SYNTHESIS OF CARBON NANOTUBES BY MICROWAVE PLASMA ENHANCED CVD ON SILICON USING IRON AS CATALYST

By

ANANDHA G R NIDADAVOLU

Bachelor of Technology

Jawaharlal Nehru Technological University

Hyderabad, India

July, 2001

Submitted to the Faculty of the
Graduate College of the
Oklahoma State University
in partial fulfillment of
the requirements for
the Degree of
MASTER OF SCIENCE
May, 2005

SYNTHESIS OF CARBON NANOTUBES BY
MICROWAVE PLASMA ENHANCED
CVD ON SILICON USING IRON
AS CATALYST

Thesis approved:

Dr. Ranga Komanduri

Thesis Advisor

Dr. Hongbing Lu

Dr. Lionel M. Raff

Dr. A. Gordon Emslie

Dean of the Graduate College

SUMMARY

Microwave plasma enhanced chemical vapor deposition (MPECVD) technique has been successfully used to synthesize vertically aligned carbon nanotubes with uniform diameter on a silicon wafer using iron as catalyst. A template has been used to pattern the catalyst film and grow nanotubes on the patterned blocks. Critical process parameters, such as source gas concentration, pretreatment time of catalyst film and growth time are varied and their effect on nanotube growth is studied. Pulsed laser deposition technique is used to deposit thin film of the catalyst film (1-5 nm) on the substrate surface. Improvement in alignment is observed with increase in methane flow rate. The optimum flow rate of methane is found to be between 20 and 30 sccm. Entire catalyst coated area has deposition with increase in pretreatment time. Growth time of 5 min with methane flow rate of 15 sccm and a pretreatment time of 5 min is found to be optimum for obtaining vertically aligned CNTs. Multi-walled nanotubes with diameters in the range 20-125 nm are synthesized in the present investigation.

ACKNOWLEDGEMENTS

I would like to express indebtedness to my advisor Dr. Komanduri, for his guidance, support and advice. Thank you for giving me an opportunity and believing me. Thanks for your support in times of hardship and giving me hope. I would like to convey my appreciation to Dr. Raff and Dr. Lu and thank them for serving on my thesis committee.

I would like to thank my colleagues and friends Madhan Ramakrishnan and Devanathan Raghavan in this collaborative effort. I truly enjoyed your company and learnt the value of team work. Thanks to Sony, Choo, Ganesh, Lee, Hari, Anand and other members of our research group for their support and friendship. I would also like to thank Phoebe Doss and Terry Colberg of electron microscopy laboratory.

My masters program would not have realized without the constant support and encouragement of my parents, brother and sisters. Thank you for having belief in my abilities and pushing me forward.

TABLE OF CONTENTS

LIST OF TABLES

LIST OF FIGURES

CHAPTER 1

INTRODUCTION

Carbon is found in four allotropic forms, namely, graphite, diamond, fullerenes and nanotubes. Of all these members of the carbon family, carbon nanotubes are relatively new and are interesting because of their unique structure, remarkable mechanical and electronic properties. Carbon nanotubes can be thought of as a sheet of graphite rolled into a cylinder. They can be either single-walled nanotubes (SWNTs) or multi-walled nanotubes (MWNTs). A MWCNT can be thought of as a stack of graphene sheets rolled into concentric cylinders. The walls of the MWCNT can either be parallel to the central axis or inclined as in a stacked cone arrangement. In such cases they can be called as multi-walled carbon nanofibers (MWCNFs). The stacked cone arrangement is also known as chevron, bamboo, ice cream cone or piled cone structures [5]. Carbon nanotubes were first discovered by Iijima in 1991 [6] when he observed multi-walled nanotubes in the soot generated in an arc-discharge apparatus. Two years later, single-walled nanotubes were discovered simultaneously by two groups each led by Iijima [1] and Bethune respectively [1].

The basic unit cell of a carbon nanotube can be defined by the chiral vector and the chiral angle. Fig 1.1(a) shows the layout of a two-dimensional graphene sheet with the unit cell bounded by OAB´B. The nanotube is formed by rolling the unit cell such that the ends of the chiral vector meet each other i.e. O meets A and B meets B´.

The chiral vector $\vec{OA}$ or $C_h = n\bar{a}_1+m\bar{a}_2$, where $\bar{a}_1$ and $\bar{a}_2$ are the unit vectors, and n and m are integers. The chiral angle, θ, is the angle made by chiral vector with the direction defined by $\bar{a}_1$.

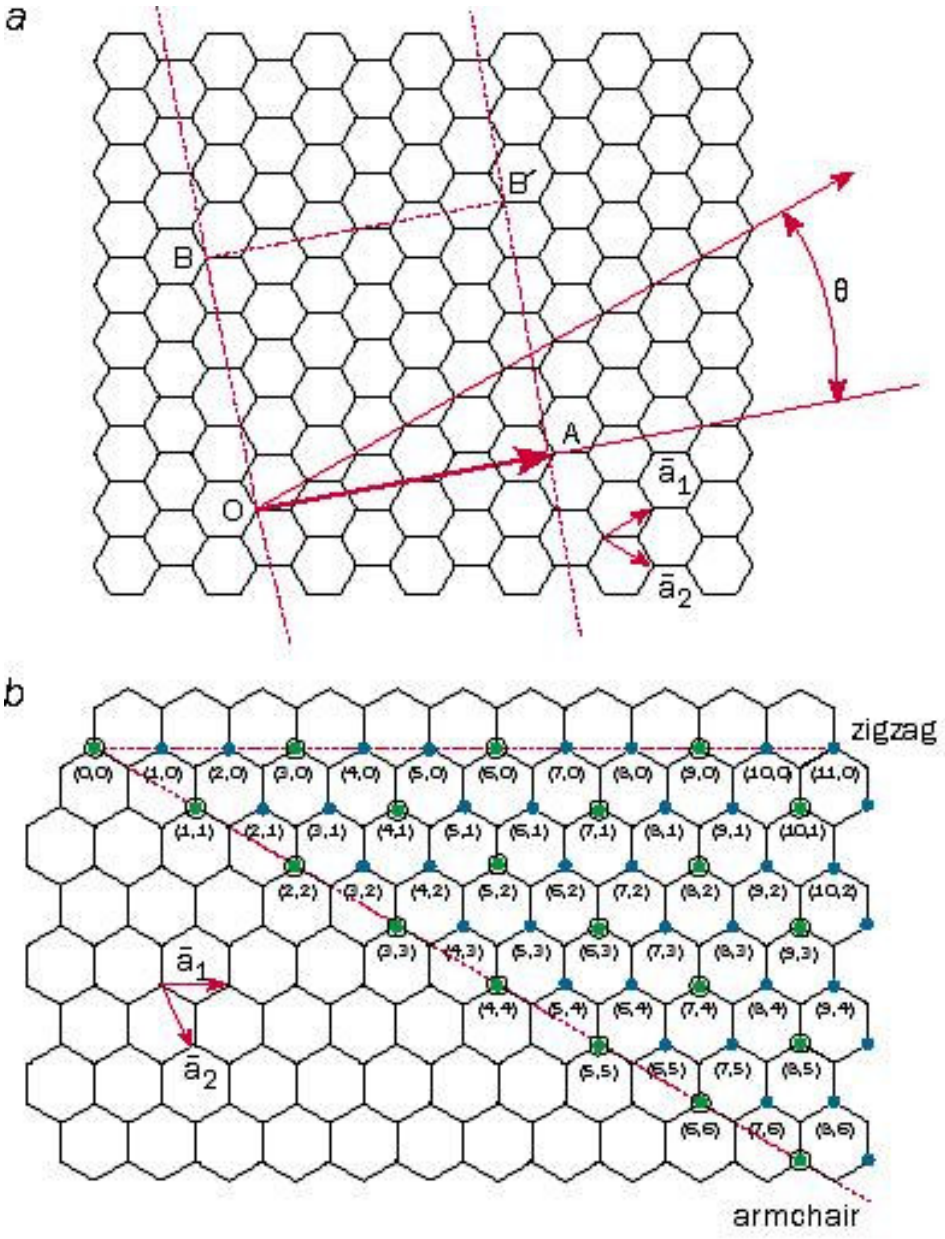

Figure 1.1(a) Schematic of the carbon unit cell OAB´B, chiral vector $\vec{OA}$ and chiral angle θ. (b) Possible vectors specified by pairs of integers (n, m) for general carbon nanotubes. [2]

The intersection of the vector $\vec{OB}$ which is normal to chiral vector with the first lattice point gives the translation vector *T*. Thus, the unit cell is defined by the rectangle formed by the chiral (C_h) and translation vectors (*T*). Fig 1.1(a) is schematic of CNT shown for (n, m) = (4, 2). If either n or m is equal to zero and the chiral angle corresponds to 0°, it is called a zigzag arrangement and the nanotubes are known as zigzag nanotubes. If n = m and the chiral angle is 30º, the nanotubes are known as armchair nanotubes. Chiral nanotubes can take any values for n and m and the chiral angle is between 0º and 30°. Figs. 1.1(b) and 1.2 show all possible arrangements [3].

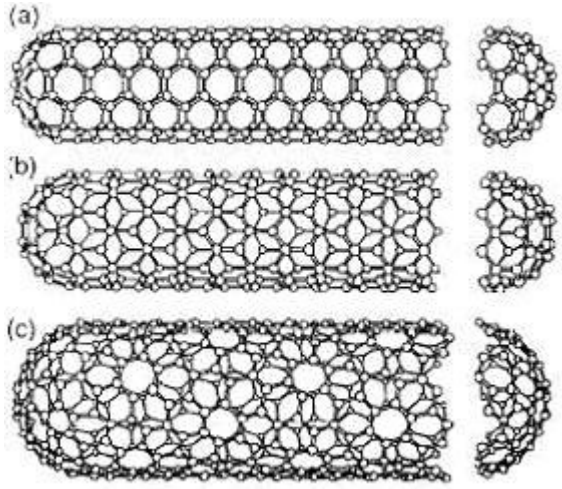

Figure 1.2 Schematic of different arrangements of SWNTs. (a) arm chair nanotube (5, 5), (b) zigzag nanotube (9, 0) and (c) chiral nanotube (10, 5).

Carbon nanotubes can be several micrometers long and have diameters as low as ≤1 nm. This huge aspect ratio makes them one-dimensional structures. They have Young's modulus of elasticity of ~ 1 TPa [1], yield strength as high as 120 GPa [5] and thermal conductivity 2000 $W.m^{-1}.K^{-1}$ [50]. The choice of n and m determines whether the nanotube is metallic or semiconducting. It is interesting to note that the chemical bonding between the carbon atoms is the same in metallic and semi-conducting nanotubes.

Because of their quasi-one dimensional shape and sp^2 and π-bonding between carbon atoms, they have interesting electronic properties. Graphite has excellent thermal properties and high mechanical strength due to the strong graphene bond. It has π-electrons above and below the individual graphene layer which are free to move and form an electron band, which explains the semi-metallic nature. Because of their finite circumference, nanotubes have a limited number of electron states which are free to move. This reduces the number of scatterers and carriers. The resistivity of a conductor depends on these two features and the number of available states into which the electrons or holes can be scattered. Due to the limited number of scatterers available, electrons can be transported without scatter or ballistically over long distances depending on the quality of the tube [4].

The mechanical properties of carbon nanotubes indicate that they are very strong, highly flexible and resist fracture under tension. They perform much better in compression than carbon fibers and do not fracture easily. SWNTs can be bent, twisted, flattened and can be made into small circles without breaking [2]. It is observed that the nanotubes do not undergo any permanent deformation when subjected to loads in an AFM.

Individual Carbon nanotubes can be used as field emission sources by utilizing their electrical properties. CNTs can be used as tips for scanning probe microscopes because of fine tip radius and high aspect ratio (>1000). There are also efforts to use them as interconnects in IC's instead of metals because of the problems associated with ever decreasing feature size and also as transistors. Ensemble of nanotubes in bulk

quantities are used for making composites with improved mechanical properties; media for hydrogen storage, field emission based flat panel displays, ionization gauges.

These properties make them exciting materials and there is a worldwide research effort in progress to have better control on their synthesis and optimization of process parameters to realize their immense potential. Nanotubes need to be produced on the kilogram scale in order to be used in bulk quantities. For microelectronics applications, self-assembly or controlled growth techniques are to be coupled with microfabrication techniques for scale-up, which still has a long way to go. There is a need to grow defect free, structurally perfect nanotubes to macroscopic lengths. Better control is needed on the chirality, diameter and selective growth of the nanotubes. These and other challenges need to be resolved before nanotubes can be integrated into devices.

Carbon nanotubes (CNTs) are grown by various methods including arc-discharge, laser ablation and chemical vapor deposition (CVD) [1]. Arc discharge and laser ablation processes are reported to yield single-walled nanotubes (SWNTs) of high quality but require very high temperatures (3000ºC-4000ºC). Chemical vapor deposition techniques (CVD) allows the growth of CNTs at low temperatures (600ºC-1200ºC) and control the orientation which is not possible with the other two techniques.

Chapter 2 will examine the various PECVD methods by which the CNTs are grown. Chapter 3 presents a review of the literature on nanotubes produced by plasma enhanced CVD. Chapter 4 presents the problem statement of the present investigation. Chapter 5 describes the experimental set up and methodology used. Results and discussion are covered in Chapters 6, and 7. Conclusions of the work are presented in chapter 8.

CHAPTER 2

PECVD TECHNIQUES

Chemical vapor deposition techniques have been in use to synthesize carbon filaments, fibers for more than 20 years [1]. As the name indicates, in CVD the reactants are in gaseous form and the growth takes place due to the chemical reaction between them. The process involves heating the catalyst material to high temperatures and allowing the reactants generally hydrocarbon gas into the reactor for the desired amount of time. The deposition or growth takes place on the catalyst surface and is collected upon cooling the chamber to room temperature. Hydrocarbons (carbon source), catalysts and growth temperature are the critical parameters in a CVD system. Transitional metals such as iron, cobalt, nickel are generally used as the catalyst material for synthesizing nanotubes. The growth process involves dissociation of hydrocarbon gas on the catalyst nanoparticles, dissolution or adsorption of carbon atoms, saturation and precipitation of carbon in tubular form on the catalyst nanoparticles leading to nanotube growth. Tubular form is favored because of the low energy associated with it. Methane, ethylene and acetylene are the most commonly used carbon feedstock and temperatures are in the range of 800-1000ºC. Methane is preferred because it does not undergo self pyrolysis at such high temperatures.

PECVD first emerged as an alternative to Thermal CVD in microelectronics industry because of the low temperatures involved. The high temperatures in thermal CVD are detrimental in microelectronics industry (charring of photo resist at elevated temperatures). A variety of CVD techniques using plasma sources are used to grow CNT. They are listed in the following [5]:

- Direct Current
- Hot-filament aided with D.C
- Microwave
- Inductively coupled plasma reactors
- RF with magnetic enhancement

DC plasma reactor contains a pair of electrodes in which one is grounded and the other connected to a power supply in a grounded chamber. Negative bias is applied to the cathode and the chamber is filled with the precursor gases. The bias applied helps in dissociating the feed gas. The substrate is placed either on the anode or cathode. The electrode holding the substrate might have an independent heating system, generally a resistive heater to raise the substrate to the desired temperature. A tungsten wire suspended in the plasma stream can also serve as a heating source. This is called hot-filament aided with D.C plasma.

Plasma dissociates the hydrocarbons creating a large number of reactive radicals which may lead to amorphous carbon deposition. So, they are diluted with gases such as hydrogen, ammonia, and argon. The reactor pressure typically varies from 1 to 20 torr and the percentage of hydrocarbon up to 20%. Operation at atmospheric pressure is

difficult due to power coupling problems whereas operation in millitorr range results in slow growth rates. So, PECVD reactors are generally operated in the 1-20 Torr range. Microwave sources are very popular in this pressure range.

Catalysts are needed to grow CNTs by PECVD. They are prepared using either solution-based techniques or physical techniques. Solution based techniques involve steps such as dissolution, stirring, precipitation, refluxing, separation, cooling, reduction, etc. They are cumbersome and time consuming. It is also difficult to confine the catalyst to small patterns. Physical techniques, such as electron-gun evaporation, ion-beam sputtering, thermal evaporation, magnetron sputtering are easy to use and can be employed to create small patterns. Particle size and the resultant nanotubes diameter are dependent on the film thickness. Thin films result in smaller particle size and tube diameters. In the PECVD process the catalyst film is first subjected to plasma treatment in inert gas or hydrogen to break the continuous film of catalyst into smaller nanoparticles which are suitable for nanotube growth. Longer pretreatment times lead to melting of the catalyst nanoparticles and they agglomerate forming bigger islands, which is not desired. The substrate must be subjected for the optimum pretreatment time so that the particles of the right size are formed.

CHAPTER 3

LITERATURE REVIEW

3.1 Alignment

In order to exploit the field emission properties of carbon nanotubes, they should be synthesized as an ensemble and vertically aligned. Ren *et al.* [9, 46] grew aligned carbon nanotubes on glass at temperatures below 666ºC using a plasma-enhanced hot filament CVD as shown in Fig 3.1. RF magnetron sputtering is used to coat nickel catalyst on the glass surface. Acetylene is used as the carbon source and ammonia as the diluent.

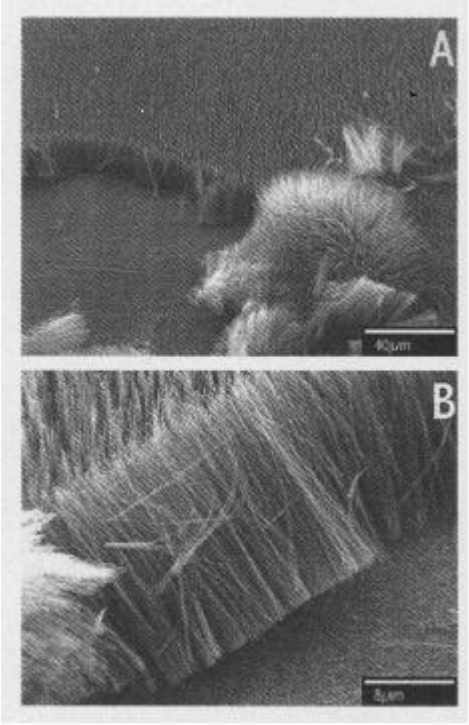

Figure 3.1 (a) SEM micrograph of carbon nanotubes aligned perpendicular to the substrate over large areas. b) Enlarged view of (a) along the peeled edges [9]

Ammonia along with the nickel layer plays an important role in the formation of CNTs. In one series of experimentation, they subjected the catalyst layer to plasma etching to reduce the thickness of the catalyst layer and then introduced acetylene. In another series, they introduced both acetylene and ammonia simultaneously. In either case, nanotubes are observed, but when nitrogen is used instead of ammonia, no tubes were observed. They were also not observed when acetylene is allowed before ammonia. They determined that the diameter of the nanotubes depend on the thickness of the catalyst layer. The thinner the catalyst layer, the smaller the size of nanotubes. MWNTs are synthesized in all cases with diameters ranging from 20 to 400 nm and lengths from 0.1 to 50 μm. The low temperatures involved are suitable for cold-cathode flat panel displays which require carbon nanotube emitters grown perpendicular to the glass surface.

3.1.1 Electrical self-bias

Bower *et al.* [8] reported the growth of uniform films of aligned carbon nanotubes. They showed that the alignment is due to the electrical self-bias imposed by the plasma on the substrate surface and not due to the van der Waals interactions between the nanotubes. They also observed curly nanotubes in the absence of plasma. The nanotubes always grew perpendicular to the local substrate surface irrespective of its contour or tilt. Fig 3.2(a) shows aligned nanotubes grown on the circumferential surface of a hair-thin telecom-grade silicon dioxide optical fiber. Cobalt is used as the catalyst, which is sputter deposited on the substrate surface, C_2H_2 and NH_3 are the process gases used. Growth rates as high as 100 nm/s are reported. Ammonia, which is relatively heavier when compared with other plasma forming gases such as hydrogen, helps in establishing a strong local field at the surface.

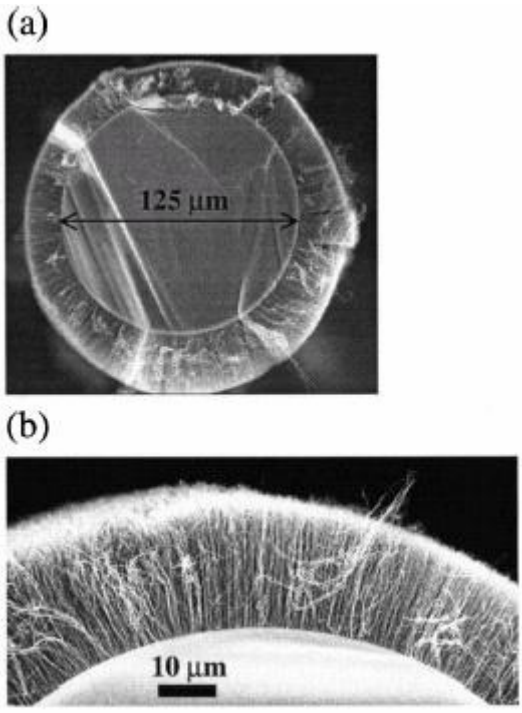

Figure 3.2 (a) SEM micrograph of radially grown nanotubes on the surface of a 125 µm diameter optical fiber. (b) Close up of (a) showing conformal perpendicular nature of the nanotubes growth on the fiber [8]

Stoner *et al.* [11] synthesized aligned MWNT on silicon substrates using CH_4 and NH_3 as process gases. An iron film of 10 nm is sputtered onto the substrates and later subjected to plasma pretreatment in NH_3 atmosphere to break the thin Fe layer into discrete islands of 100 nm to 200 nm. They observed bamboo shaped growth for the majority and some had concentric hollow structures which are shown in Fig 3.3. The temperature is varied from 660ºC to 1000ºC and the pressure is fixed at 21 torr for experimentation.

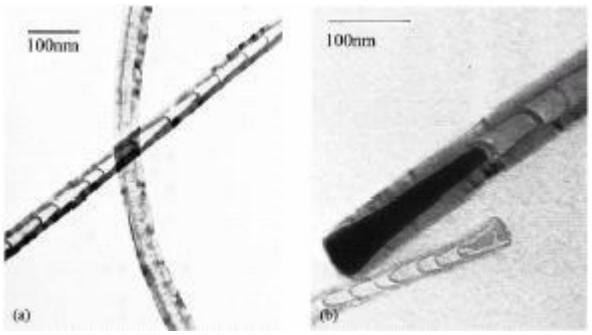

Figure 3.3 (a) TEM micrograph of bamboo and hollow concentric structures. (b) Catalyst particle at the end of carbon nanotubes [11]

3.1.2 Inductively coupled plasma reactor (ICP)

Meyyappan *et al.* [10] used an inductively coupled plasma (ICP) reactor to grow carbon nanotubes on silicon substrates with multilayered Al/Fe catalyst. ICP reactors are simple to construct and have high ionization and power utilization efficiencies. First a thin layer of Al is sputtered followed by a thin layer of Fe. The coated Fe layer consisted of particles less than 10 nm. This helps in avoiding the pretreatments such as exposure to H_2 plasma or ion bombardment or NH_3 etching needed to prepare the growth surface. A CH_4 and NH_3 mixture is used to grow vertically aligned MWNTs and MWNFs. They showed that presence of atomic hydrogen is suitable for growing MWNFs.

3.2 Room temperature synthesis

Silva *et al.* [12] reported the growth of carbon nanofibers at low temperature (Fig 3.4). They used RF (13.56MHz) PECVD technique to synthesize them at room temperature, 100ºC and 250ºC. They used nickel powder, which has an average grain size of 4-7 µm, on different substrates, such as silicon, graphite and plastic. Methane and hydrogen are used as the precursor gases.

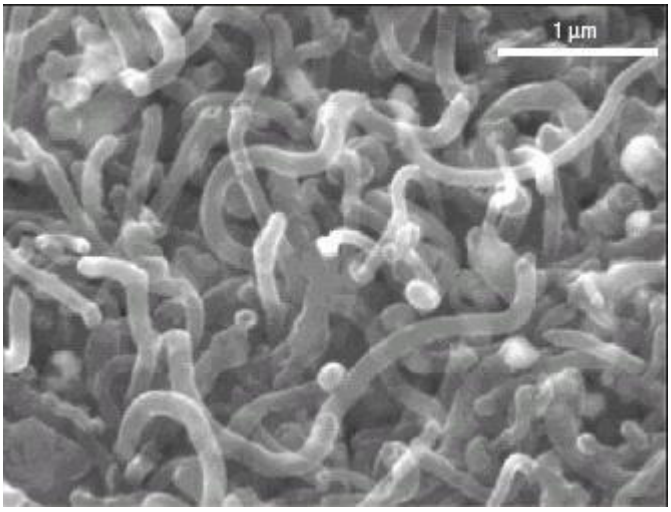

Figure 3.4 SEM micrograph of carbon nanofibers produced at room temperature [12]

3.3 Role of hydrogen plasma

Lin *et al.* [13] argued that H_2 plasma is responsible for the alignment of nanotubes. Carbon nanotubes are synthesized using RF plasma-enhanced CVD using acetylene and hydrogen mixtures on Fe coated silicon substrates. They observed that aligned nanotubes are formed only when H_2 plasma is used. Acetylene plasma resulted in randomly oriented carbon fibers and using just hydrogen in the absence of plasma resulted in randomly oriented CNTs.

3.4 Terminating clusters

Tomanek *et al.* [14] synthesized high density of carbon nanotubes by MPECVD. The diameters ranged from 20 to 400 nm and densities in the range of 10^8-10^9 cm^{-2}. They observed higher growth rates on Fe catalyst than on Ni. They also observed cluster formation on top of the nanotubes at temperature of 650ºC during deposition. With increase in temperature, the size of the cluster decreased and the diameter increased. They call them terminating clusters which are shown in Fig 3.5. The tube diameter is not

affected by growth time. As shown in Fig 3.6, they also observed nanotubes with different morphologies, such as the repeating arrow head shape (bamboo like growth) and hollow core. The average tube diameter of hollow core type is 20 nm greater than that of arrow head shape.

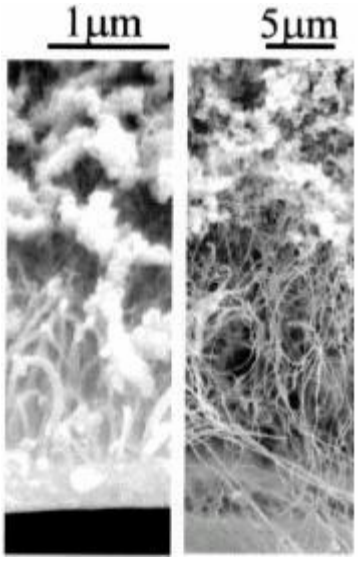

Figure 3.5 SEM micrographs showing nanotubes and terminating clusters on top of them [14]

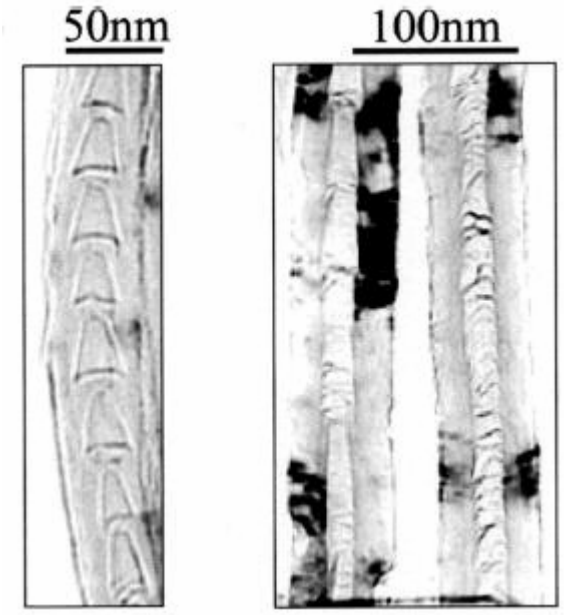

Figure 3.6 TEM micrographs of carbon nanotubes showing arrow head and hollow core patterns [14]

3.5 Plasma breaking of thin films

Gao *et al.* [15] determined optimum plasma breaking conditions for Fe catalysts for a particular thickness. A PLD method is often used for catalyst deposition due to the high deposition rates possible at low temperatures. The highly energetic ablated plume strongly adheres to the substrate forming a uniform layer. Only nanoparticles of the catalyst act as nucleation sites for CNT growth. Thus, it is highly desirable to have uniformly distributed, high-density nanoparticles for high quality synthesis. The catalyst size and distribution are highly dependent on the plasma breaking conditions. They determined the catalyst density as a function of size of catalyst by subjecting the thin film to plasma pretreatment at various powers and arrived at the optimum combination.

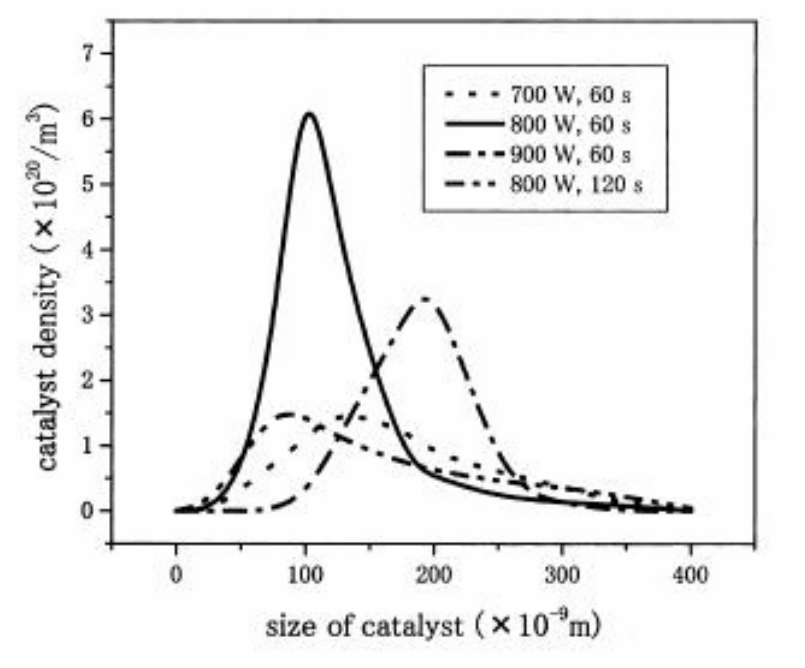

Figure 3.7 Size distributions of iron catalysts, produced by plasma bombardment on Fe films [15]

From Fig 3.7, it can be seen that optimum plasma breaking conditions were obtained at 800 W and heating time of 60 sec at a fixed gas pressure of 15 torr for a 200 nm thick Fe film. With increase in the duration of plasma treatment, the peak of the catalyst density is lowered and the film melted as shown in the Fig 3.8.

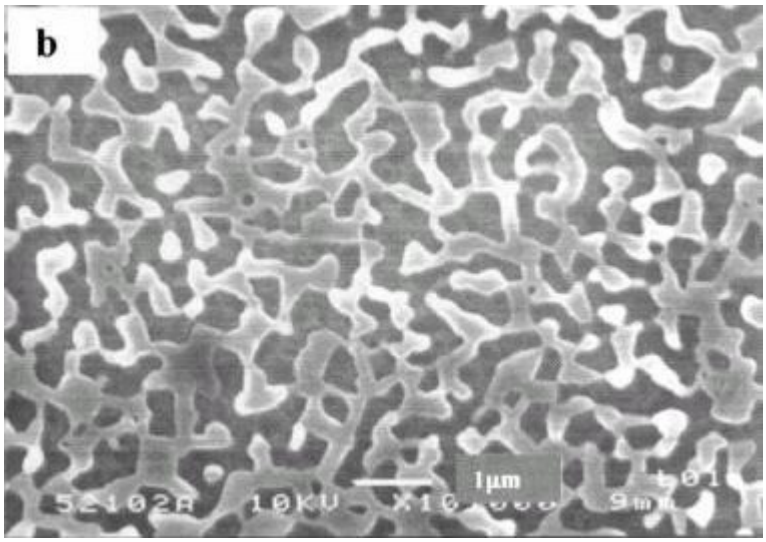

Figure 3.8 SEM micrograph of Fe film showing melt pattern after being subjected to 5 min of plasma pretreatment [15]

3.6 Nitrogen incorporation

Kim *et al.* [16] showed that enhanced CNT growth in a N_2 or NH_3 environment takes place as a result of nitrogen incorporation to the CNT wall or cap. N_2 incorporation can reduce the strain energy required for tubular graphitic layer of CNTs, so it decreases the activation energy required for both nucleation of graphitic layer and structural evolution of CNT during growth. They also showed that pretreatment in a N_2 environment is not necessary for vertically aligned CNT growth. Lee *et al.* [17] showed that the growth rate and diameter of CNT can be controlled by varying the concentration of nitrogen in the process gas.

3.7 Catalyst film thickness

Chhowalla *et al.* [18] used a direct current glow discharge system to synthesize vertically aligned carbon nanotubes. Ni and Co are used as the catalyst materials and either magnetron sputtering or thermal evaporation is used to deposit a thin film of catalyst on silicon substrate.

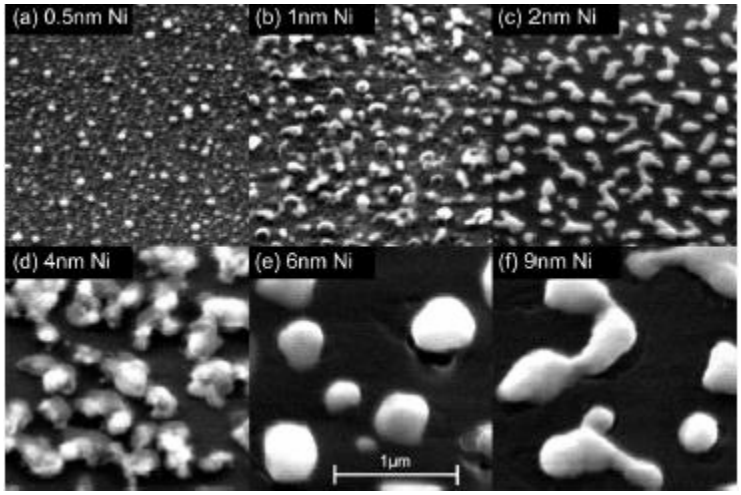

Figure 3.9 SEM micrographs of Ni films with varying thickness deposited using magnetron sputtering on 50 nm of ECR SiO_2 after annealing at 750°C in 20 torr of H_2 for 15 min [18]

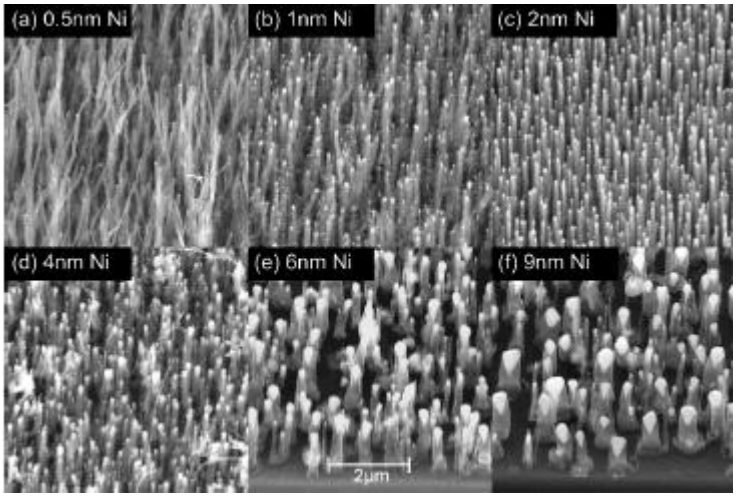

Figure 3.10 Nanotubes grown on Ni layers of various initial thicknesses shown in Fig 3.9. Same growth conditions are used for all samples. C_2H_2:NH_3 = 75:200, time = 15 min and bias voltage = -600V [18]

The film thickness is varied from 0.5 nm to 20 nm. The catalyst film after annealing is shown in Fig 3.9. The film breaks into small nanoparticles when it is thin and agglomeration of catalyst particles is observed as thickness increases. As seen in Fig 3.10 with increase in catalyst film thickness, the tubes become thicker and shorter in length. C_2H_2 and NH_3 are used as the process gases. Silicon substrates with three different surface morphologies are used. Substrates with a thin native oxide, pristine surface and 50 nm layer of SiO_2 grown by electron cyclotron resonance (ECR) are used. No islands are formed after annealing the nickel film on pristine silicon surface and on silicon with a native oxide. They attribute it to the diffusion of nickel into silicon forming a silicide above 300ºC. No such phenomenon is observed with a cobalt film. With increase in acetylene content, the growth rate initially increases and then decreases. They applied a bias voltage of -600V in all cases to obtain aligned nanotubes. With increase in bias voltage they observed that the deposition rate decreases, which is due to the fact that there are a larger number of NH_3 species which results in greater etching.

Qin *et al.* [19] used a microwave plasma enhanced CVD to produce bundles of carbon nanotubes on alumina substrates employing a CH_4 and H_2 mixture. Iron is the catalyst material, which is reduced from ferric nitrate solution. The lower portion of the plasma was always in contact with the substrate. The nanotubes are 10-50 nm in diameter and more than 20 µm long. Typical processing conditions are: Chamber pressure 15 torr, Microwave power 600 W, Flow rates 15/10 sccm for CH_4/H_2 and Temperature 850-900ºC.

3.8 Morphology of thin film

Lee *et al.* [20] determined that surface morphology of the catalyst film influences the growth of nanotubes. They sputtered Ni films of 70 nm thickness by varying the RF power during the sputtering process. It was observed that the distribution of the catalyst grain size is not uniform with increase in RF power which is shown in Fig 3.11. Films coated at lower power had uniform grain size distribution. Carbonaceous particles are synthesized on top of the aligned CNTs for particles with larger grain sizes. The length and density of CNTs also decreased with increase in rf sputtering due to larger grains. The average diameter of the CNTs is smaller than the grain size of Ni films due to etching of the Ni surface by atomic hydrogen in the early stages of growth. The catalyst film is not subjected to any pretreatment because of the grain size of catalyst obtained by the sputtering process is very small.

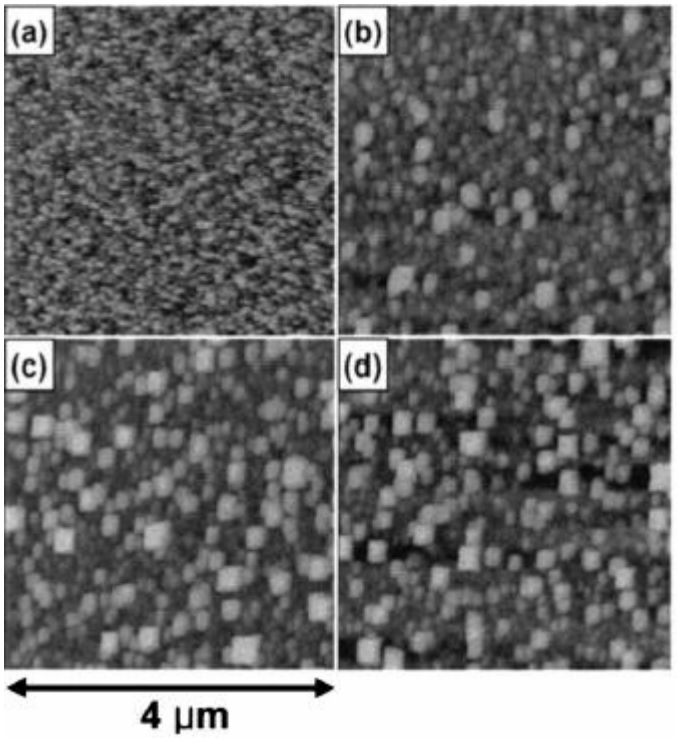

Figure 3.11 AFM images of Ni films deposited at rf powers (a) 10 (b) 20 (c) 40 (d) 80 W [20]

3.9 Off-normal orientation

Off-normal orientation is required for some applications such as tips of probes used in scanning probe microscopy. If the cantilever tip is oriented at a relatively large angle to the normal of the cantilever surface, it will be possible to map the sidewalls of the vertical trenches which would be of great use in the semiconductor industry. The orientation is controlled by the direction of electric field lines. When the plasma completely engulfs the substrate which is on the cathode, the substrate surface is surrounded by electric field lines which are straight and normal except for the corners or regions around the edges.

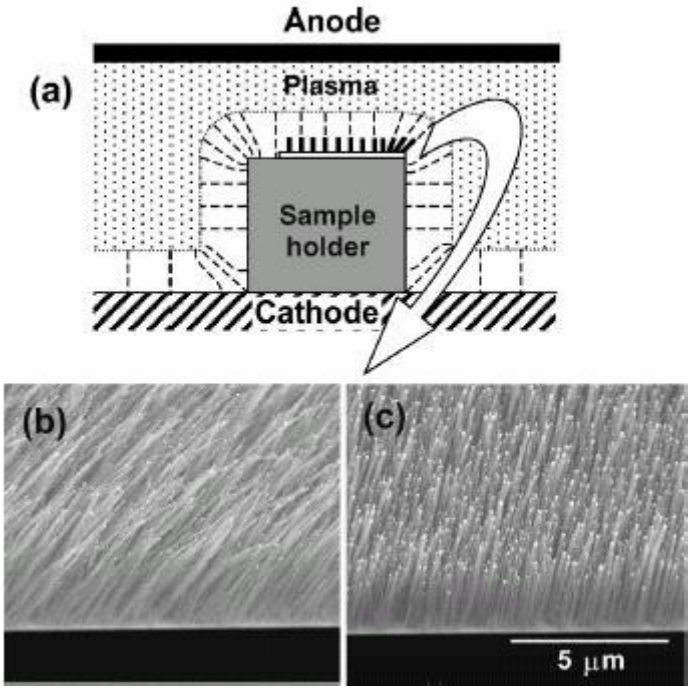

Figure 3.12 (a) Schematic of the experimental setup used and (b) and (c) SEM micrographs of the forests located at 100 μm and 1000 μm away from the edge aligned at ~38º and 12º angles to the substrate normal, respectively [21]

It has been observed by Merkulov *et al.* [21] that the direction and shape of the field lines is different at the edges and significant bending takes place. This bending is greater at the edges and decreases as one moves away from the edges. So, by positioning the substrate

closer to the edges of the cathode surface, they have grown CNTs which are aligned at angles other than the substrate normal which is shown in Fig 3.12.

3.10 Entanglement

Sato *et al.* [22] studied CNT film thickness as a function of plasma pretreatment time. The thickness of the CNT film is determined by the H_2 plasma pretreatment time and the growth time.

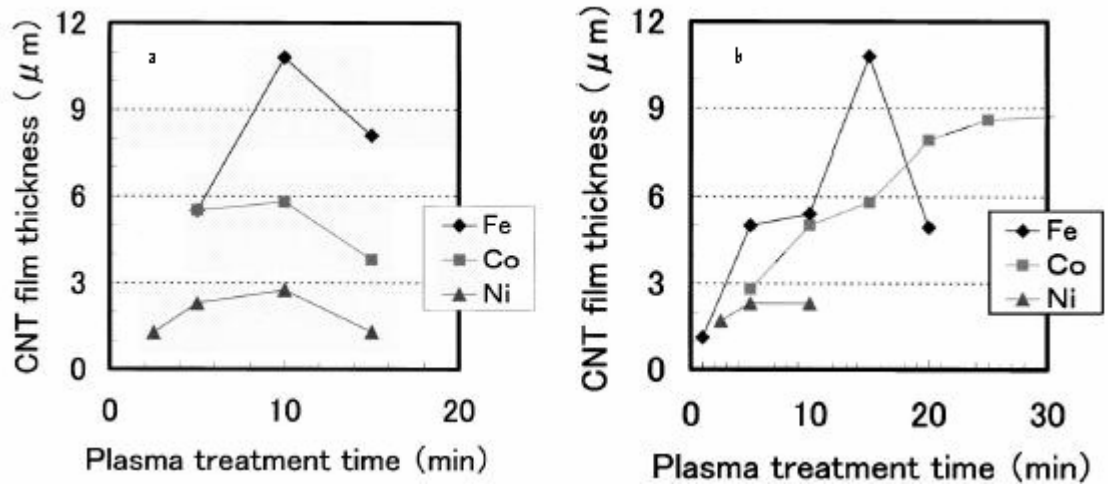

Figure 3.13 CNT film thickness as function of (a) pretreatment time in H_2 plasma. (b) Growth time in H_2+CH_4 plasma [22]

Figure 3.13 (a) shows that film thickness reaches its maximum value of 10 μm in 10 min of pretreatment time. The growth times were 15 min for Fe and Co and 5 min for Ni. Fig 3.13 (b) shows CNT film thickness as a function of growth time. It can be clearly seen that Fe gives the largest film thickness among the three catalysts. The film thickness decreases after reaching a maximum of 11 μm in 15 min. They have reported that bundles are observed when the tube length is more than 10 μm which brings about entanglement of CNTs. They believe that this entanglement prevents the CNTs from growing upwards and destructs the well-aligned CNT layer. In Co and Ni samples the

film thickness increases and then levels off. Bundle formation is also observed in both these catalysts. The difference in growth rates is presumed to be due to the differences in solubility of the three metals in carbon. Fe and Ni have the highest and least solubility in carbon which coincides with the fact that they have the highest and least growth rates.

3.11 Gas phase environments

Meyappan *et al.* [23] compared the gas phase environments of thermal and plasma CVD when methane is used as the feed stock. In thermal CVD at temperatures below 900ºC (which are commonly used for the synthesis of SWNT and MWNTs), the feedstock does not dissociate in the gas phase and the nanotube growth is solely due to surface reaction of CH_4 on the catalyst surface. Whereas in plasma CVD, the feed stock is readily dissociated by plasma to produce significant amount of C_2H_2, CH_4, variety of C_xH_y radicals and ions through electron impact as well as neutral reactions, all of which contribute to nanotube production. The large amount of carbon available at catalytic surfaces in plasma CVD is the reason behind MWNTs being synthesized in that process. So, it might be possible to synthesize SWNTs in plasma CVD by controlling the dissociation of methane which can be achieved by lowering the partial pressure or lowering the input power. Copious amount of atomic hydrogen is present in plasma CVD. The atomic hydrogen assists in dehydrogenation of adsorbed hydrocarbons, enhance the surface diffusion of carbon and etch away amorphous carbon.

3.12 RF PECVD

Kato *et al.* [24] used rf PECVD techniques to grow aligned multiwall nanotubes. They synthesized nanotubes on the rf electrode which is covered with a nickel plate and also on a zeolite substrate. The Ni plate on the rf electrode is subjected to plasma

pretreatment in three different atmospheres, namely, H_2, He, Ar and the resulting nanotubes growth is compared, with all other conditions remaining the same. The plasma sputters the nickel plate leaving projections of various sizes depending on the plasma type and this controls the density of the tubes as shown in Fig 3.14.

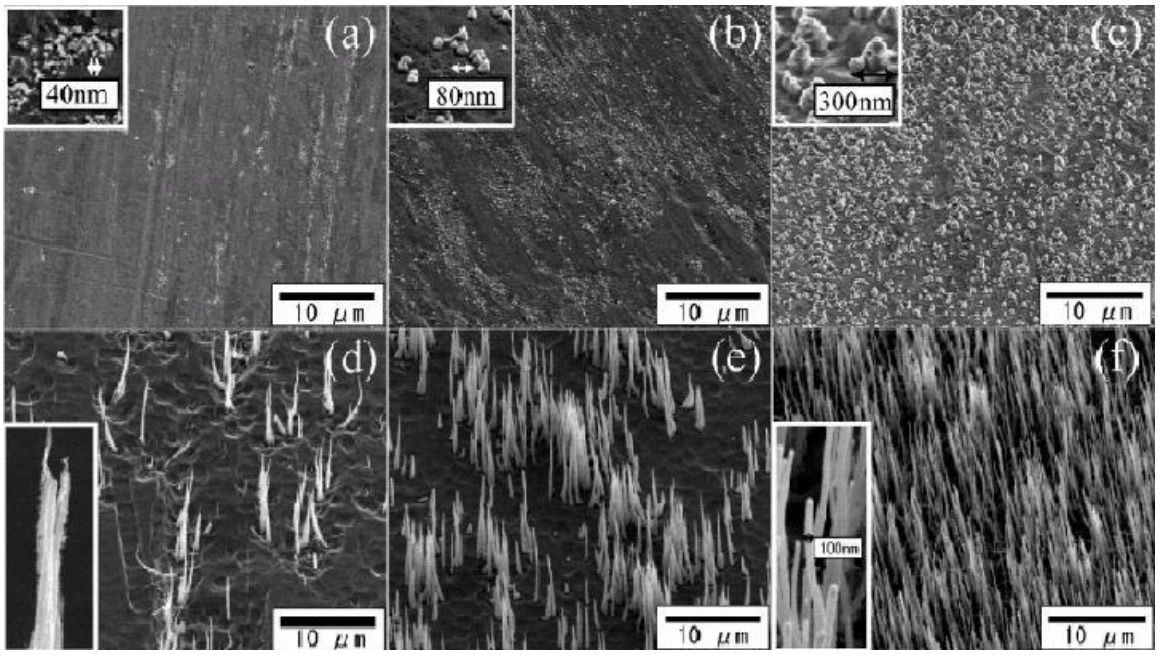

Figure 3.14 SEM micrographs showing the relationship between pretreatment gases and MWNTs produced by 15 min of PECVD. (a) and (d) in H_2; (b) and (e) in He: and (c) and (f) in Ar [24]

The pretreatment was carried at 650ºC. The density of projections varies as the gases change and Ar pretreatment is the best giving rise to dense growth of CNTs. SWNTs are observed on the zeolite substrate when Fe/Co catalyst is used.

3.13 Carbon nanocones

Merkulov *et al.* [25] reported synthesis of vertically aligned carbon nanocones (CNC) and CNFs on CNCs. A nanocone consists of central cylindrical CNF and a sloped solid outer wall. This can be achieved by adjusting the growth parameters, in this case the

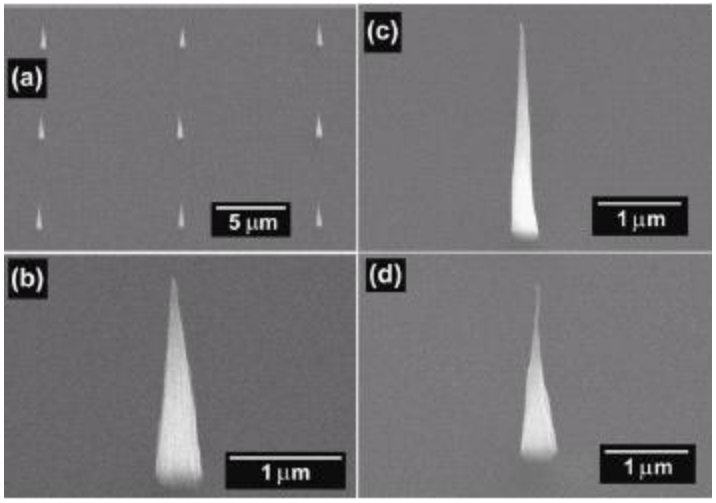

Figure 3.15 SEM micrographs of (a) an array of carbon nanocones fabricated using PECVD with high amounts of acetylene; individual carbon nanocones with different cone angles (b) ~15º and (c) ~5º (d) CNT on top of nanocone synthesized by first growing nanocone as in (b) followed by reduced acetylene content. The growth times for nanocones in (a), (b), (c) were 15 min and for (d) 15 and 5 min [25]

ratio of acetylene to ammonia. With increase in the ratio, it is observed that carbon precipitates on the outer walls of the vertically aligned CNFs resulting in lateral growth and forming carbon nanocones. This takes place due to the deposition rate of carbon being higher than the etching rate of ammonia. By adjusting the flow rate of acetylene, first a nanocone can be synthesized and after it reaches the desired height, the flow rate can be changed to produce CNFs. Fig 3.15 shows CNCs and CNT on top of CNCs.

Fig 3.16 depicts the schematic of the growth process. Fig 3.16 (a) shows the normal growth process of a CNT, where the hydrocarbon decomposes on the surface of catalyst, diffusion of carbon through the catalyst particle and subsequent precipitation. In a CNF in addition to this, growth also takes place in a lateral direction when the deposition rate is greater than the etching rate as shown in Fig 3.16 (c). This happens when the acetylene content is increased relative to ammonia or the ammonia content is

too low. Fig 3.16 (b) shows the reactive radicals, ions formed during plasma decomposition of acetylene and ammonia.

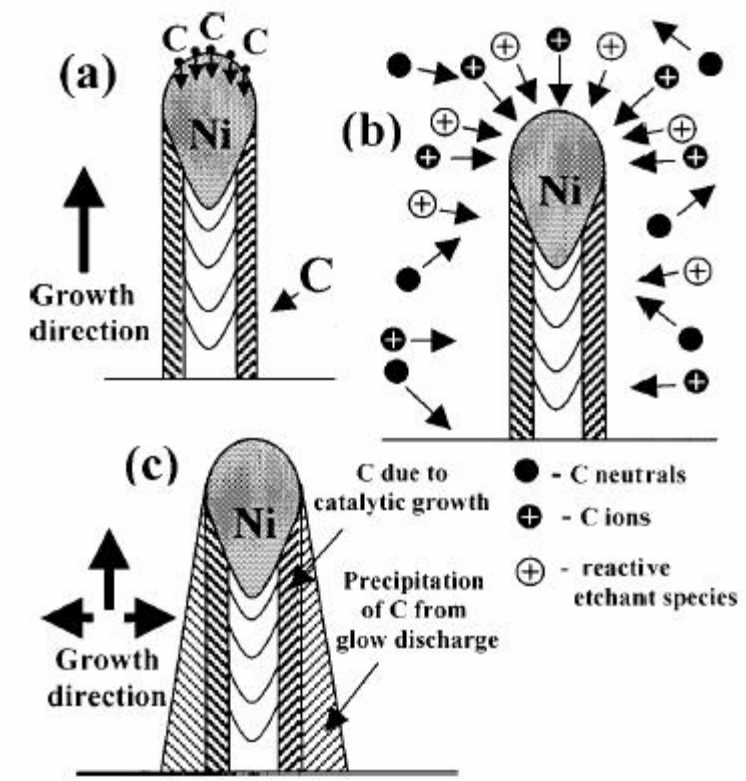

Figure 3.16 Schematic representation of the growth of (a) a CNF using conventional thermal CVD, (b) a vertically aligned CNF using PECVD, and (c) a carbon nanocone formed due to additional precipitation of carbon at the outer walls during PECVD [25]

3.14 Bundles of aligned nanotubes

Dai *et al.* [26] synthesized massive arrays of aligned MWNTs on patterned porous and plain silicon substrates using thermal CVD. The schematic is shown in Fig 3.17 and SEM micrographs in Fig 3.18. A thin layer of iron (5 nm) is used as the catalyst and ethylene as the source gas. They observed that porous silicon substrate is more conducive to the nanotube growth than plain silicon. The average diameter of the nanotubes, which are synthesized in bundles, is 16 nm. The bundles are held together by van der Waals

forces. The rigidity of the bundle helps the nanotubes to keep growing along the original direction, which is normal to the substrate surface. For growth times of 5, 15, 30, and 60 min they observed tubes which are 35, 100, 160, and 240 µm long, respectively.

Plain silicon substrates are purchased and are used without cleaning or removing the native oxide. Porous silicon is obtained by electrochemical etching of P-doped n^+-type Si (100) wafers. All are patterned with Fe films 5 nm thick by electron beam evaporation through shadow masks containing squared openings with side lengths of 10 to 250 µm at pitch distances of 50 to 200 µm.

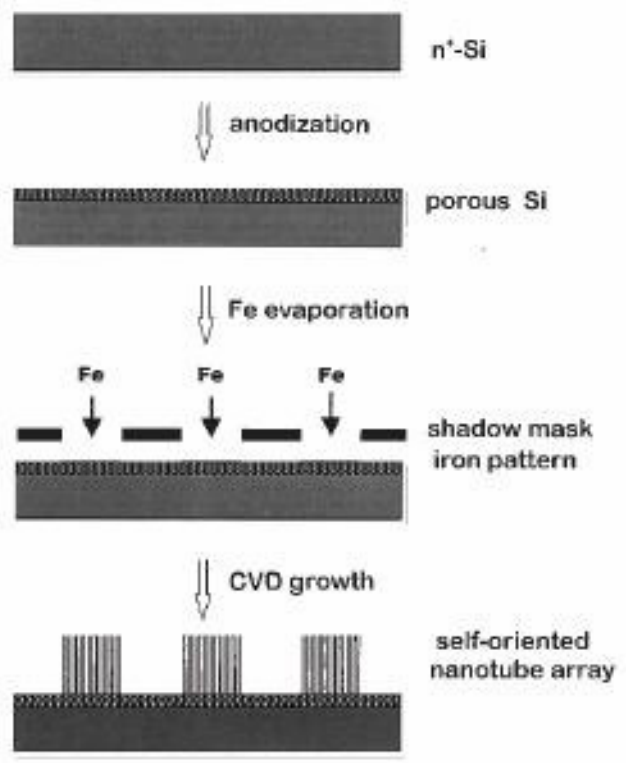

Figure 3.17 Schematic of the synthesis of regular arrays of oriented nanotubes on porous silicon by catalyst patterning and CVD [26]

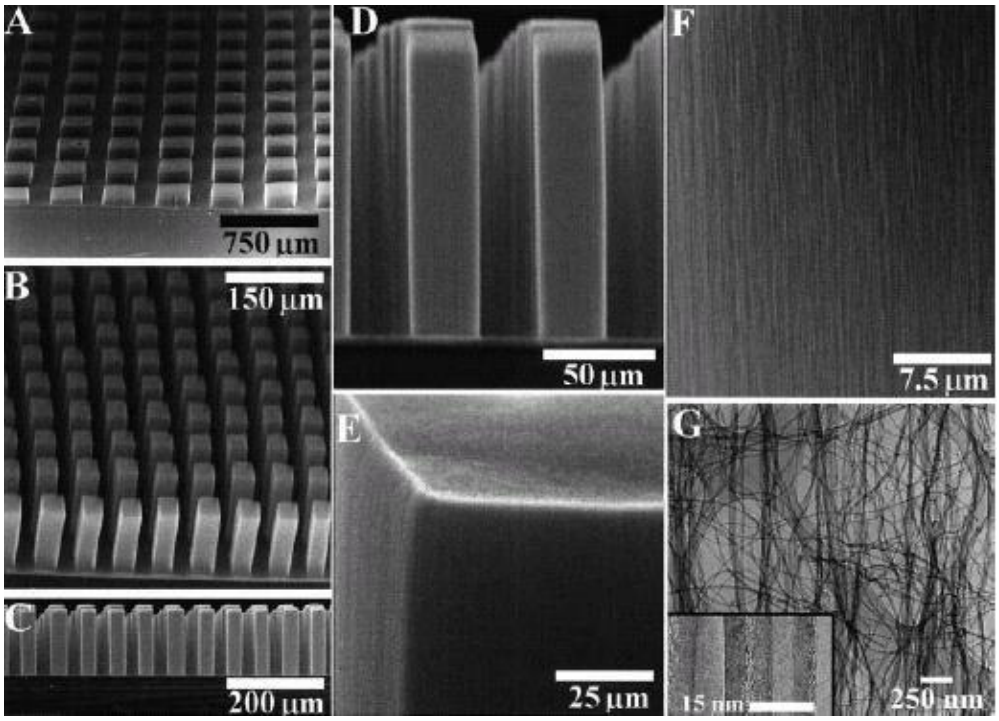

Figure 3.18 SEM micrographs of self-oriented nanotubes synthesized on porous silicon substrates. (a) SEM micrographs of nanotubes synthesized on 250 µm X 250 µm pattern, (b) Nanotubes synthesized on 38 µm X 38 µm pattern, (c) Side view of the nanotowers in (b), (d) Higher magnification of (c), (e) SEM micrograph showing sharp edges and corners, (f) SEM micrograph showing the nanotubes in a single block well aligned perpendicular to the substrate surface, and (g) TEM micrograph of pure multiwalled nanotubes [26]

Ren *et al.* [27] employed a plasma-enhanced hot-filament CVD technique to synthesize aligned carbon nanotubes on polycrystalline and single crystal nickel substrates. The temperature is maintained below 666ºC and the tube diameter ranges from 10 to 500 nm and 0.1 to 50 µm in length. Acetylene and ammonia are used for supplying carbon and dilution, respectively. They observed that the intensity of plasma is crucial in determining the diameter and length of the nanotubes. With increase in plasma intensity, the size of the Ni catalyst particle is reduced, which results in reduced tube diameter. The length of the nanotubes increases dramatically.

3.15 Low temperature synthesis

Ren *et al.* [9] synthesized aligned nanotubes on glass at temperatures as low as 666ºC. The growth temperature still needs to be lowered for FED applications in which soda lime glass is often used for the manufacture of devices. Lee *et al.* [28] were further able to reduce the temperature to 520ºC and synthesize carbon nanotubes. A microwave PECVD technique is used to achieve this, employing a mixture of CH_4 and H_2 on silicon substrates which are sputter coated with Ni. All the nanotubes formed are curly without any alignment suggesting that they are highly defective. They observed that diameter of the nanotube increased with increase in methane content and decreased with an increase in growth time.

3.16 Aligned SWNTs

Dai *et al.* [29] surmised that the substrate also plays an important role in the formation of nanotubes. Fe_2O_3 catalyst supported on crystalline alumina nanoparticles produced abundant individual SWNTs and small bundles of SWNTs using thermal CVD of methane. Only SWNT bundles are produced when the catalyst is supported on amorphous silica particles. The nanotubes thus produced are nearly free of amorphous carbon. This is attributed to the fact that methane is used as the carbon source at temperatures of the order of 1000ºC. Methane is the most kinematically stable hydrocarbon that undergoes the least pyrolytic decomposition at higher temperatures. Due to this, the carbon atoms needed for the growth of nanotubes are provided by catalytic decomposition of methane at the surface. They also ran experiments for a short period (10 min) employing high flow rates for methane, which might have also contributed towards the synthesis of amorphous-free nanotubes.

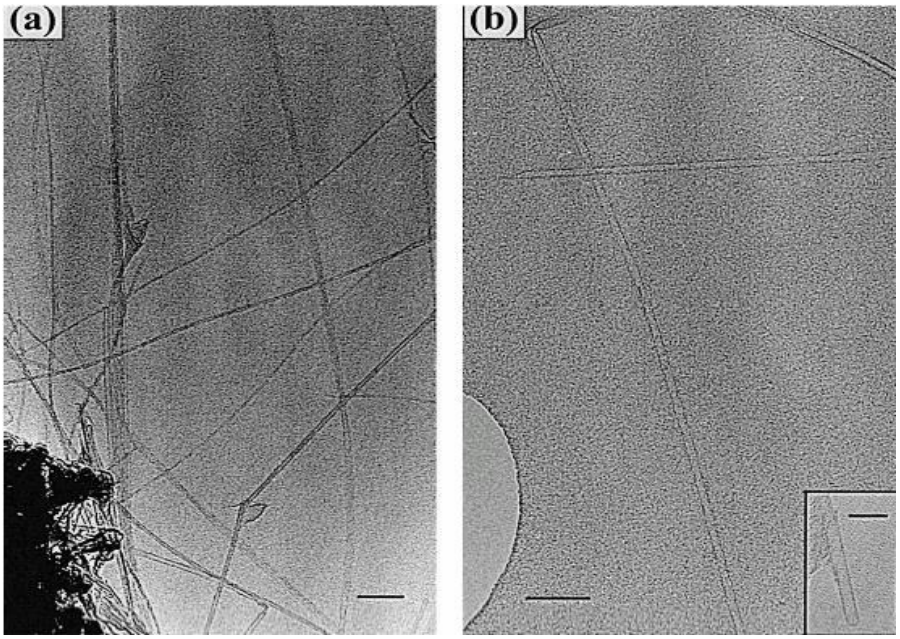

Figure 3.19(a) TEM micrographs of individual and bundled SWNTs produced on Fe_2O_3/alumina catalyst. Scale bar: 100 nm. (b) High resolution TEM of an individual SWNT (5 nm). Inset shows the closed end of a 3 nm SWNT [29]

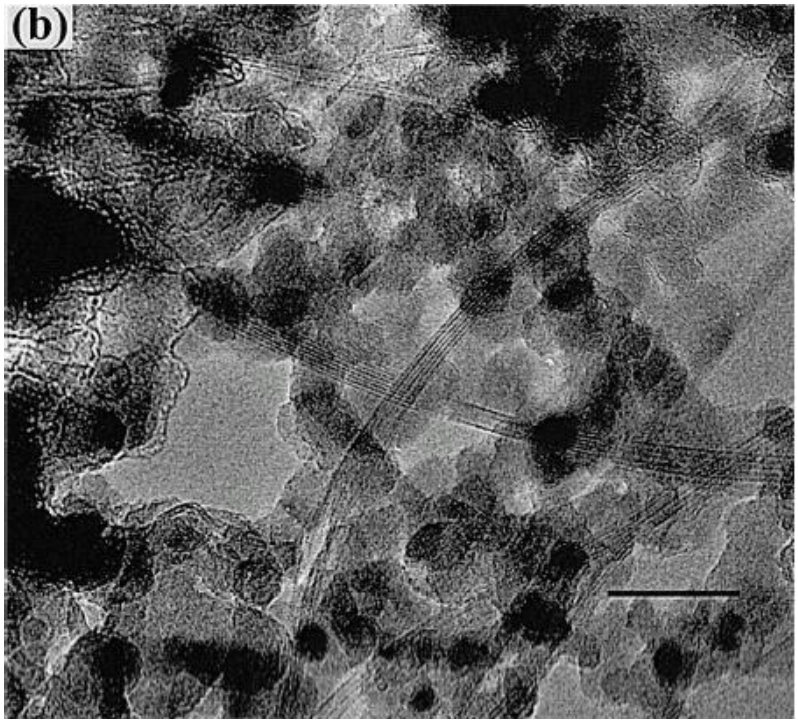

Figure 3.20 High resolution TEM micrograph of SWNT bundles synthesized on Fe_2O_3/silica catalyst exhibiting fringes of individual SWNTs in the bundles. Scale bar: 50 nm [29]

Xie *et al.* [30] synthesized aligned CNT using CVD on iron particles embedded in mesoporous silica as shown in Fig 3.21. The nanotubes are aligned perpendicular to the substrate surface and their orientation can be controlled by the pores from which they grow (Fig 3.22). Aligned arrays of tubes which are well graphitized are formed with spacing of about 100 nm between them and 50 μm long.

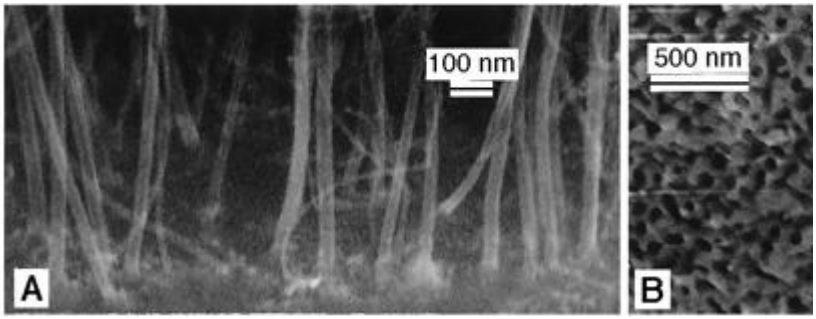

Figure 3.21 (a) SEM micrograph of an array of carbon nanotubes growing out of mesoporous iron/silica substrate (b) SEM micrograph of mesoporous iron/silica before deposition [30]

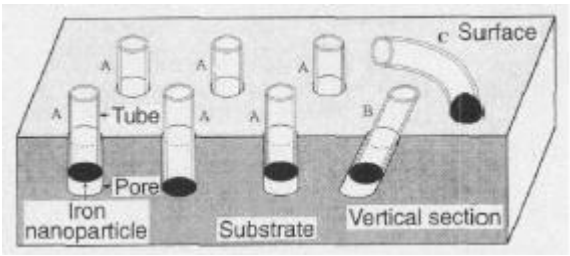

Figure 3.22 Possible growth models of carbon nanotubes formed on iron nanoparticles embedded in mesoporous silica [30]

Carbon nanotubes formed on iron nanoparticles embedded in vertical pores grow perpendicular to the substrate (marked A) and those from inclined pores were tilted along the axes (marked B) in Fig 3.22. Tubes from nanoparticles on the surface might grow freely (marked C).

3.17 Role of nitrogen

Kenny *et al.* [31] studied the growth behavior of carbon nanotubes as a function of catalyst layer thickness and amount of nitrogen. RF plasma enhanced CVD was used in this study with Ni as the catalyst material. With increase in nitrogen content (0% to 25%), a progressive transition from random to aligned CNTs is observed. No nanotube growth is observed when the catalyst film is thicker than 20 nm. Amorphous carbon is formed in the absence of nitrogen.

3.18 Temperature Dependence

Ducati *et al.* [32] synthesized randomly oriented and aligned carbon nanotubes by chemical vapor deposition at temperatures 550ºC, 700ºC, 850ºC. The diameter of the tubes and the degree of crystallization of the graphitic walls are determined by the temperature.

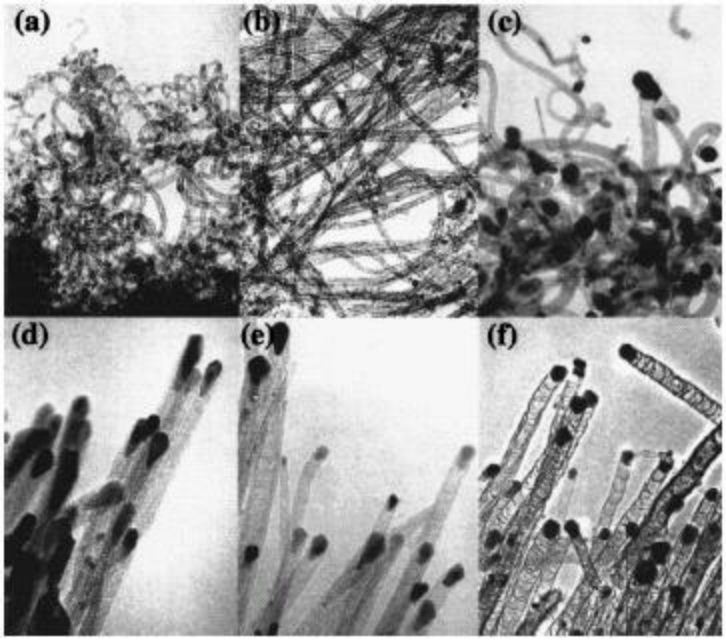

Figure 3.23 TEM micrographs of carbon nanotubes grown by thermal CVD (a-c) and dc PECVD (d-f). (a, d) at 550ºC; (b, e) at 700ºC; (c, f) at 800ºC. Scale 5mm corresponds to 50 nm in (a, d); 100 nm in (b, e); 200 nm in (c, f) [32]

With increase in temperature, the diameter of the tubes increased in both thermal CVD and PECVD techniques as shown in the Fig 3.23. For a given thickness of the initial catalyst layer it is possible to grow nanotube films of different morphology by simply varying the growth temperature.

Wang *et al.* [33] synthesized aligned carbon nanotubes on an iron tube coated with a Ni catalyst, at temperatures as low as 550ºC. The catalyst was electrodeposited onto the iron substrate and CH_4/H_2 mixture is used. Vertical aligned growth occurred due to the plasma effect. When plasma, which is the sole source of thermal energy, was not in contact with the substrate only randomly entangled CNTs are grown.

3.19 Significance of plasma heating

Meyyappan *et al.* [34] have characterized the effect of plasma on heating the growth substrate in a PECVD technique. They showed that plasma alone can be used to reach substrate temperatures as high as 700ºC and synthesized well-aligned carbon nanofibers without an external heater. The morphology of the nickel nanoclusters which form after the pretreatment, with or without external heating, is very similar. The alignment of the nanofibers in plasma heated process is due to the high sheath electric field resulting from the high direct current bias at the cathode where the substrate is placed. Addition of a heater provides a high level of process control and flexibility as the plasma can be varied independent of the substrate temperature.

3.20 Patterned growth

Meyyappan *et al.* [35] used an iron catalyst layer and aluminum under layer deposited by ion beam sputtering onto silicon wafers for the growth of nanotubes. Use of methane as the feedstock yielded SWNTs in a thermal CVD set up and MWNFs in an

inductively coupled plasma reactor when the feed stock is ethylene. A 400 mesh TEM grid is used as mask. The catalyst and underlayer are deposited through the holes of the grid. The composition of the multilayer is 20 nm Al/1 nm Fe/ 0.2 nm Mo. The growth temperature was 900ºC in thermal CVD which produced SWNT and 700-800ºC for PECVD which produced MWNFs.

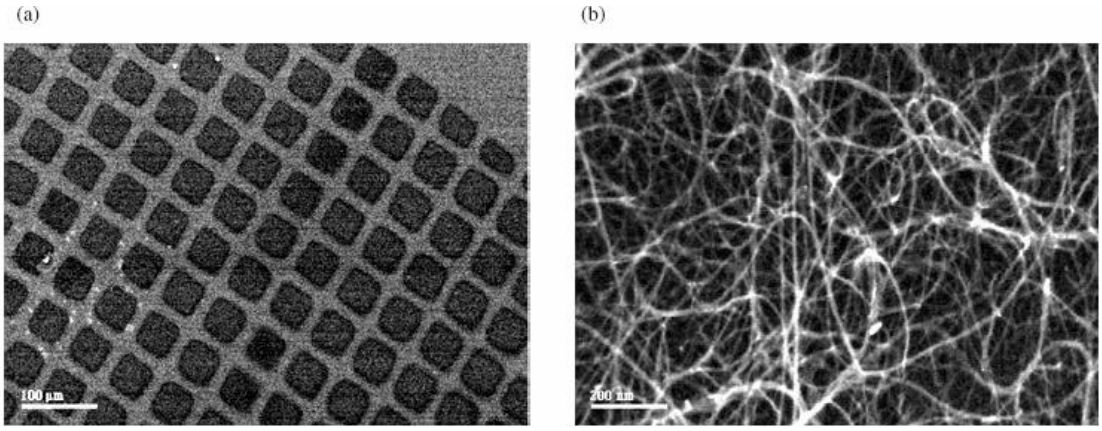

Figure 3.24 SEM micrograph of SWNT grown on patterned silicon surface. (a) Si surface masked with 400 mesh TEM grid and catalyst is deposited through the holes of the grid [35]

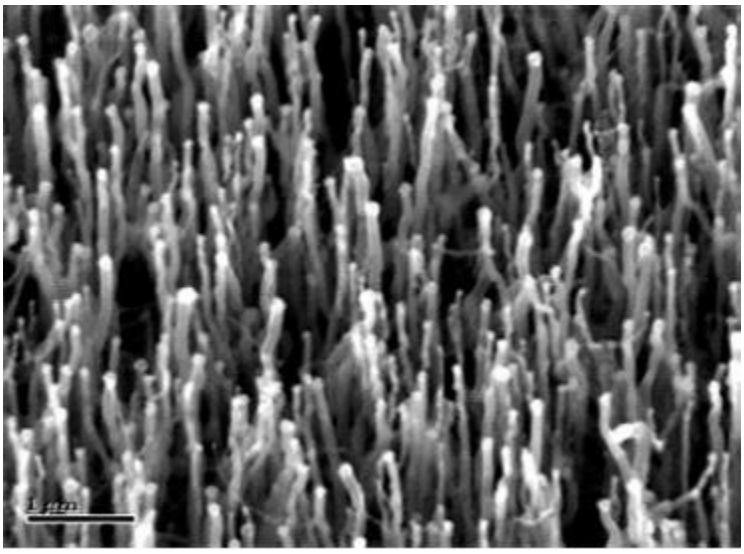

Figure 3.25 SEM micrograph of MWCNFs grown in ICP reactor [35]

It can be seen from Fig 3.24 that dense mat of SWNT ropes grow in the open area of the grids where catalyst is deposited. No nanotubes growth was observed in the regions which are covered by the grid. The MWCNFs grown by PECVD are well aligned (Fig 3.25) and can be used in the fabrication of electrodes and sensors.

3.21 SWNT by PECVD

Catalyst application-dip coat

Maruyama *et al.* [36] synthesized high quality SWNTs on silicon and quartz substrates employing a dip-coat approach. In this approach, the substrate is submerged partially into the catalyst solution (metallic acetate solution in this case) and then drawn up at a constant rate. The surface of the substrate dries rapidly as it is drawn from the solution. The substrate is heated to decompose the acetates or other organic residue. All the tubes formed are randomly oriented as shown in Fig 3.26. According to the authors this process is easy, versatile and economic.

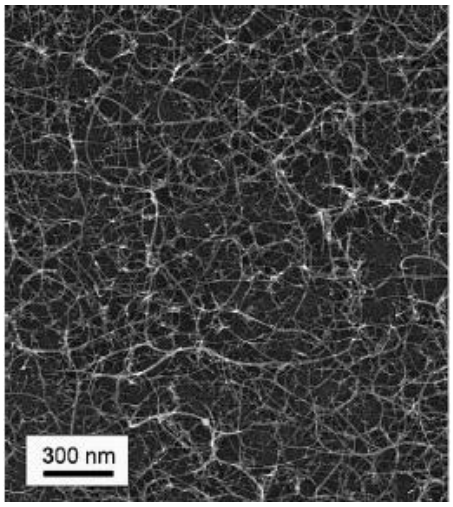

Figure 3.26 SWNTs synthesized by PECVD on silicon substrate [36]

Dai *et al.* [37] synthesized single walled nanotubes employing a PECVD technique at 600ºC. Nanotubes are grown on SiO_2/Si wafers or on holey-SiO_2 films supported on TEM grids. Two different types of catalyst were used. Discrete ferritin particles with an average of ~300 Fe atoms per ferritin are adsorbed randomly onto the substrate. The density of the ferritin particles, controlled by ferritin concentration and adsorption time was less than one monolayer. The other type of catalyst was ~1A° thick Fe film deposited by slow electron beam evaporation at a rate of 0.1A° for 3-12 sec. CH_4 and Ar are the source gases used and the deposition time was 3 minutes. Electrical characterization revealed that 90% of the nanotubes produced are semi-conducting. Laser ablation preferentially produces metallic SWNT (~70%) which shows that PECVD technique preferentially forms semi-conducting SWNTs when compared to other methods. Lower temperatures employed in this method have great potential such as enhancing the compatibility of CNT synthesis process with CMOS technology for hybrid electronic applications.

3.22 Importance of plasma

Yoo *et al.* [38] investigated the effect of growth parameters, such as plasma intensity, filament current and substrate temperature on the growth characteristics of MWNTs. They employed a hot filament plasma-enhanced CVD to grow vertically aligned MWNTs on nickel coated glass substrates at temperatures below 600ºC. They found that plasma intensity was the most critical parameter controlling the growth of MWNTs.

3.23 Methane/nitrogen-ammonia plasma

Wong *et al.* [39] used N_2 and NH_3 as carrier gases and CH_4 as the carbon source to grow well-aligned MWNTs by MPECVD technique. Electron beam deposition is used to deposit iron catalysts of different thickness 1, 2, and 5 nm on a silicon substrate. It is observed that the nanotube alignment degraded with increasing Fe film thickness which is shown in Fig 3.27. With increase in film thickness, the diameter of the tubes also increases. They obtained a MWNT as small as 6 nm in diameter with a 1 nm iron film.

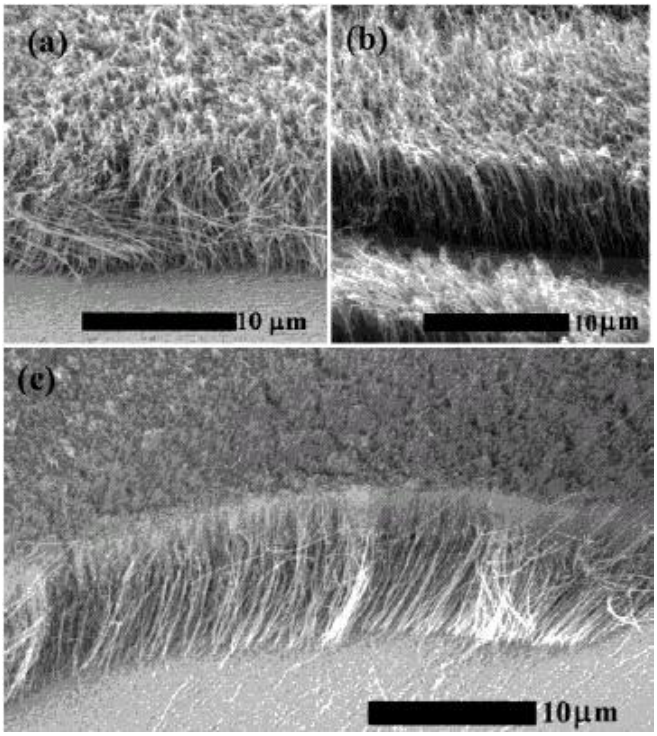

Figure 3.27 CNTs deposited on Fe film of varying thickness; (a) 5 nm (b) 2 nm (c) 1 nm. Note the degree of alignment reduces with increase in film thickness [39]

The presence of amorphous carbon suggests the possibility of H_2 incorporation in the nanotubes during growth. Pure nanotubes are grown by using N_2 in the absence of NH_3 and aligned carbon nanotubes are grown only by adding a small amount of NH_3 to the carrier gases.

3.24 Integration of CNFs into devices

Cassell *et al.* [40] studied the integration of CNFs into devices using high throughput methodology. A growth compatibility chip consisting of five different metal contact underlayers namely Cr, Ir, Ta, Ti, W and five catalysts from transition metals namely, Co, Fe, Ni, Fe/Ni, Ni/Co are employed to explore the growth pairings of these two layers. The underlayer materials are deposited in rows using an Ar ion-beam sputtering and a 0.5 mm X 15 mm shadow mask. The substrate is rotated 90º after the underlayer is deposited and subsequently, the catalysts are deposited to a total thickness of 20 nm. The schematic is given in Fig 3.28 (a).

The growth compatibility chip was then run for 10 min in a PECVD chamber. NH_3/C_2H_2 feedstock was used at temperatures below 600ºC. It was found that the Ni catalyst layer afforded the best growth for each underlayer material. Cr showed highest growth rate for all underlayer materials except when Fe is used. They suggested that Ni catalyst is more active at lower temperatures when using the above feedstock as compared to Fe.

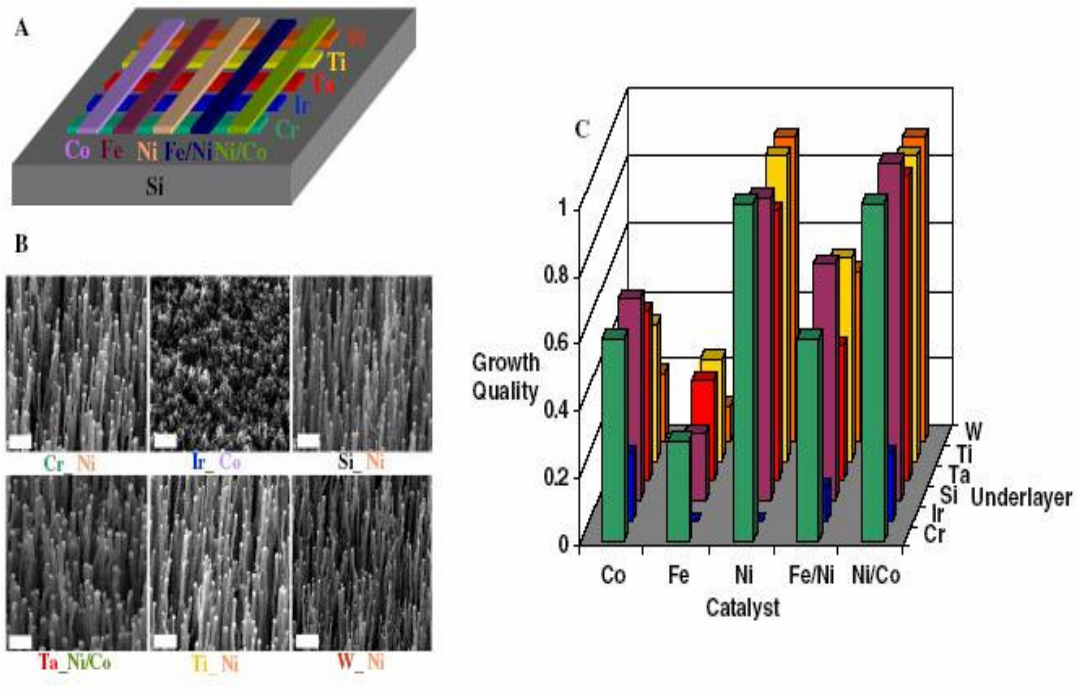

Figure 3.28 Underlayer/catalyst compatibility library for screening growth activity. (a) Five underlying metals (Cr, Ir, Ta, Ti, and W) that are sequentially deposited (40 nm) and rotated 90° before the catalyst layers were deposited on top of the underlayers. (b) catalyst/underlayer combinations that displayed the highest activity and growth quality for each of the candidate underlayer material. (c) Growth activity map for each of the catalyst/underlayer combinations [40]

3.25 Aligned tubes-PLD

Terrones *et al.* [41] synthesized aligned carbon nanotubes over thin films of cobalt catalyst patterned on silicon substrates using thermal CVD. Pulsed laser deposition technique was employed to deposit a thin film of catalyst. It is patterned by laser etching to create linear tracks of widths 1-20 µm and length ≤5 mm as shown in Fig 3.29. The nanotube bundles are closely aligned with the laser tracks, uniform in length (≤50 µm) and diameter (~30-50 nm) as shown in Fig 3.30. Laser etching generates tracks free of cobalt and leaves cobalt particles positioned evenly along the edges of the eroded tracks or stripes. This helps in the alignment of nanotube bundles along the tracks.

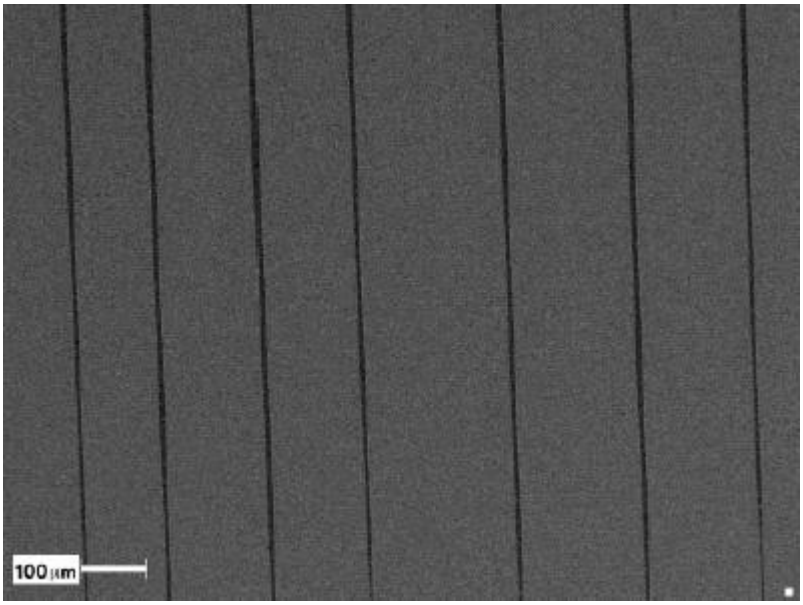

Figure 3.29 SEM micrograph showing uniform tracks etched by laser beam [41]

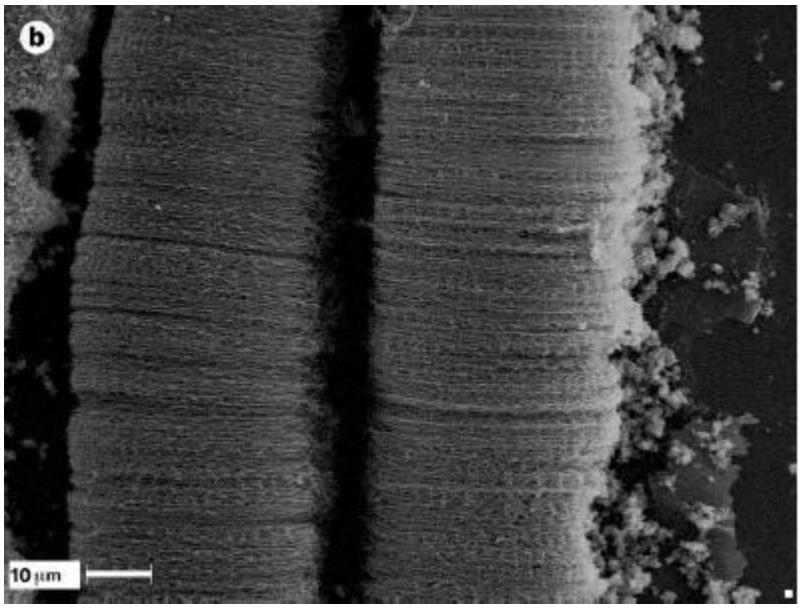

Figure 3.30 SEM micrograph of a bundle of aligned nanotubes [41]

Gupta *et al.* [7] synthesized single and double walled nanotubes using a thin film of Fe catalyst. They used two layers of 0.3 nm and 0.5 nm and found that with decrease in catalyst layer thickness, smaller catalyst particles are formed during pretreatment, which leads to hollow concentric tubes with fewer walls. C_2H_2 and NH_3 are used as the

precursor gases at 850ºC, and a pressure of 20 torr. The growth time was varied from 30-40 sec. Single and double walled CNTs are shown by the presence of well defined bands in the lower frequency region at ~187 and ~266 cm^{-1}, which correspond to the radial breathing modes obtained by μ-Raman spectroscopy. A tangential displacement mode associated with the stretching of the SWNTs in the high frequency region at ~1540, 1560 and 1593 cm^{-1} is also seen. A weak D band at ~1350 cm^{-1} arises due to disorder. The role of ammonia is to etch away amorphous carbon and prevent passivation of the catalyst.

3.26 Scanning probe microscopy

Diameter of a scanning probe determines the image resolution. So, CNT tips can offer high resolution due to their small radius and the length of the CNTs permits tracing of features with high aspect ratio [42]. CNT probes are robust because of their extraordinary strength and their ability to retain structural integrity after deformation. Because of the above mentioned reasons they are relatively hard and last longer than traditional silicon scanning probes.

CNTs in conjunction with AFM will be of immense help in imaging on a nanometer scale. In IC industry, as gate dielectric layers become thinner (on the order of several tens of angstroms), the imaging becomes difficult with conventional probes. In order to image non-conducting surfaces with SEM, they will be coated with a conducting layer which alters the surface morphology. AFM with nanotube tips can be helpful in such cases, and they can be operated in ambient environments.

A SWNT probe with its small diameter has greater resolution than MWNT probe. But the concentric cylinder structure is much stiffer than SWNT and they are much longer which can be exploited to image features with high aspect ratios.

3.26.1 Nanotubes for microscopy tips

Nyugen *et al.* [42] used SWNT and MWNTs as probes in AFM to image ultra thin films which are 2-5 nm thick. MWNTs are attached to the tips of silicon pyramids by applying electric filed between the cantilever and the nanotubes source whereas SWNT tip probe is fabricated on the cantilever itself.

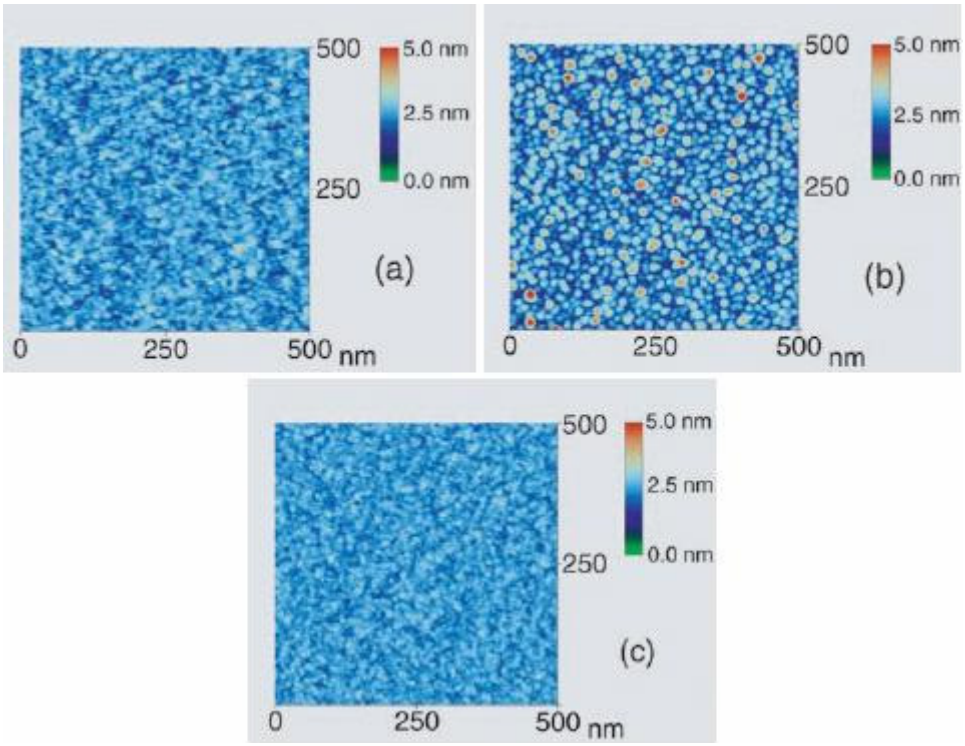

Figure 3.31 AFM images of thin films acquired with SWNT as probe tip. (a) Silicon nitride surface showing grains as small as 3 nm; (b) 2 nm gold film on mica showing grains ranging from 30 nm to less than 10 nm; (c) Iridium film on mica showing IR grain sizes about 2-3 nm [42]

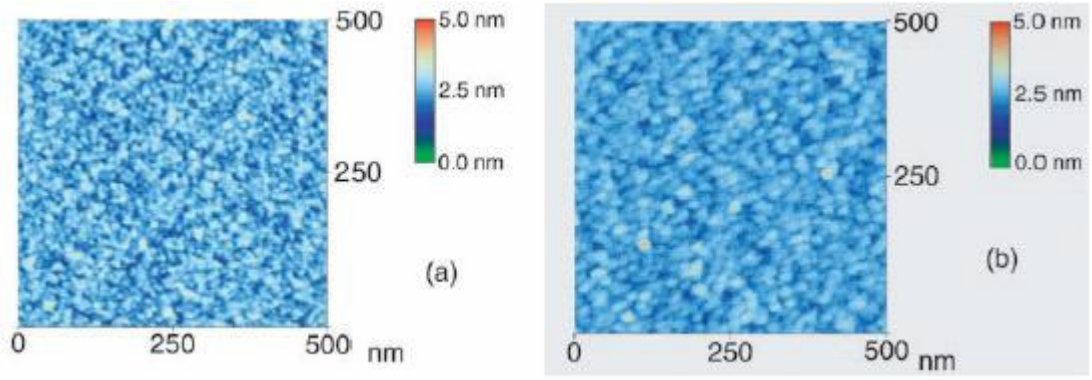

Figure 3.32 AFM image of a 2 nm thick silicon nitride film comparing MWNT probe and a commercial silicon probe; (a) after 15+h continuous scanning with MWNT tip and (b) after 12 h continuous scanning with regular silicon probe [42]

They showed that these tips have high lateral resolution and good stability as shown in Fig 3.31 where grain sizes from less than 10 nm to 30 nm have been imaged. From Fig 3.32 it can be seen that the MWNT probe showed no degradation after continuous scanning for 15 hrs and that SWNT is capable of lateral resolution as small as 2 nm.

Lieber *et al.* [44] developed a CVD technique to grow aligned carbon nanotube probe tips directly on the ends of silicon tips. Conventional silicon tips are flattened at its apex by contact AFM imaging and anodizing them in HF to create nanopores of 50-100 nm along the tip axis. Iron catalyst is electrodeposited into these pores and nanotubes are grown by employing C_2H_4 and H_2 as process gases at 750ºC for 10 min. MWNTs produced by this method have a diameter of 5-15 nm but is too long to be used as tips. They shortened them by an in situ AFM technique. Nanoprobes have been characterized using gold nanoparticles standards and the results showed that high resolution tips with end radii of 3-6 nm can be readily obtained. The probes can be used several times, and

when a tip fails, it is ultimately removed by oxidation and a new tip is grown by CVD. Even after 20 cycles they have observed no loss of yield or resolution.

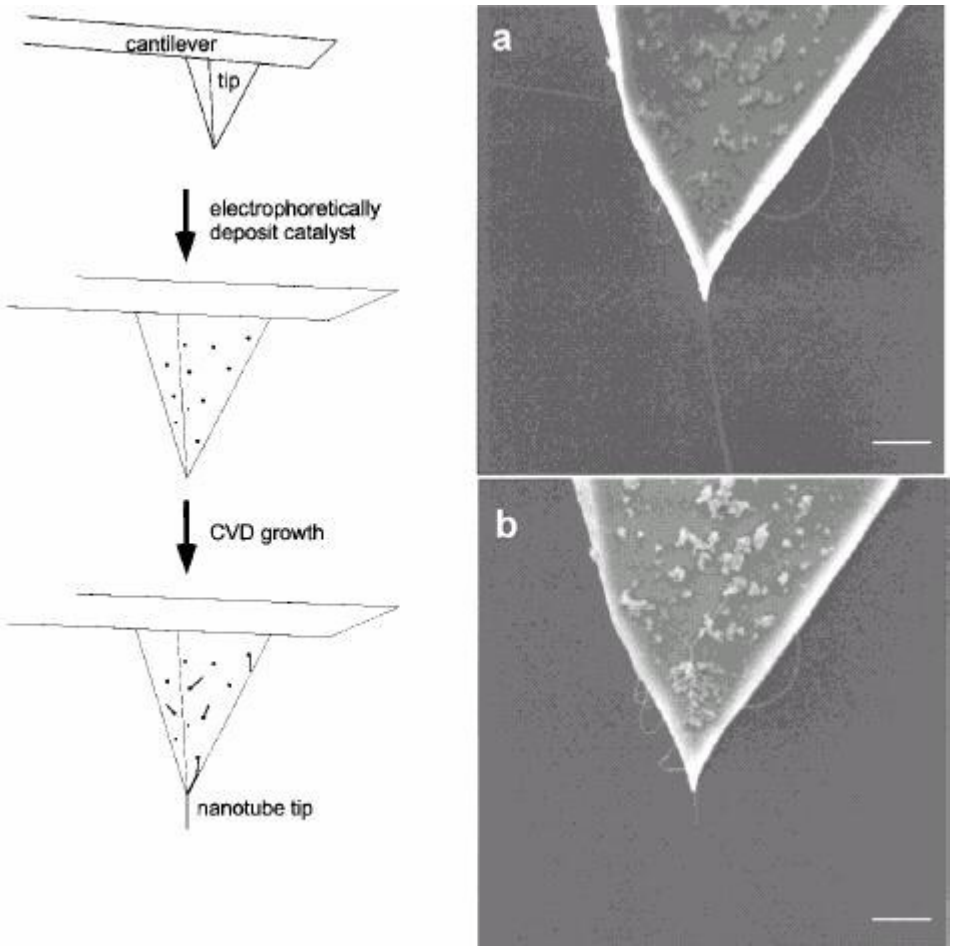

Figure 3.33 Left panel: Schematic of the approach used to prepare SWNT tips. Right panel: FE-SEM micrographs of a nanotubes probe grown on a silicon cantilever/tip assembly using CVD (a) before and (b) after shortening. Scale bar 500 nm [45]

The same group later synthesized aligned single-wall nanotubes for use as probes using CVD [45]. They eliminated the pore etching step and electrophoretically deposited Fe-Mo and colloidal Fe-oxide catalysts onto the pyramidal tip of the commercial cantilever

assembly. The schematic is shown in Fig 3.33. The left panel shows schematic of the process used to attach SWNT to the tip. The right panel shows the nanotube at the tip before and after shortening. They have observed that SWNTs and small diameter MWNTs preferentially grow along the surface and stay in contact rather than grow out from the surface when they encounter an edge. This is due to the attractive nanotube-surface interactions. The tips exhibit reversible buckling similar to mechanically attached SWNT nanotubes and CVD MWNT tips which demonstrates that they have structural quality and remain attached to the pyramids. Tubes with an effective tip radius of 3 nm or less can be obtained and the CVD process can be repeated 5-6 times to provide new tip without replacing the catalyst.

3.27 Gas ionization sensors

Ajayan *et al.* [43] developed miniaturized gas ionization sensors using carbon nanotubes. The sensor consists of an Al sheet which acts as a cathode and the anode is a film of MWNTs. They are separated by a glass insulator as shown in Fig 3.34. CVD technique is used to grow vertically aligned MWNTs on a SiO_2 substrate. The nanotubes are ~25-30 nm in diameter, ~30 μm long, and a spacing of 50 nm between the nanotubes. Because of their small tip radius MWNTs create very high nonlinear electric fields near their tips. This hastens the breakdown process of gases due to the formation of corona or conducting filament of highly ionized gases that surrounds the tips. Due to this, a powerful electron avalanche is formed that bridges the gap between the electrodes and allows a self-sustaining interelectrode discharge to be created at relatively low voltages. They have observed that due to this, the breakdown voltages are lowered several fold (from 960V to 346V for air) in comparison to traditional electrodes (aluminum in the

above cited case) enabling compact, battery-powered and safe operation of such sensors. For fixed interelectrode spacing, the breakdown voltage of each gas is unique which depends on the electric field and the discharge current provides a means to quantify the concentration of species being detected.

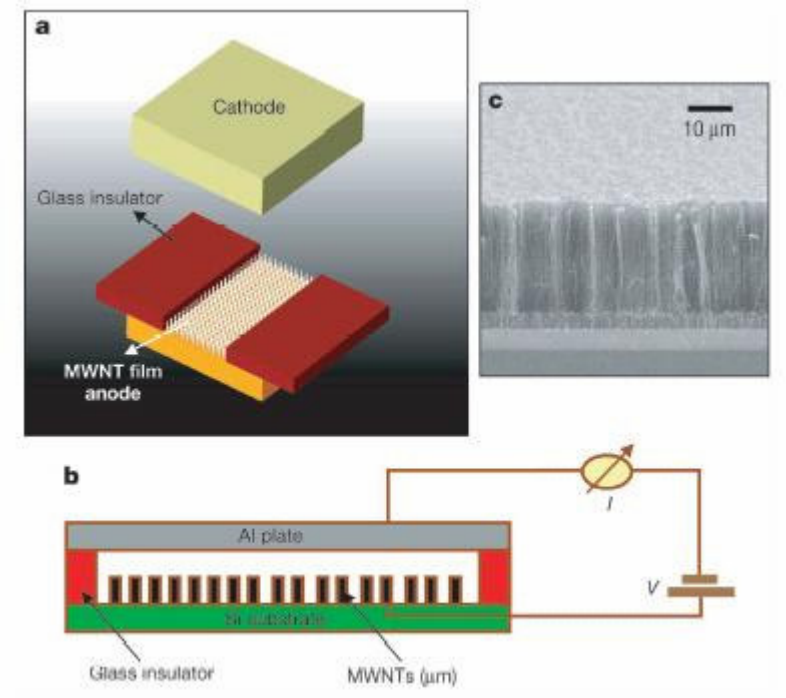

Figure 3.34 Nanotube sensor device (a) Exploded view of sensor showing MWNT film as the anode, 180-µm thick glass insulator plates, and Al as cathode; (b) diagram of the actual set-up; (c) SEM micrograph of vertically aligned MWNT film used as the anode [43]

CHAPTER 4

PROBLEM STATEMENT

Synthesis of carbon nanotubes for commercial applications can be realized only when they can be produced on a large scale, efficiently, economically and with minimum defects. Though high purity nanotubes can be synthesized by laser ablation, the process cannot be scaled up easily. Arc-discharge can be used to produce nanotubes on a large scale but the purity is low. Chemical vapor deposition techniques provide a viable alternative because of the low temperature involved and low cost of the apparatus as compared to the other two methods. They are also promising because of the ability to control the nanotube growth and amenable to scale-up.

Plasma-enhanced microwave CVD is a simple and inexpensive technique to grow carbon nanotubes and has great implications for the microelectronics industry because of the ability to grow complex structures from smaller building blocks. In order to realize this immense potential, a thorough understanding of the growth process using MPECVD is needed. This will help in obtaining a better control of the growth process of carbon nanotubes, reduce defects and optimize the process parameters.

The aim of the present investigation is to optimize the process parameters for the synthesis of carbon nanotubes, the objective would be to obtain well aligned, uniform geometry CNTs. To be specific, it is desired:

- To synthesize aligned carbon nanotubes on silicon wafer and achieve growth at selective locations and
- Identify the process parameters and study their effect on carbon nanotube growth.

The following are important parameters of MPECVD for carbon nanotube synthesis:

- Duration of deposition
- Thickness of the catalyst
- Pretreatment time
- Concentration of carbon source gas
- Pressure
- Temperature

Some of the above parameters are varied in the present investigation to optimize the process parameters for carbon nanotube synthesis on a silicon wafer.

CHAPTER 5

EXPERIMENTAL SETUP AND TEST METHODOLOGY

In the current investigation carbon nanotubes are synthesized using microwave plasma enhanced CVD. An ASTEX S-1500, 1.5 KW microwave power generator operating at 2.5 GHz is employed for this purpose. A ball of plasma is generated on the substrate surface by microwave energy coupled to a symmetric plasma coupler. The chamber consists of a cylindrical stainless steel that houses the substrate assembly. The set up also consists of mass flow meters, control valves and stainless steel tubing for transporting gases to the reaction chamber and controlling their flow. The chamber pressure is measured and controlled by a pressure transducer and pressure controller, respectively. A mechanical pump is used to evacuate the chamber and maintain it in the desired pressure range.

5.1 EXPERIMENTAL SETUP

5.1.1 Description of the reaction chamber

The chamber consists of a substrate stage and a motorized drive, such that the stage can be moved up and down thereby varying the proximity of the plasma with the substrate as shown in Fig 5.1. The substrate stage also consists of resistive heater which is capable of reaching 1200°C. A graphite susceptor sits on top of the heater assembly. The substrate is loaded onto this graphite susceptor. The chamber has two sapphire view ports to observe the progress of the deposition and measure the temperature. The

substrate temperature is measured by a Williamson dual-wave length optical pyrometer. The chamber is provided with a door to load and unload the samples. The picture of the chamber is shown in Fig 5.2.

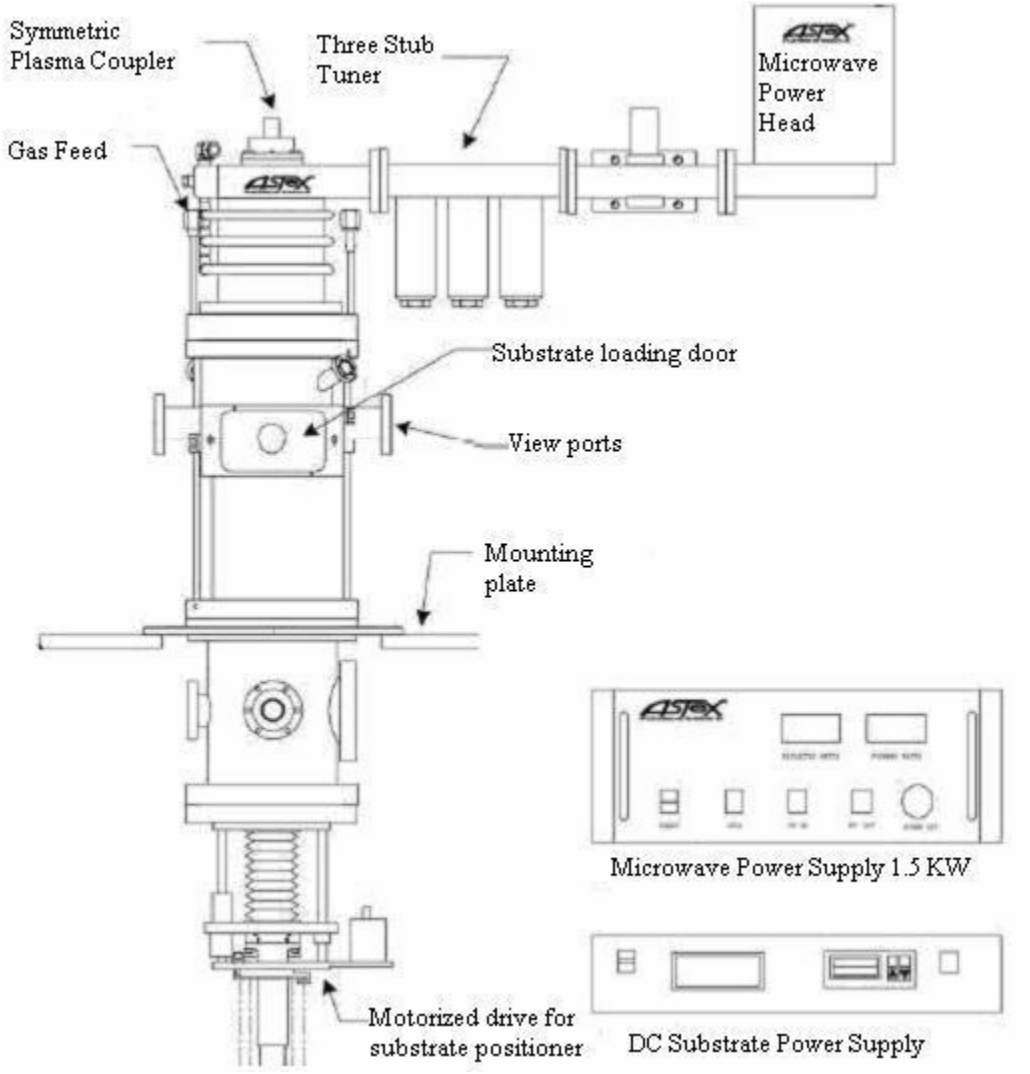

Figure 5.1 Schematic of the CVD chamber.

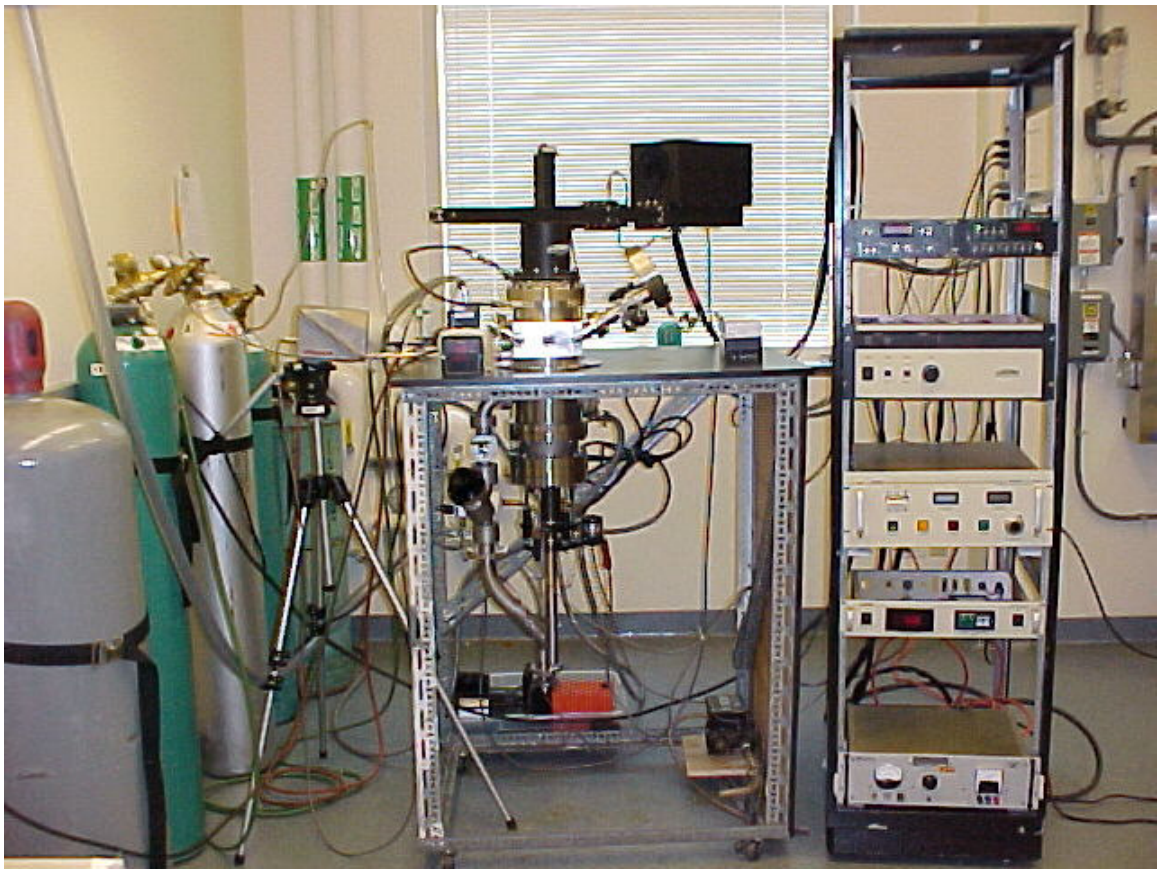

Figure 5.2 Picture of the MPECVD chamber.

5.1.2 Description of gas flow and controls

The gas flow system consists of mass flow controllers (MKS Type 1159B), mechanical valves, a Baratron pressure transducer (MKS Type 127), pressure controller (MKS Type 250), mass flow meters (MKS Type 247C), and stainless steel tubing. The chamber is connected to an Alcatel mechanical pump which can take the chamber to 10^{-2} torr. The gases are introduced into the chamber through an inlet port. High purity grade CH_4, H_2 and N_2 are used as the process gases in the present investigation. The gases flow downstream past the substrate surface and are pumped out by the mechanical pump. The flow between the pump and the chamber is controlled by a throttle valve. When the valve is closed, the pressure inside the chamber is maintained by the actions of a solenoid

actuated butterfly valve, a pressure transducer and the pressure control units. In this way, the chamber can be maintained at the desired pressure. Mass flow controllers monitor and control the flow rate of the gases.

5.1.3 Description of PLD chamber

In the present set of investigation, both and n and p-type silicon wafers were used as substrates. Iron is used as the catalyst. It is deposited on silicon wafers using a pulsed laser deposition technique (PLD). An excimer laser was used for this purpose. This instrument consists of a short-pulse (FWHM = 25 ns) KrF (λ = 248 nm) Lambda Physik COMPex205 excimer laser. The following specifications of the laser are used [47]: wavelength: 248 nm, maximum pulse energy: 650 mJ, maximum average power: 30 W, maximum pulse repetition rate: 10 Hz, nominal pulse duration: 25 ns, orientation of the laser beam: horizontal, and type of homogenizer: dual axis.

The PLD system consists of an excimer laser, cylindrical stainless steel chamber, motor systems for rotating the target, control unit and a turbo molecular pump working in conjunction with a mechanical pump. The target is mounted on a multiple target carousel which can be rotated. The substrate to be coated is mounted on a supporting block and placed opposite to the target on a resistive heater. The laser strikes the target at an inclined angle and ablates the material generating a plume which is then deposited on the substrate. The deposition is performed under a vacuum of 10^{-2} torr. The target rotation is controlled externally by a CPU. Fig 5.3 shows a schematic of the PLD set up and the picture is given in Fig 5.4.

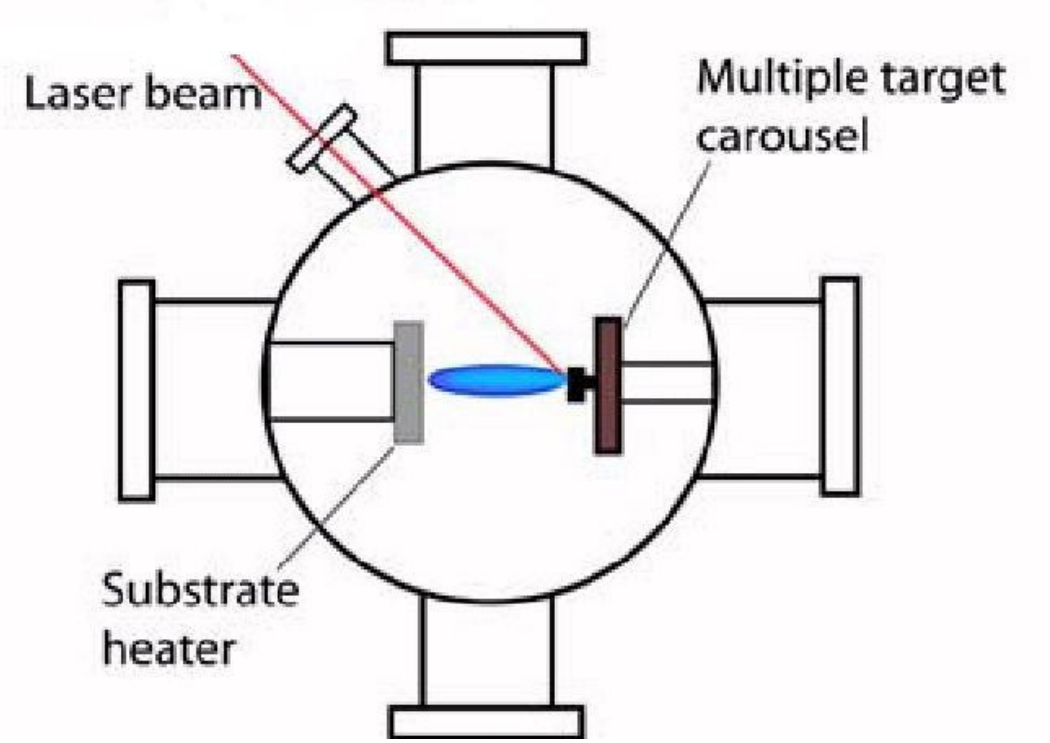

Figure 5.3 Schematic of the PLD set up.

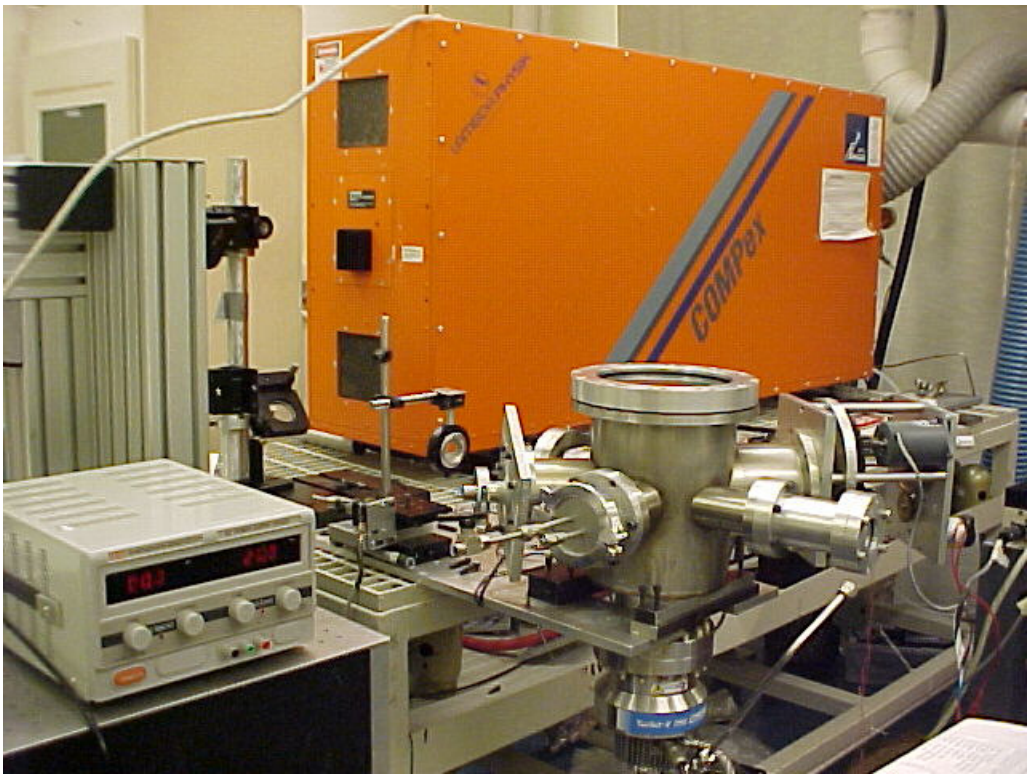

Figure 5.4 Picture of the PLD set up showing excimer laser and the chamber.

5.2 METHODOLOGY

Silicon wafers are cut into pieces of 2.5 cm X 2.5 cm and ultrasonicated in acetone for 5-15 min to remove any organic films on the surface and present a clean face. Iron is used as the metal catalyst and it is coated on the substrate using the PLD technique. The iron target is 99.995% pure. It is 1" in diameter and 0.25" thick (supplied by Kurt J. Lesker company). The substrate is loaded in the chamber and the laser is turned on. The beam hits the rotating target generating a plume. The target is rotated to avoid the laser hitting the same spot again and the whole target rotor assembly moves back and forth in the axial direction to cover the entire substrate surface. The deposition of the catalyst takes place for the desired amount of time. After deposition, the vacuum is turned off and the chamber is slowly brought back to atmospheric pressure. This sample is removed from the PLD apparatus and transferred onto the CVD chamber in air for further experimentation.

The substrate is now placed on the graphite susceptor and loaded into the CVD chamber. The substrate is kept at 10~12 mm below the window base and the chamber is pumped down to 10^{-2} torr. After reaching the desired pressure, H_2 gas is admitted into the chamber and the pressure is increased to 11 torr. After the chamber pressure is stabilized, plasma is initiated by turning the microwave generator on and the power is increased to 500 W. A plasma ball forms on top of the substrate surface and N_2 is allowed into the chamber while the pressure is increased to 15 Torr. The substrate is subjected to plasma pretreatment for the desired amount of time and then CH_4 flow is begun. At the end of experimentation plasma power is turned off after stopping the flow of CH_4 and H_2. The substrate is allowed to cool in an atmosphere of N_2 for 5 min before the vacuum pump is

turned off. The chamber is slowly vented and the substrate is taken out and subjected to further analysis using SEM, TEM, AFM and μ-Raman techniques. The temperature of the substrate is measured using the optical pyrometer by viewing it through the sapphire view port.

5.3 Characterization techniques

Scanning electron microscopy (SEM), Scanning transmission electron microscopy (STEM), Atomic force microscopy (AFM) and μ-Raman spectroscopy are used to study the morphology and elemental composition of the nanotubes.

5.3.1 Scanning electron microscopy (SEM)

A JEOL JSM-6400 SEM is used for viewing the nanotubes produced by CVD. The SEM with an accelerating voltage from 0.2 to 40 KV has a resolution of 3.5 nm at 8 mm working distance. Magnifications from 10X to 300,000X can be achieved and the sample can be tilted -5º to 90°.

5.3.2 Scanning transmission electron microscopy (STEM)

JEOL 100 CX II STEM is used in the present investigation to study the structure of the nanotubes. The operating voltage is from 20 to 100 KV and can be increased in steps of 20. The resolution is 0.2 nm. Magnifications from 100X to 850,000X can be achieved.

5.3.3 Atomic force microscopy (AFM)

AFM is used to map the surface of the nanotubes. A Dimension 3100^{TM} Digital scanning probe microscope is used in the present investigation. The instrument operates in tapping mode to map the surface profile of the nanotube.

5.3.4 μ-Raman spectroscopy

A SPEX 500 M double monochromator equipped with a Lexel 95 Argon ion laser is used to record Raman spectra. The laser power can be varied from 50 mw to 2 W. The non-lasing plasma is filtered by a 1450 tunable excitation filter through which the 5145 nm argon laser line passes. An Olympus BH-2 microscope is used to focus the incident laser beam on the sample. The beam splitter in the microscope reflects part of the laser radiation towards the objective and simultaneously allows Raman radiation collected by the same objective to pass through and enter the spectrometer. A CCD detector is used to collect the scattered light in 180° back scattered geometry. The CCD detector is cooled to 140 K by liquid nitrogen.

CHAPTER 6

RESULTS

Experiments were conducted to study the critical process parameters which effect the carbon nanotube growth. These experiments were part of a collaborative study on carbon nanotube synthesis by various catalysts and were conducted along with two other members of the group namely, Ramakrishnan [48] and Raghavan [49]. Growth time, pretreatment time, flow rate of feed gas are identified as some of the critical parameters and their effect is studied.

6.1 Effect of methane

In order to study the effect of methane on the carbon nanotube growth, experiments were conducted at four flow rates 10, 15, 20, and 30 sccm. Rest of the process parameters and sample names are given in Table 6.1.1.

Table 6.1.1 Process parameters used in the study of effect of methane

Growth time, min	10
Pressure, Torr	15
PLD time, sec	30
Pretreatment time, min	5
Microwave power, watts	500
Substrate temperature, ºC	750-950

Table 6.1.2 Sample identification for various flow rates

Sample name	Methane flow rate, sccm
Fe-8-8	10
Fe-8-7	15
Fe-8-4	20
Fe-8-9	30

Carbon nanotubes are not formed at a methane flow rate of 10 sccm. When the flow rate was increased to 15 sccm nanotubes are observed. Figure 6.1.1 is a representative sample of the growth showing long and straight nanotubes initiated at the bottom and with terminating clusters at the top. The nanotube film has been scratched to examine the alignment of the nanotubes. Fig 6.1.2 is a higher magnification micrograph of the long tubes found in Fig 6.1.1. It can be observed that the tubes are randomly oriented. They tend to align along the direction of scratch. This can be thought of as a bushy growth where the tubes are long and straight and are not entangled. When this bush growth is plowed they all try to align in that direction.

When the flow rate is increased to 20 sccm, there is a marked improvement in the alignment of nanotubes. They are oriented perpendicular to the surface of the substrate as shown in Figure 6.1.3.

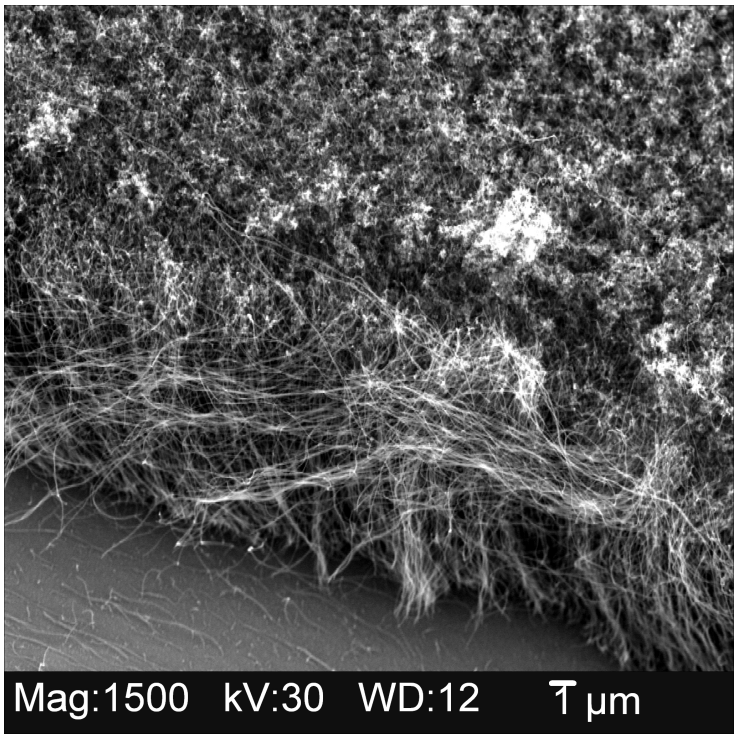

Figure 6.1.1 SEM micrograph showing nanotubes initiating at the bottom and with terminating clusters on top

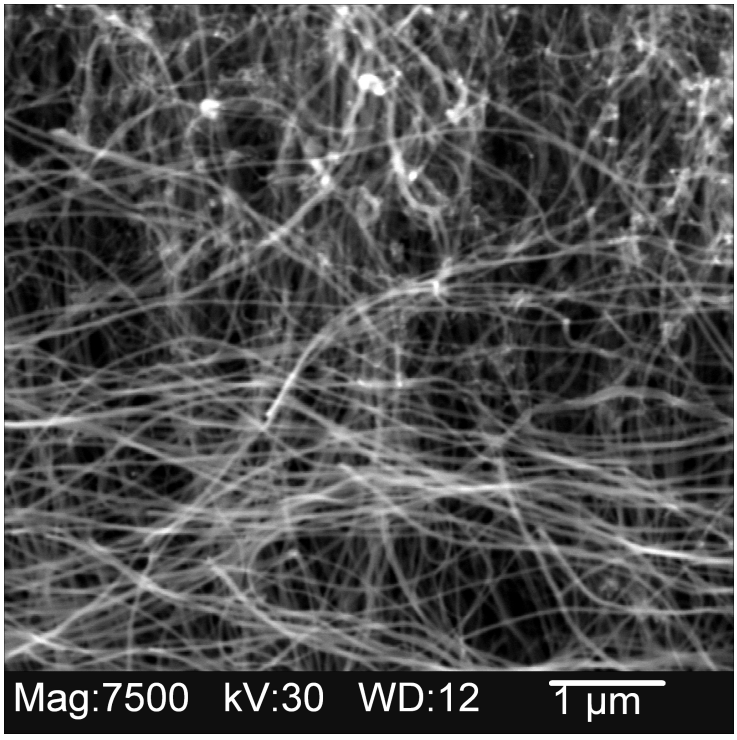

Figure 6.1.2 High magnification SEM micrograph of Fig 6.1.1 showing long and straight nanotubes

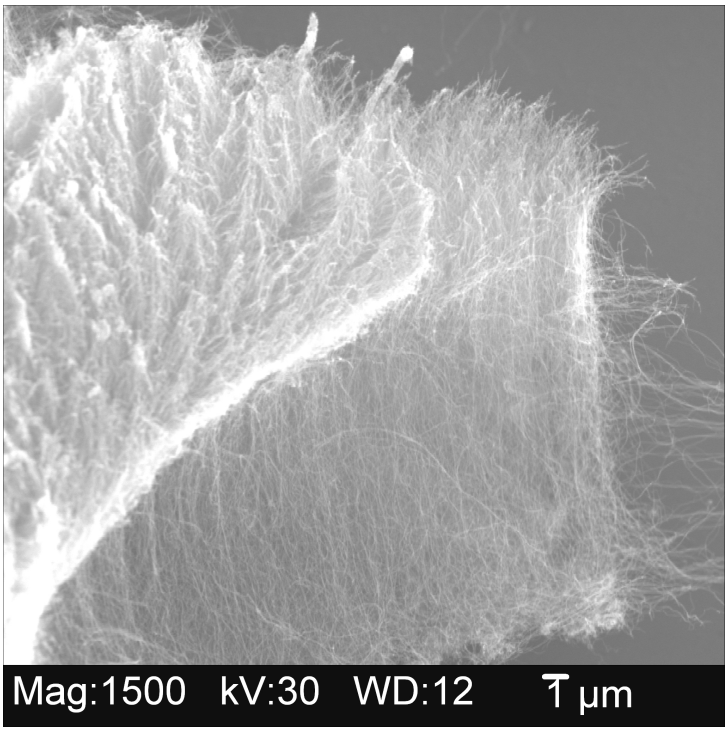

Figure 6.1.3 SEM micrograph showing vertically aligned nanotubes

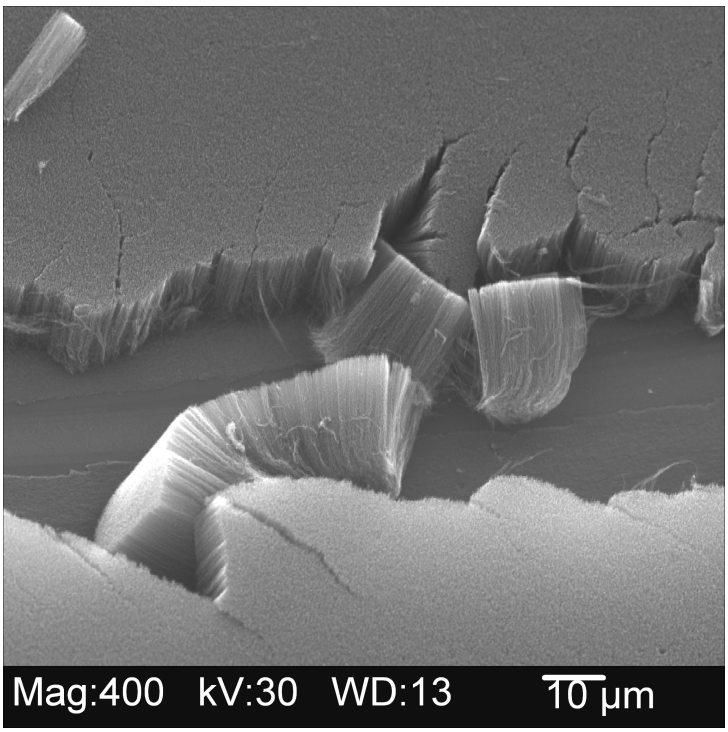

Figure 6.1.4 SEM micrograph showing broken nanotube film revealing alignment of CNTs

At 30 sccm of methane flow rate, the degree of alignment of the nanotubes is still improved as shown in Figs. 6.1.4 and 6.1.5. It can be observed that the nanotube film when scratched breaks and gives rise to pieces which clearly show aligned nanotubes. Fig 6.1.5 shows one such piece containing aligned nanotubes. The other significant change as compared to previous samples is the density of the nanotubes. It is clear that the nucleation density of the nanotubes is very high and the nanotubes are very closely packed to one another.

The deposition on the sample when viewed with a naked eye consisted of one dark annular ring surrounding an inner grey region with central portion containing scant growth or deposition. SEM micrographs revealed that both the dark and grey regions consisted of nanotubes and the central scant deposited area consisted of amorphous carbon as shown in Fig 6.1.6. The inner grey region has terminating clusters on top of the nanotubes as shown in Fig 6.1.7 which are not predominant in the outer dark region.

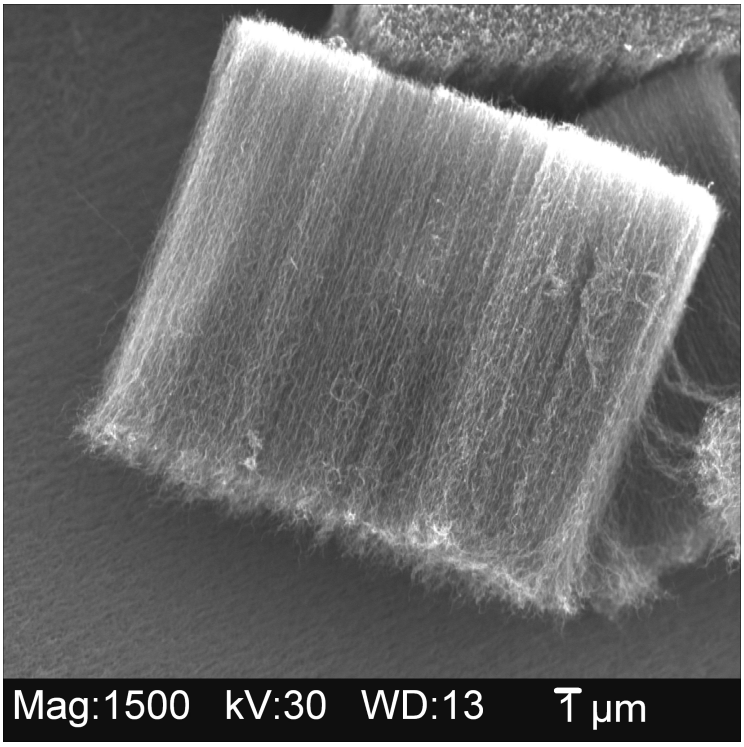

Figure 6.1.5 SEM micrograph of a broken piece showing aligned nanotubes

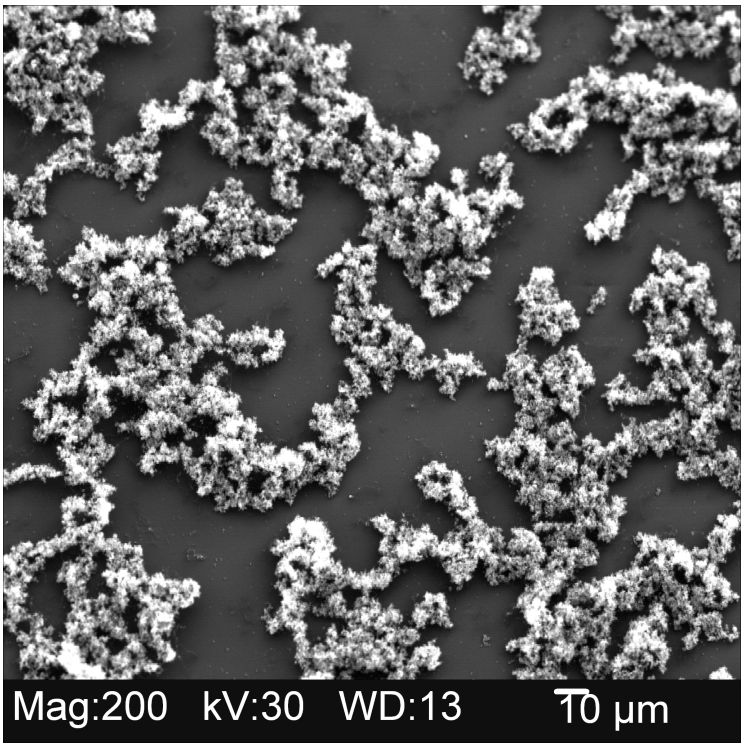

Figure 6.1.6 SEM micrograph of amorphous carbon found in the central region

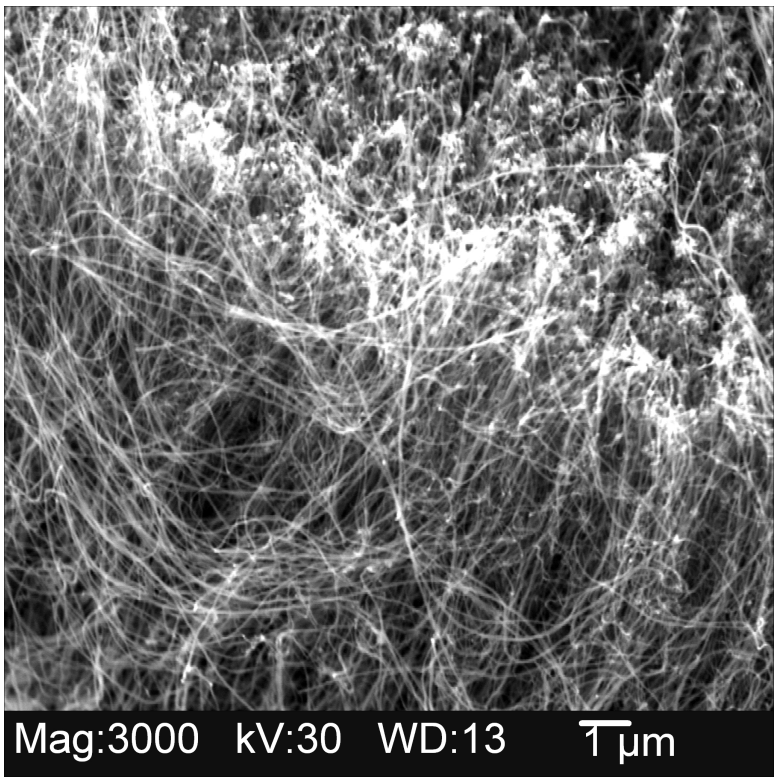

Figure 6.1.7 Terminating clusters on top of the nanotubes found in the grey region

6.2 Effect of pretreatment time

Experiments were conducted at pretreatment times of 0, 3, 5, and 10 min. The remaining process parameters are given in Table 6.2.1. When the sample was subjected to 10 min of pretreatment time, a reasonable amount of black deposition is found on the silicon substrate. Almost the entire region of the substrate with catalyst deposition is covered with the black deposit. Two distinct regions are observed. The outer region is pitch black in color and the inner region grey in color. SEM observation revealed that both contain carbon nanotubes. A scratch mark is made in each one of these regions to get an insight into the alignment.

Table 6.2.1 Process parameters used in the study of effect of pretreatment time

Growth time, min	5
PLD time, sec	30
Substrate temperature, °C	680-880
Chamber pressure, torr	15
Microwave power, watts	500
Flow rates of $H_2/N_2/CH_4$, sccm	40/50/15

Table 6.2.2 Sample identification and the corresponding pretreatment times

Sample name	Pretreatment time, min
Fe-9-4	10
Fe-9-1	5
Fe-9-3	3
Fe-9-5	0

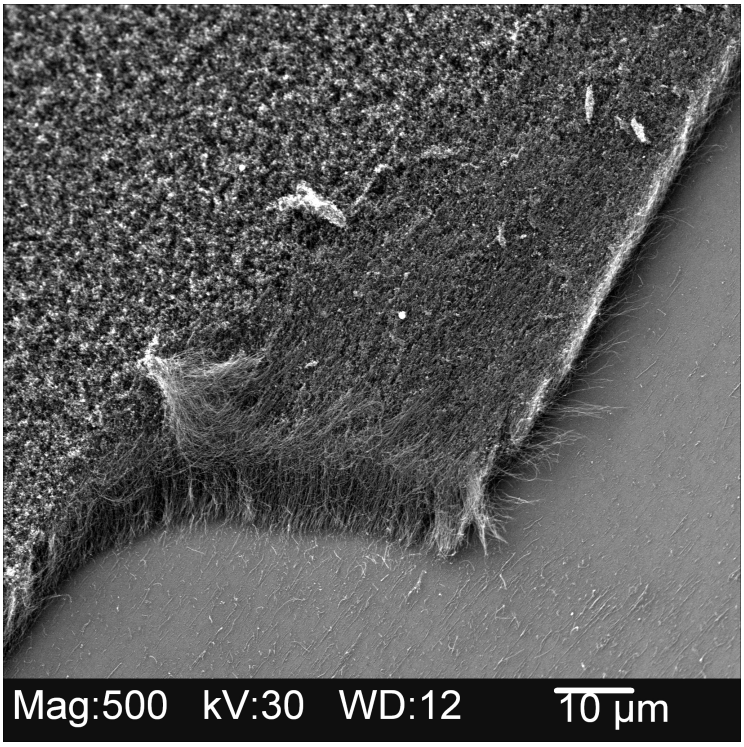

Figure 6.2.1 SEM micrograph of nanotubes aligned along the scratch in the inner grey region

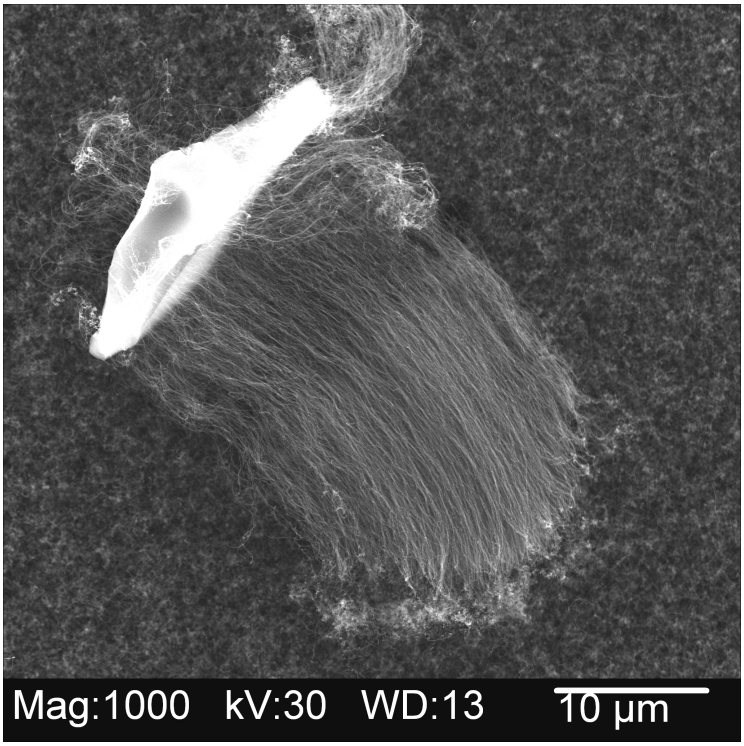

Figure 6.2.2 SEM micrograph of aligned nanotubes from a broken piece of film

Figure 6.2.1 shows aligned nanotubes along the inner grey region and Fig 6.2.2 shows long straight nanotubes from a broken piece of film. They are very uniform and straight over 10 µm long. Figure 6.2.3 shows aligned nanotubes along the scratch mark made in the outer dark region. It can be observed that the tubes tend to bundle along the scratch boundary compared to the inner grey region.

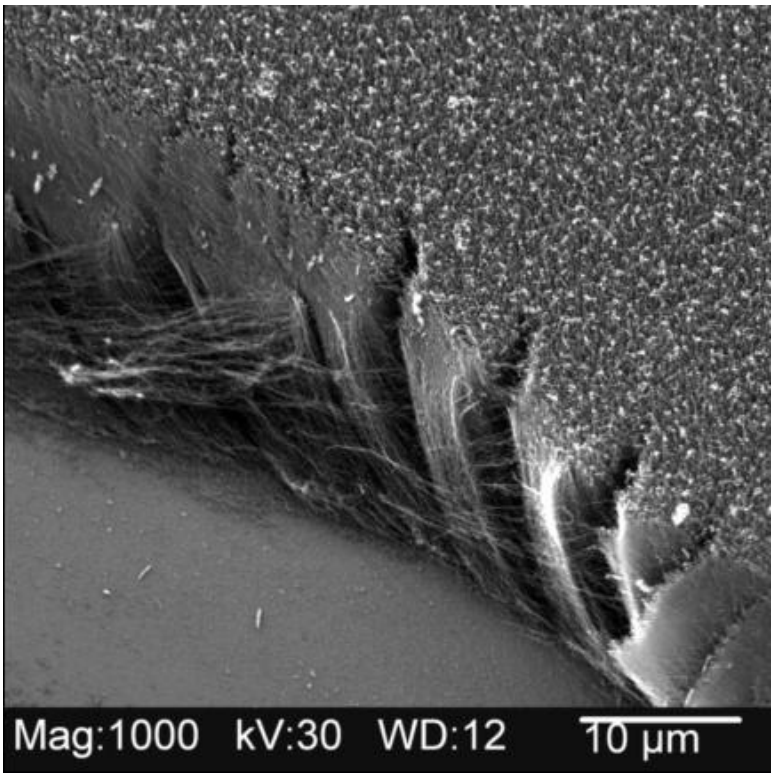

Figure 6.2.3 SEM micrograph showing bundles of aligned nanotubes along the scratch in the outer dark region

For 5 min of pretreatment time, the tubes are vertically aligned as shown in Figs. 6.2.4 and 6.2.5. Figure 6.2.4 is very similar to Fig 6.2.3 where the nanotubes are bundled. This was also taken from the outer darker region. Figure 6.2.5 shows the pile up of materials at the end of the scratch. Higher magnification micrograph (Fig 6.2.6) revealed them to be nanotubes which are well aligned, uniform in diameter and are over 10 µm long.

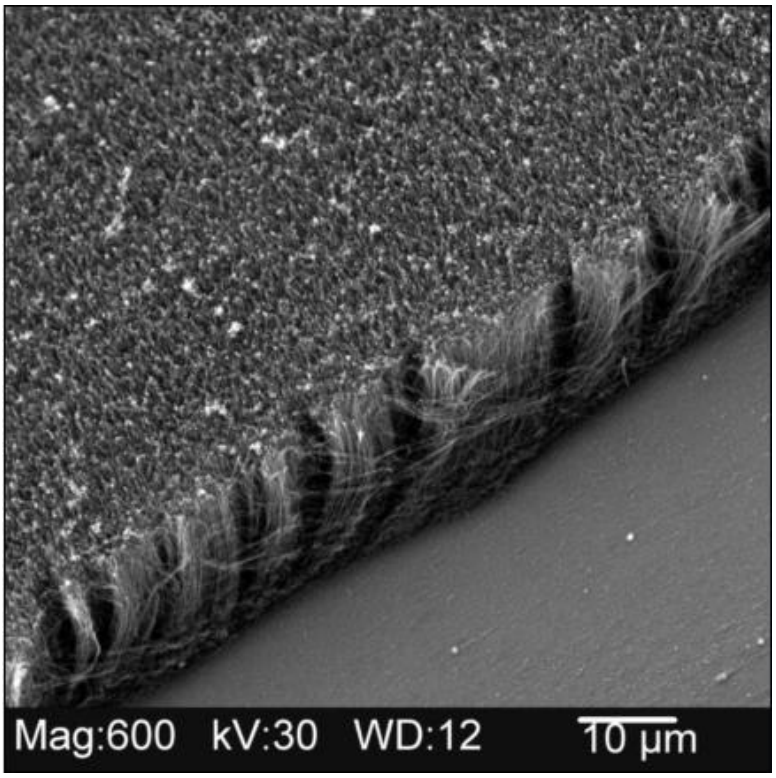

Figure 6.2.4 SEM micrograph along the scratch revealing alignment

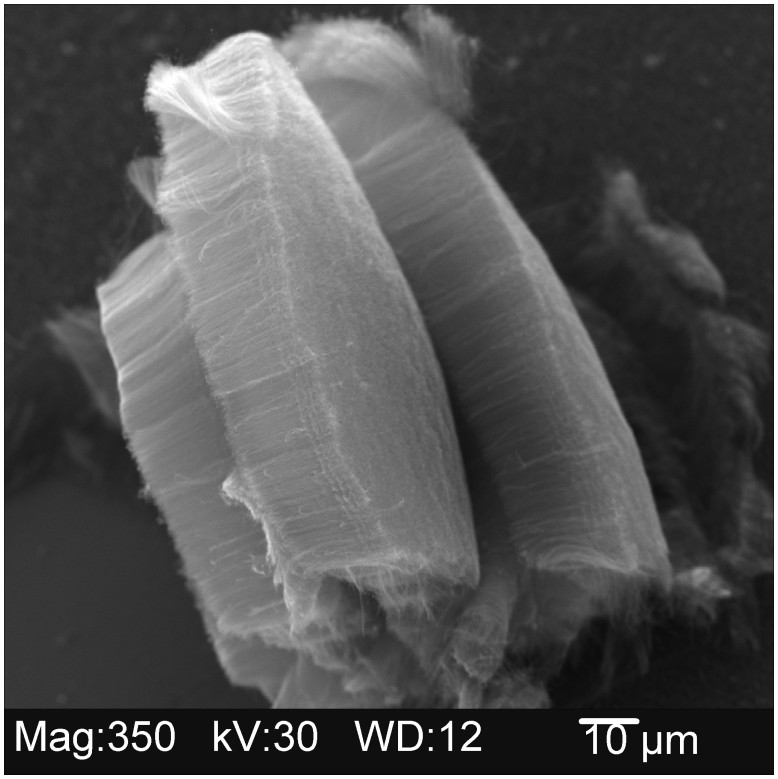

Figure 6.2.5 SEM micrograph of the piled up material at the end of a scratch

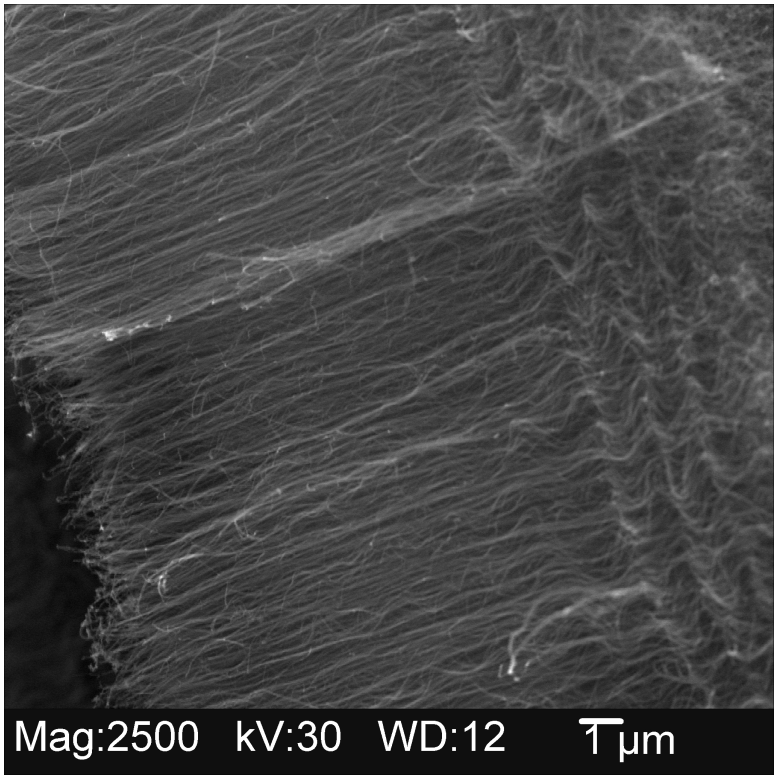

Figure 6.2.6 High magnification SEM micrograph of the pile up showing ropes of nanotubes over 10 µm long

It is observed that for 5 min of pretreatment time, the inner grey region does not completely encompass the catalyst coated region in the center. For 3 min of plasma pretreatment, the dark region on the outer periphery is predominant and the inner grey region is hardly seen. Figs. 6.2.7 and 6.2.8 are micrographs of nanotubes taken from the outer and inner regions, respectively. The tubes are well oriented as in the previous cases. The inner region has some amorphous carbon along with the nanotubes. When the substrate is directly subjected to growth without any pretreatment, nanotube growth is still observed, as shown in Fig 6.2.9, and the entire catalyst coated region has uniform deposition. Growth of nanotubes without pretreatment is possible when the size of catalyst particles deposited is very small. From Fig 6.2.9, it is clear that they are also aligned but not are well defined and closely packed as shown in Fig 6.2.10.

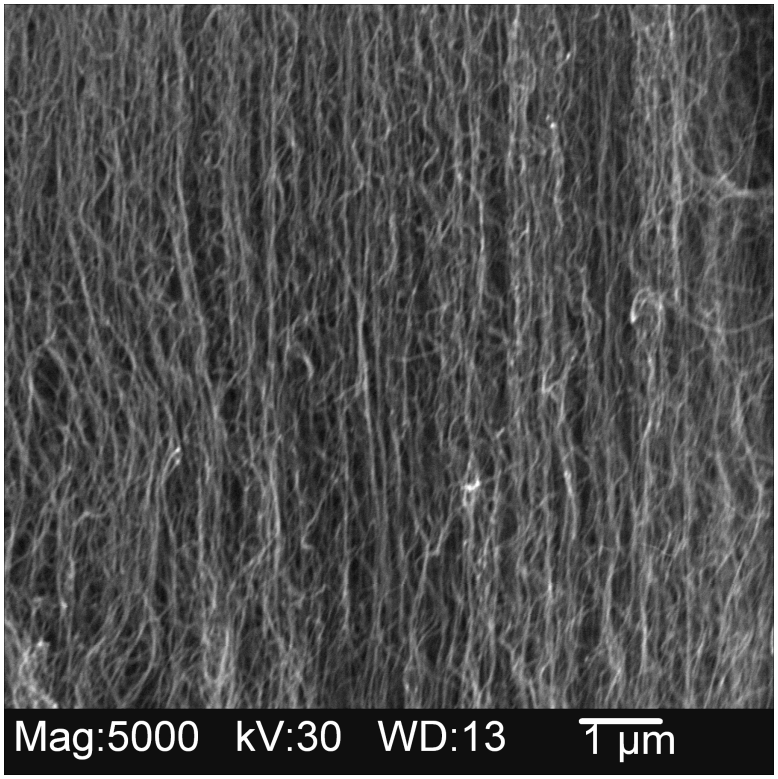

Figure 6.2.7 SEM micrograph of nanotubes grown in the outer dark region

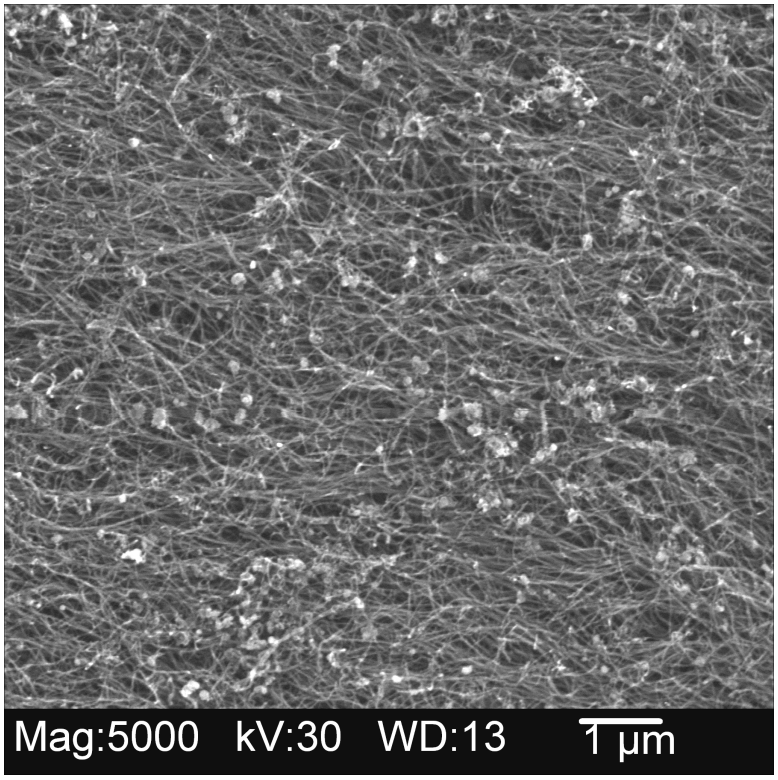

Figure 6.2.8 Nanotubes along with amorphous carbon from the inner grey region

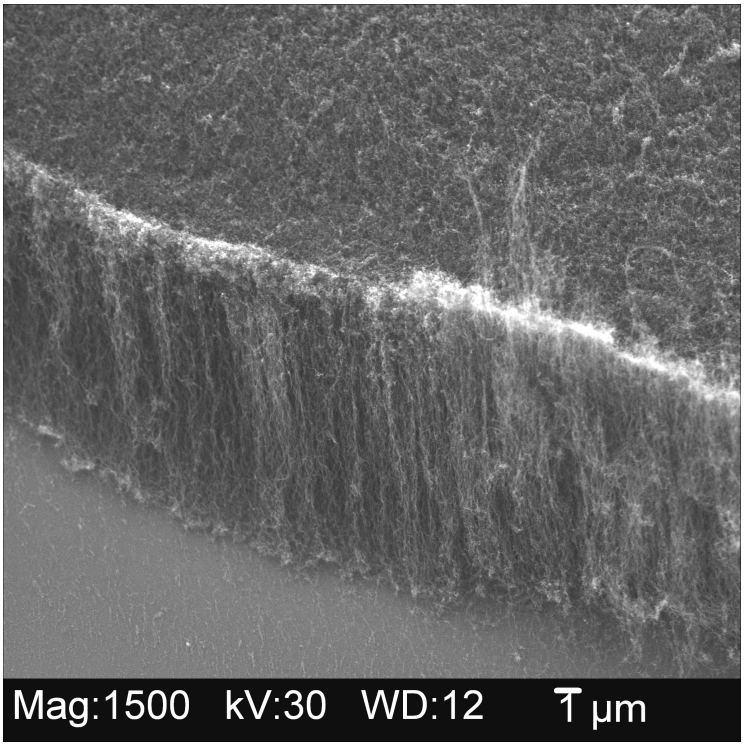

Figure 6.2.9 SEM micrograph showing vertically aligned nanotubes along the scratch

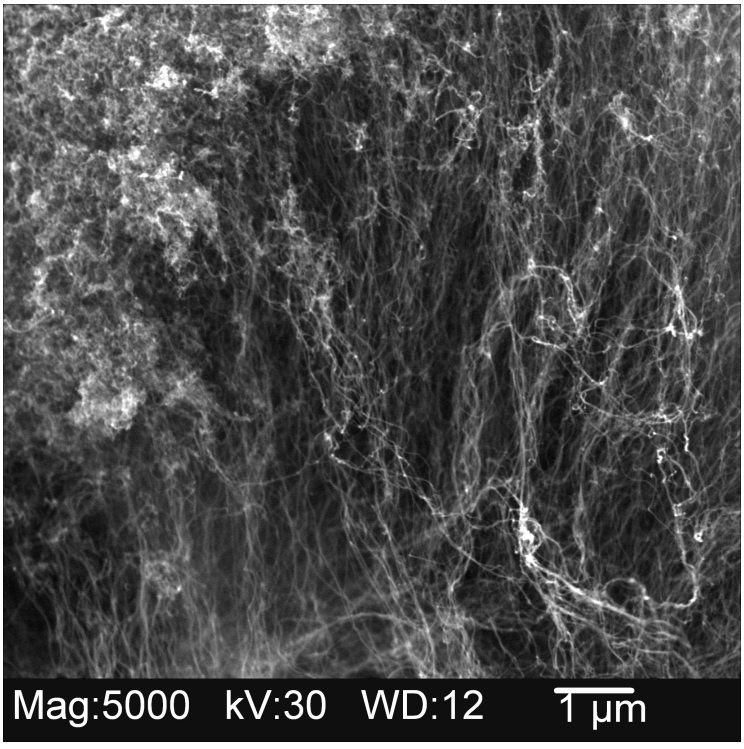

Figure 6.2.10 SEM micrograph of nanotubes which are not closely packed

6.3 Effect of growth time

The growth time has been varied at three different flow rates 10, 15, and 20 sccm and their effect studied. All the samples have iron catalyst coated for 30 sec using PLD.

Table 6.3.1 Methane flow rates and the corresponding growth times

Sample name	Methane flow rate, sccm	Growth time, min
Fe-8-2	10	15
Fe-8-3	10	10
Fe-8-4	20	10
Fe-A-2	20	5
Fe-8-7	15	10
Fe-T-1	15	10
Fe-9-1	15	5

Table 6.3.2 Process parameters employed to study effect of growth time

Pretreatment time, min	5
Flow rates of H_2/N_2, sccm	40/50
Chamber pressure, torr	15
Microwave power, watts	500
Temperature, ℃	750-900

Good amount of deposition is observed for 15 min of growth time at a methane flow rate of 10 sccm. From Fig. 6.3.1 it is clear that the nanotubes are randomly oriented, tangled and coiled. A scratch mark is made to investigate any sort of alignment, if

present. Figure 6.3.2 shows the nanotubes along the scratch boundary with amorphous carbon on top of the nanotubes. Figure 6.3.3 is higher magnification of the nanotubes shown in Fig 6.3.2. It is clear that they are straight over several micrometers long and are uniform in diameter. The tubes are ~10 µm long. No nanotube growth is observed when the duration is reduced to 10 min. The surface of the substrate after CVD growth is shown in Fig 6.3.4.

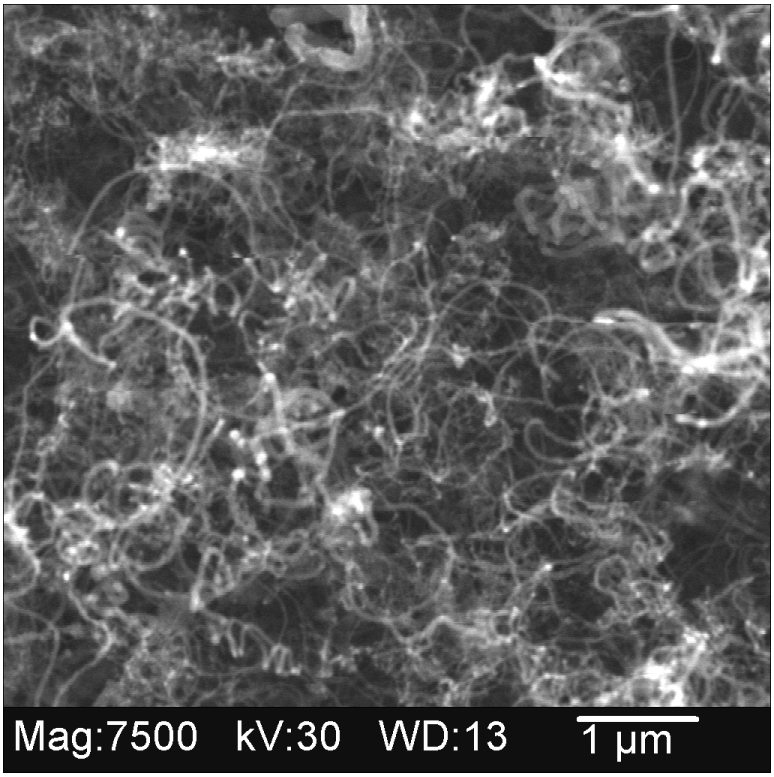

Figure 6.3.1 SEM micrograph showing randomly oriented, coiled, and tangled carbon nanotubes tubes as viewed from top

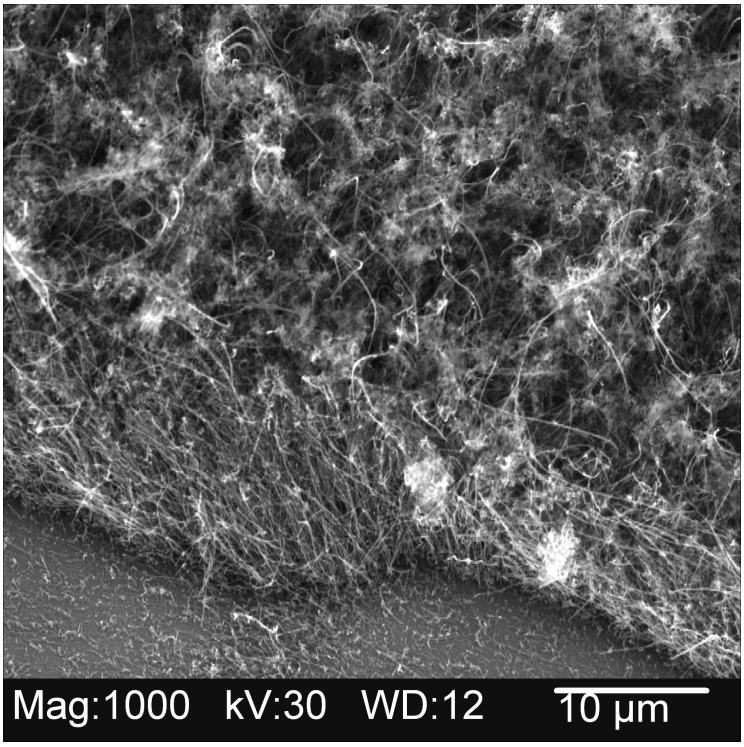

Figure 6.3.2 SEM micrograph of nanotubes along the scratch boundary with amorphous carbon on top

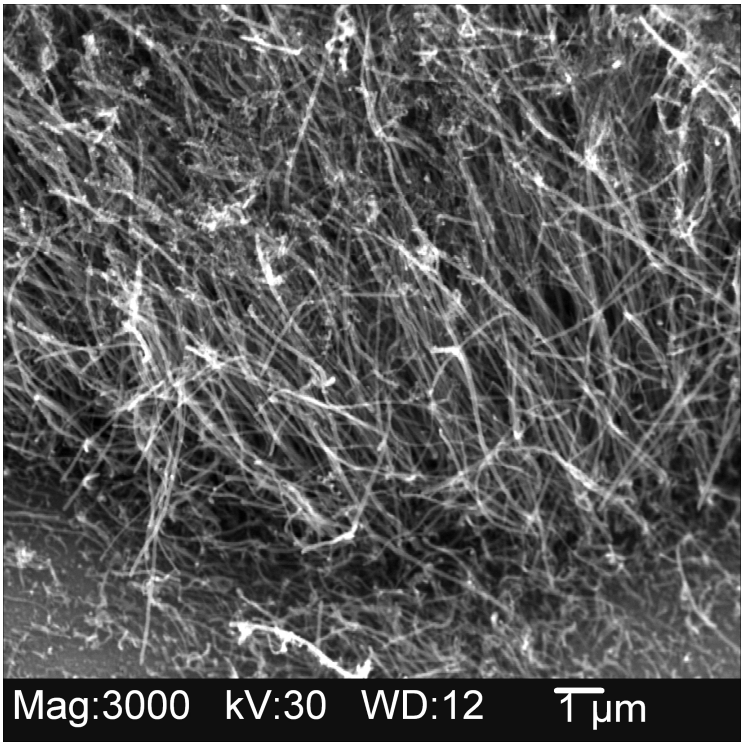

Figure 6.3.3 SEM micrograph showing long and straight carbon nanotubes

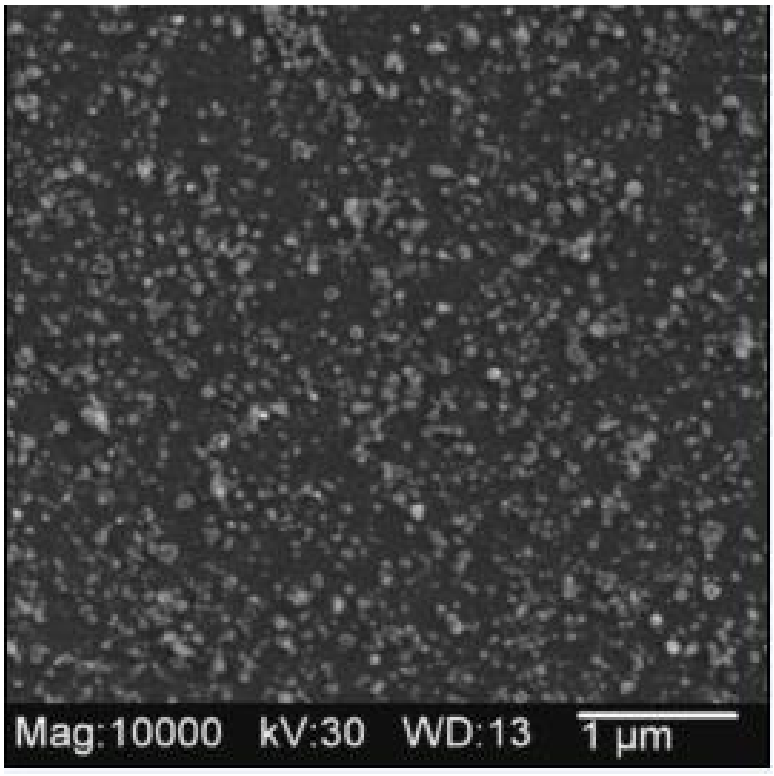

Figure 6.3.4 SEM micrograph of the substrate surface after 10 min of CVD showing no nanotube growth

As no deposition was observed for 10 min at 10 sccm of methane, the flow rate was increased to 20 sccm and the experiment was performed for 10 minutes. Figure 6.3.5 shows that the tubes are vertically oriented and no amorphous carbon deposition is seen on top.

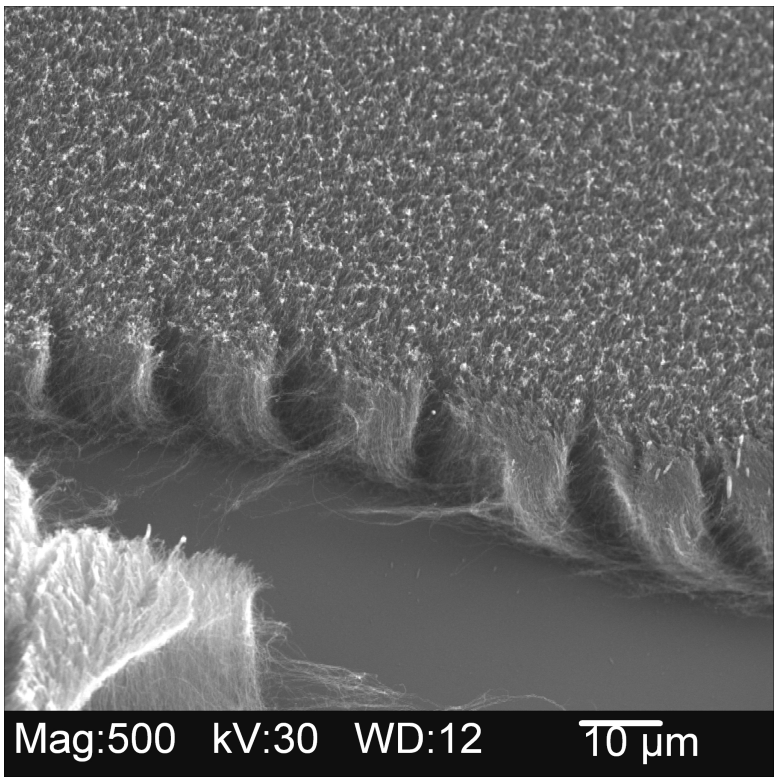

Figure 6.3.5 Aligned nanotubes on silicon substrate

Fig 6.3.6 shows another area where the nanotubes are clearly aligned perpendicular to the substrate surface. It can be seen from Fig 6.3.7 that ropes of nanotubes are formed. The nanotubes are ~20 µm long.

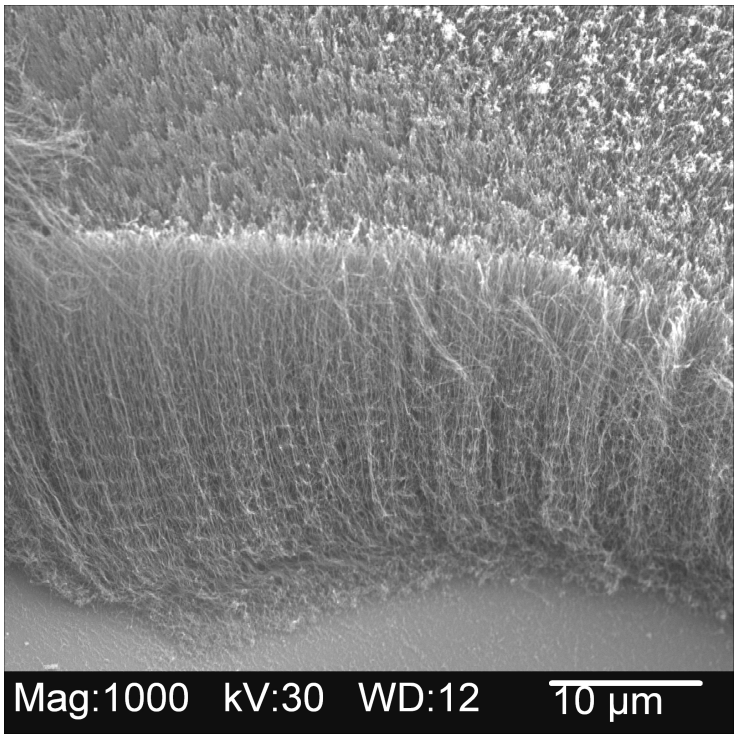

Figure 6.3.6 SEM micrograph of vertically aligned nanotubes revealed by scratching part of the deposit

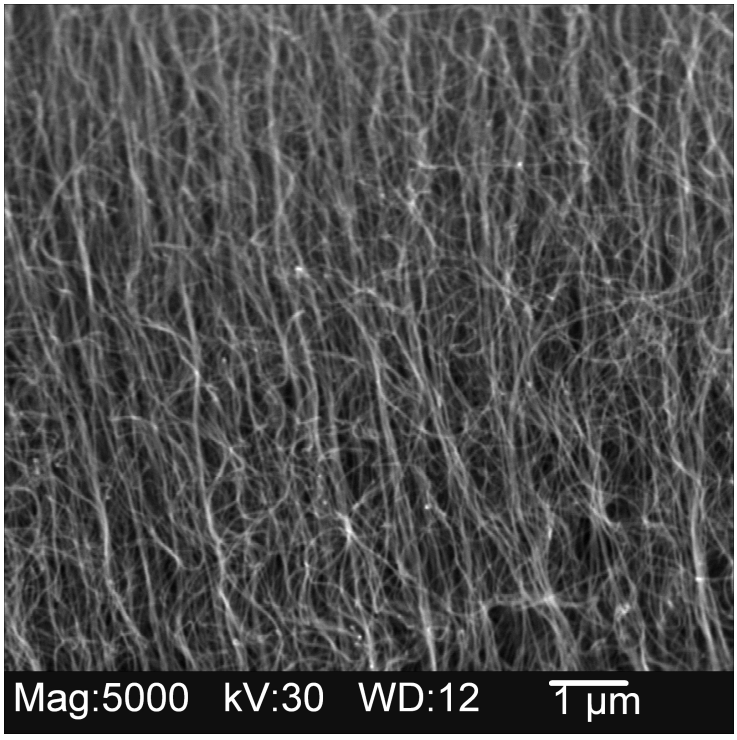

Figure 6.3.7 SEM micrograph of ropes of nanotubes grown for 10 min at 20 sccm of methane

When the growth time was reduced to 5 min, nanotubes oriented perpendicular to the substrate surface are observed, but they are of reduced length (< 10 µm). Well defined and aligned nanotubes are obtained as shown in Figs. 6.3.8 and 6.3.9. It can be seen that the deposition is very dense and the nanotubes are closely packed. There is a marked difference in the degree of alignment when compared to samples grown with 10 sccm (Fig. 6.3.1 to Fig. 6.3.3) and 20 sccm of methane (Fig 6.3.5 and Fig 6.3.6). The tubes are only 5 µm long owing to the short growth period.

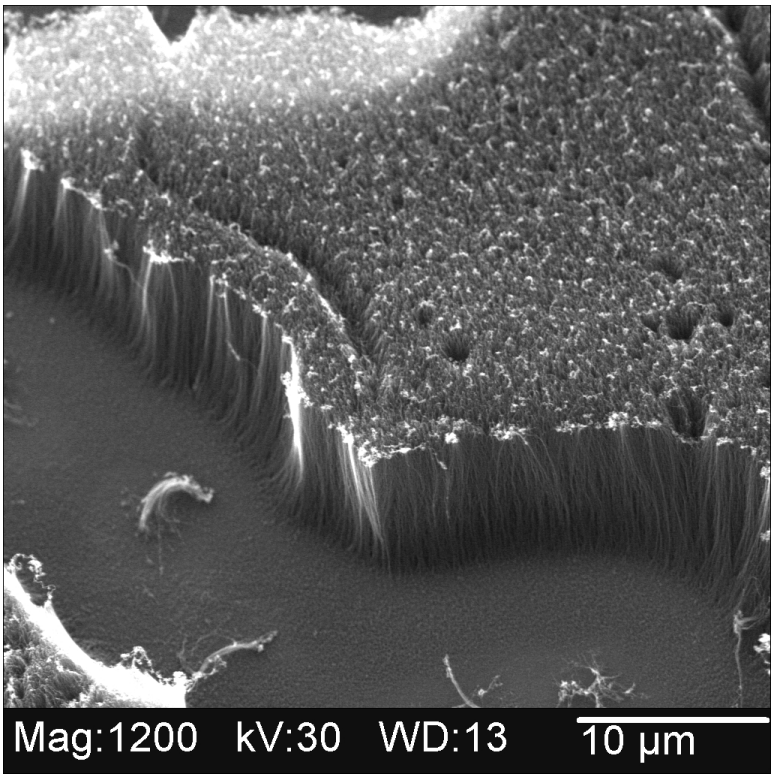

Figure 6.3.8 SEM micrograph of aligned nanotubes showing minimal clusters on top

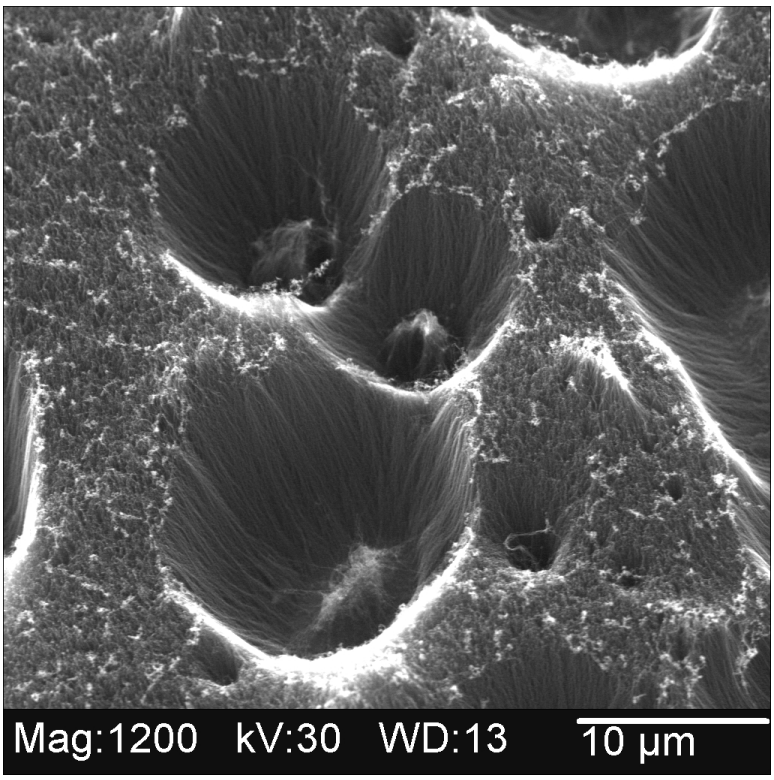

Figure 6.3.9 Dimples formed on the nanotube film reveal the orientation of tubes

Experiments were also conducted at 3, 5, 10 minutes when the methane flow rate is fixed at 15 sccm. For the sample with 10 min growth time, the deposition consisted of two distinct regions or bands. The outer dark region consisted of long ropes of nanotubes (Figs. 6.3.11 and 6.3.12) and the inner grey region consisted of short nanotubes with considerable amorphous carbon deposits (Fig 6.3.10). Terminating clusters are observed on nanotubes grown in the outer darker region and the tubes are ~15 µm long. The nanotubes are randomly aligned in both regions.

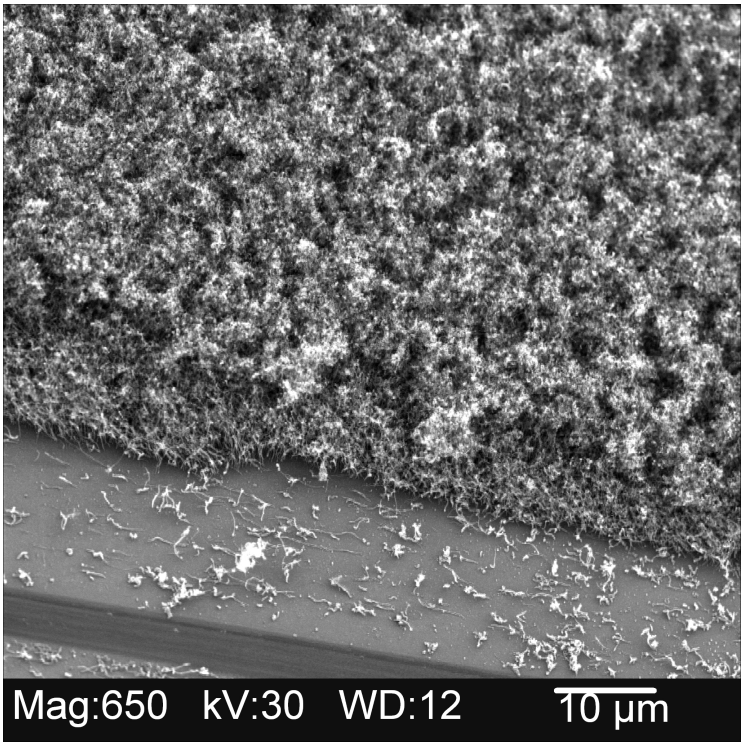

Figure 6.3.10 SEM micrograph of amorphous carbon deposits in the inner grey region

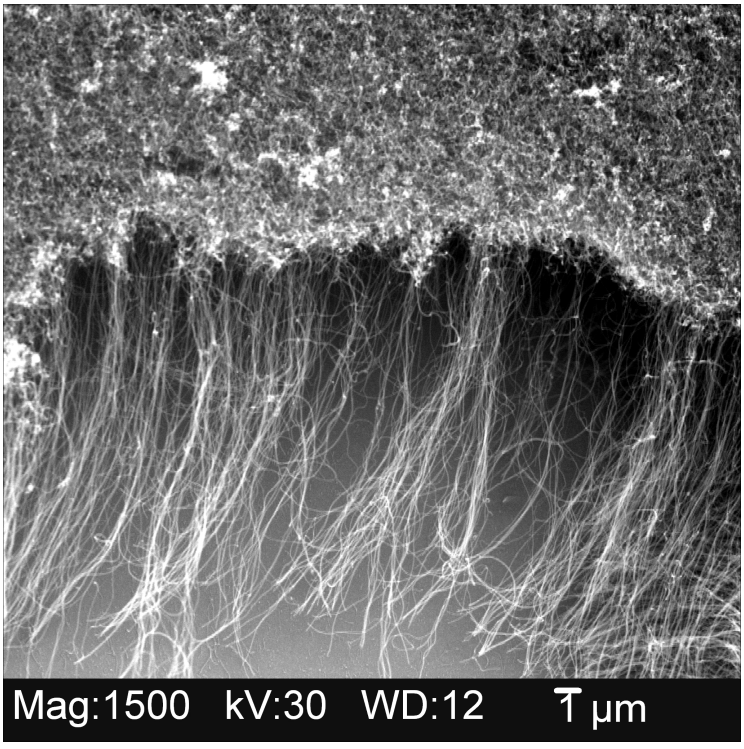

Figure 6.3.11 SEM micrograph of ropes of carbon nanotubes

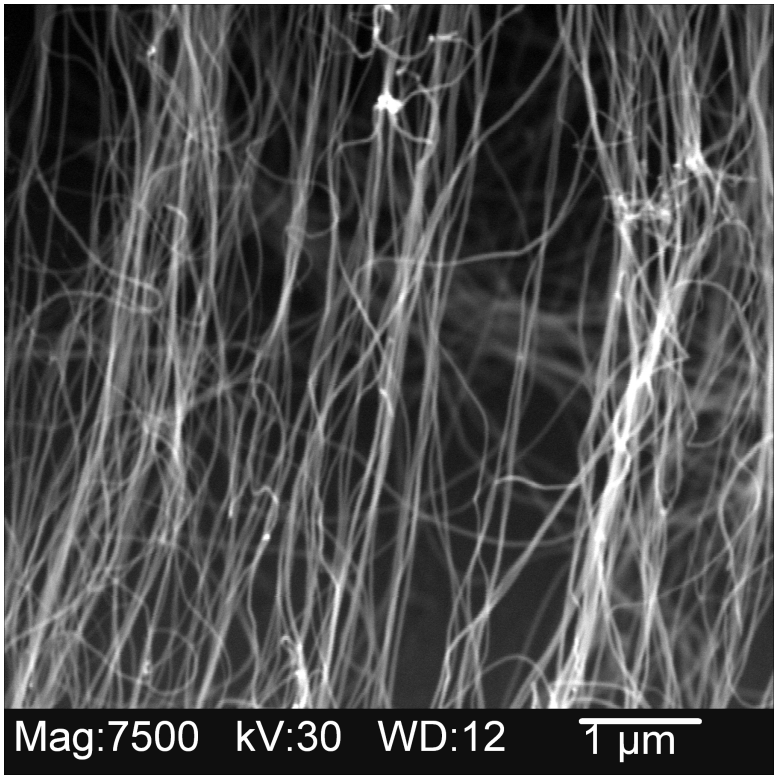

Figure 6.3.12 Higher magnification image of ropes shown in Fig 6.3.11

A mask or template was used while depositing catalyst using PLD to achieve patterning. The sample was then run for 10 minutes at 15 sccm of methane. Figs. 6.3.13, 6.3.14 show the results of these patterning. It is evident from Fig 6.3.13 that growth takes place in the patterned blocks. The nanotubes formed in the patterned blocks were curly and randomly oriented as shown in Fig 6.3.14.

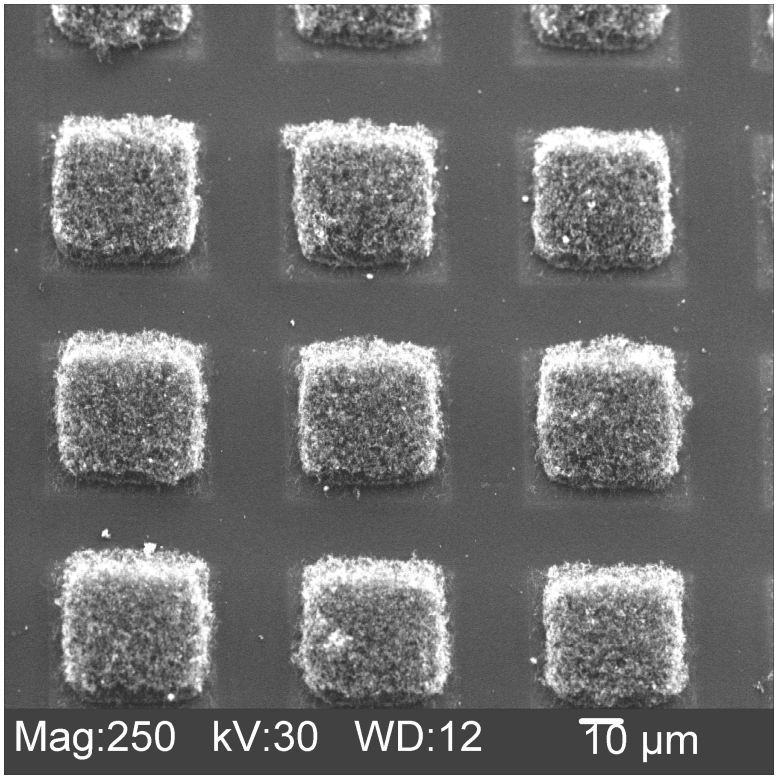

Figure 6.3.13 SEM micrograph of nanotubes grown on patterned blocks

When the growth time was reduced to 5 min under the same conditions vertically aligned nanotubes are obtained. No patterning is done for this sample. The alignment is revealed by an accidental scratch. Fig 6.3.15 shows the piled up material at the end of scratch which contains these very fine aligned nanotubes. Hardly any terminating clusters were seen and the CNTs are 10~15 µm long.

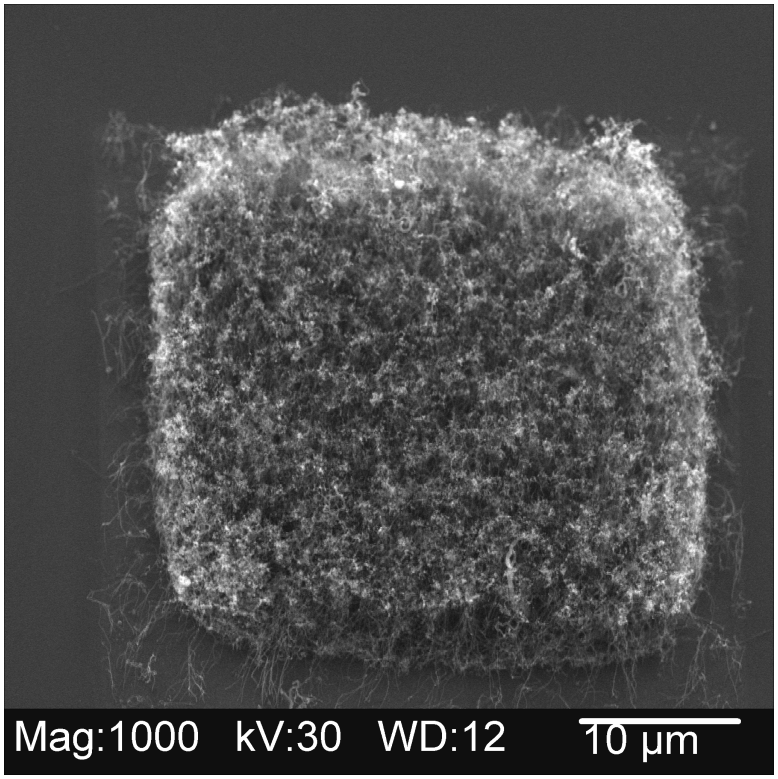

Figure 6.3.14 Randomly aligned nanotubes grown in a patterned block

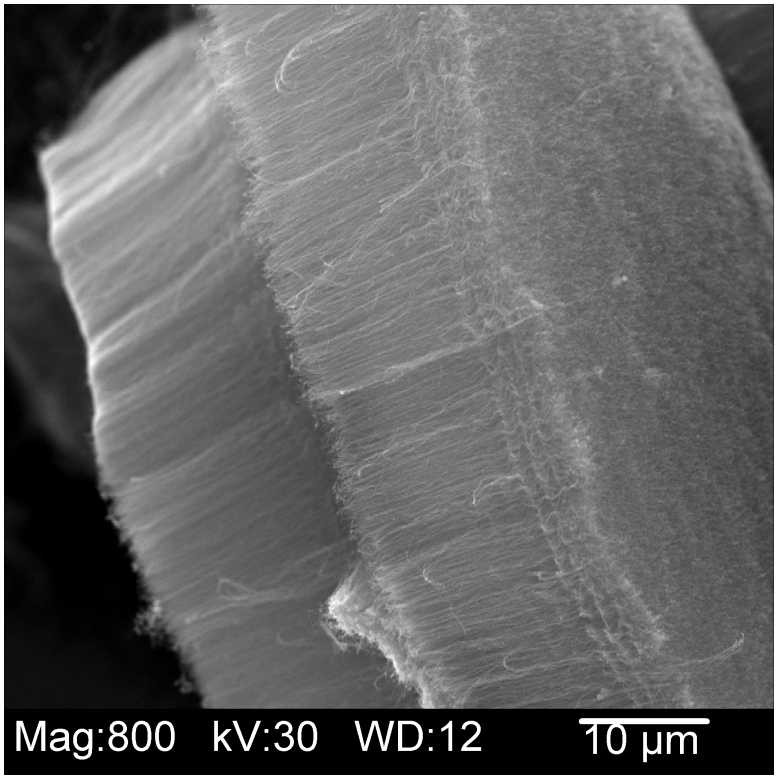

Figure 6.3.15 Aligned nanotubes in the piled up material grown for 5 minutes

As aligned nanotubes were observed for 5 min of growth time and 15 sccm of methane, the same conditions were employed again and patterning was attempted to produce aligned tubes on patterned blocks. Figure 6.3.16 shows the tubes oriented perpendicular to the substrate surface. All the following three samples were subjected to PLD for 45 sec and the methane flow rate is fixed at 15 sccm.

Table 6.3.3 Conditions employed

Sample name	Growth time, min	Pretreatment time, min
Fe-T-4	5	5
Fe-T-7	3	5
Fe-A-1	5	10

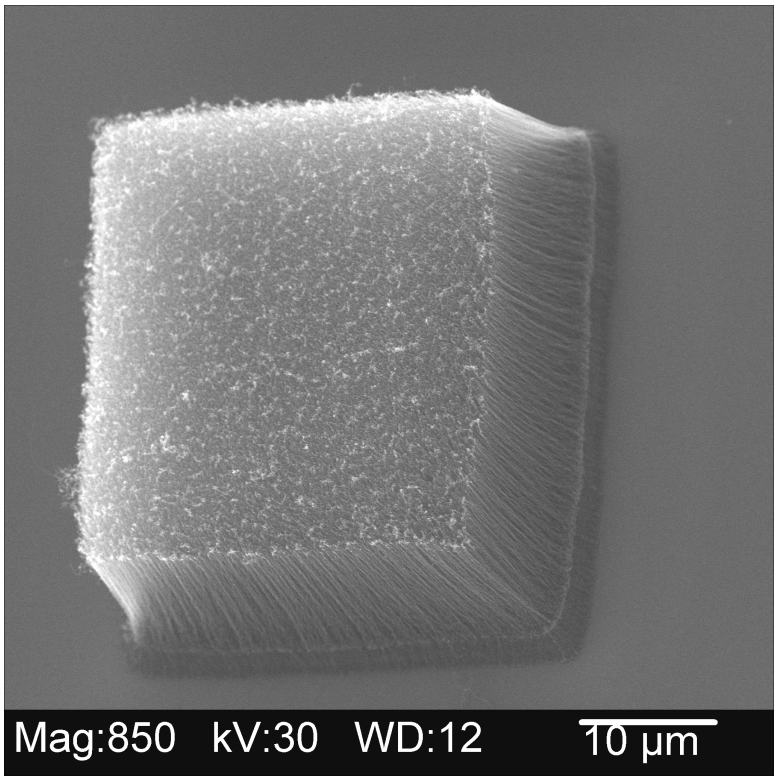

Figure 6.3.16 Vertically aligned nanotubes grown on a patterned block

The diameter of the nanotubes is uniform and the tubes grow only in the blocks where the catalyst is deposited on the silicon surface. Each block is 40 µm X 40 µm and the nanotubes are ~10 µm in length.

The growth time was further reduced to 3 min keeping all other conditions same. Fig 6.3.17 shows the vertically aligned nanotubes grown on the patterned block. It can be observed that there is no nanotube growth where the catalyst is not deposited. Terminating clusters can be noted on top of the nanotubes.

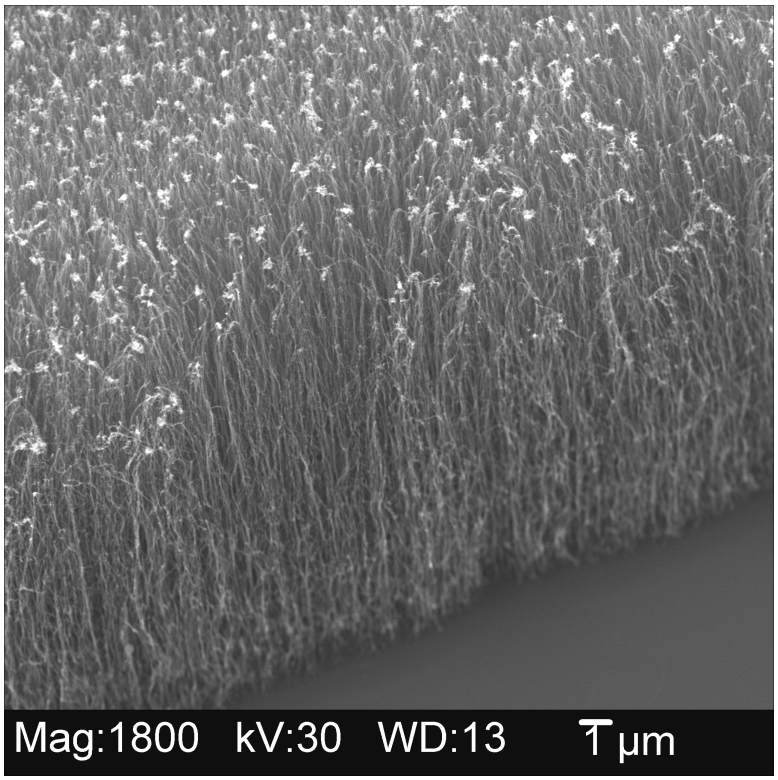

Figure 6.3.17 Vertically aligned nanotubes obtained for a 3 min growth time

These terminating clusters are much more pronounced for tubes at the centre of the pattern and reduce in number for nanotubes on patterned blocks at the edges.

Finally, sample Fe-A-1 is run for 5 min, but the pretreatment time is increased to 10 min to verify the effect of pretreatment. The catalyst layer after PLD is not uniform in thickness throughout. The central part of the coating receives intense plume and so is thick compared to edges. Figure 6.3.18 shows that catalyst nanoparticles are melted and agglomerated at the center of the coating. As one moves away from the centre of the catalyst coating, the nanoparticles size decreases and agglomeration is not observed as shown in Fig 6.3.19. Carbon nanotubes are found on the fringes of the catalyst coating where the catalyst film thickness is much less compared to the center (Fig 6.3.20). In this particular case the catalyst at the edges was ~5 nm thick.

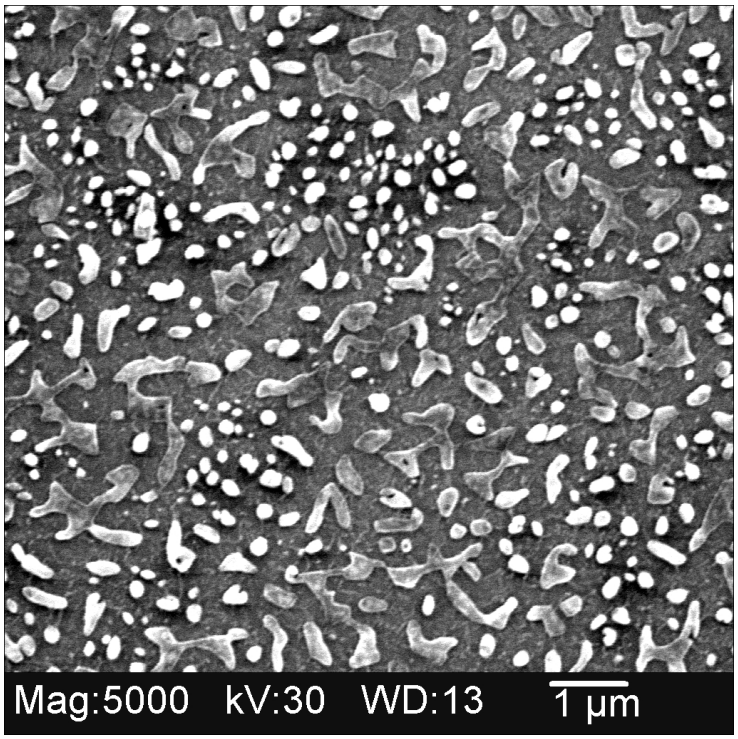

Figure 6.3.18 Nanoparticles of catalyst at the centre of deposition showing agglomeration and melt pattern

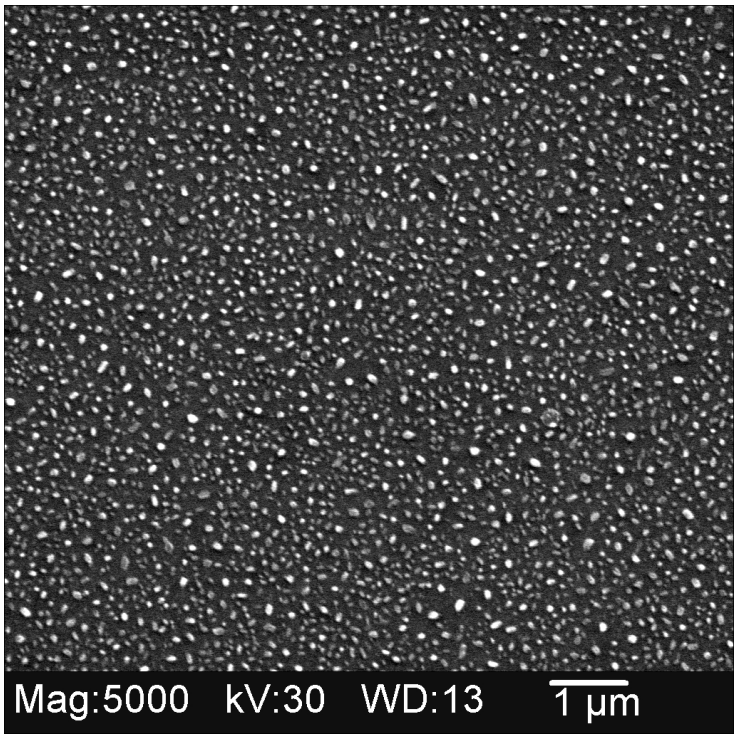

Figure 6.3.19 Catalyst nanoparticles showing no agglomeration effects farther away from the center

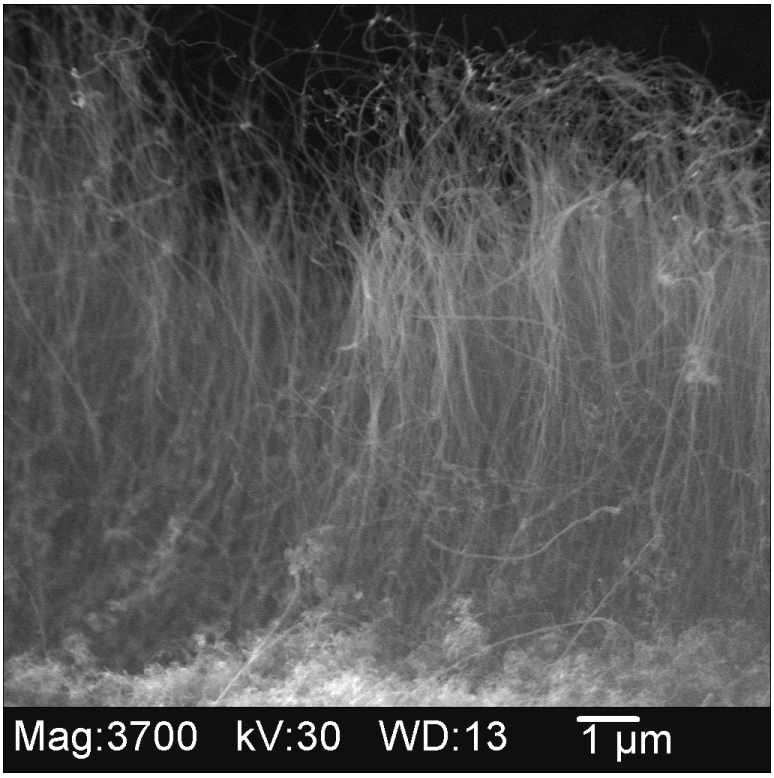

Figure 6.3.20 Nanotubes formed on the fringes of catalyst deposition area

Figs. 6.4.1 and 6.4.2 are TEM micrographs taken from a sample whose growth time is 30 min. The catalyst was coated for 90 sec and the flow rates employed are $CH_4/H_2/N_2$: 10/50/36 sccm.

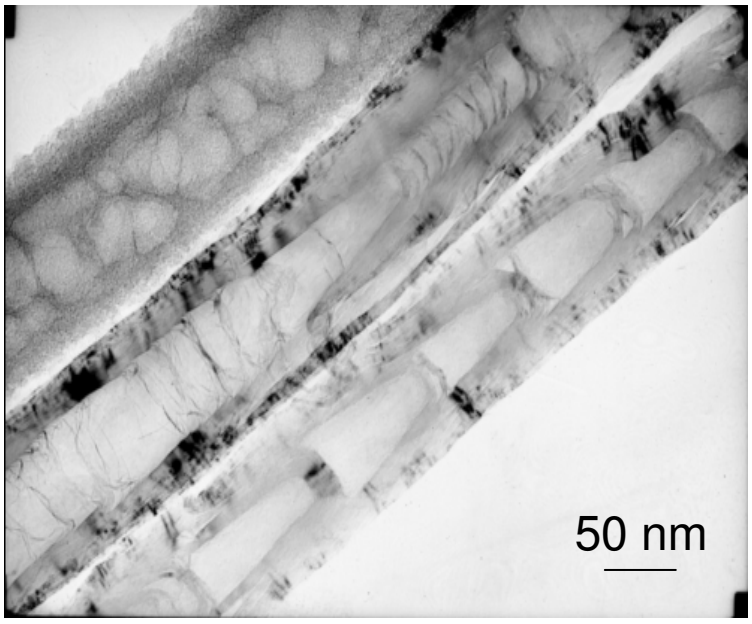

Figure 6.4.1 TEM micrograph of carbon nanotubes showing bamboo growth

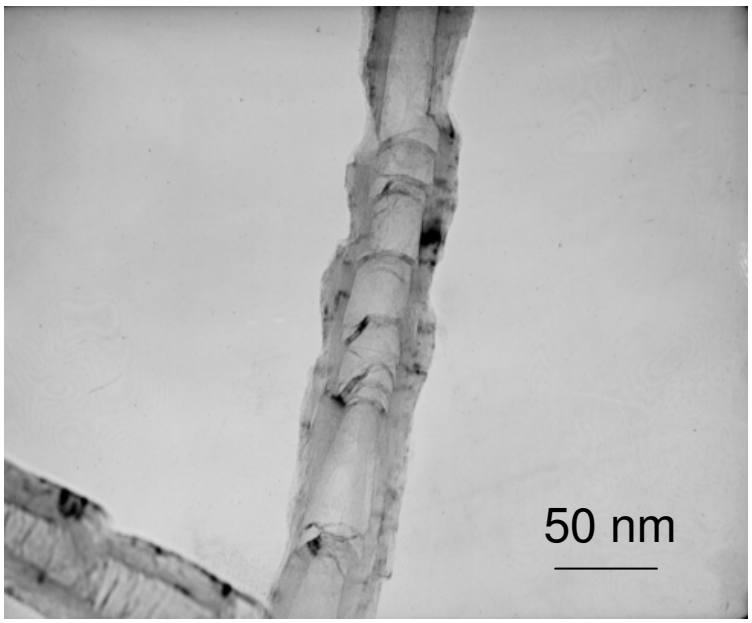

Figure 6.4.2 TEM micrograph showing stacked cone arrangement

Fig 6.4.1 shows the bamboo structure in the bottom tube. A tube with a hollow core can also be seen. It can be seen from the wall thickness that both are multi-walled nanotubes with diameter of ~100 nm. Figure 6.4.2 is another TEM micrograph showing the bamboo or stacked cone arrangement. The diameter of the nanotube is about 50 nm. The bends or kinks of the nanotube are indicative of the defective nature of the nanotube produced.

Fig 6.5.1 shows a number of nanotubes placed on a microscope cover glass and imaged under AFM. Figure 6.5.2 shows the end of another nanotube. Some defects on the surface of the nanotube can also be seen.

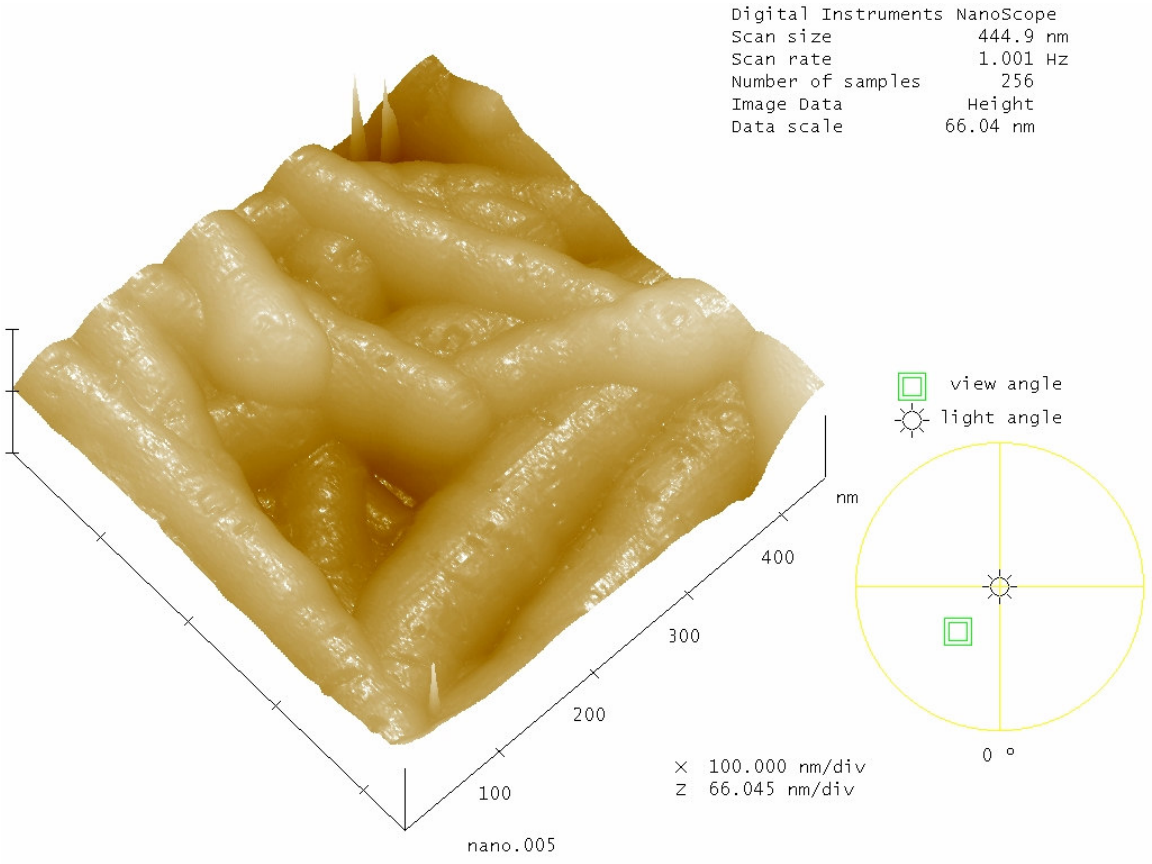

Figure 6.5.1 AFM image of nanotubes placed on a microscope cover glass

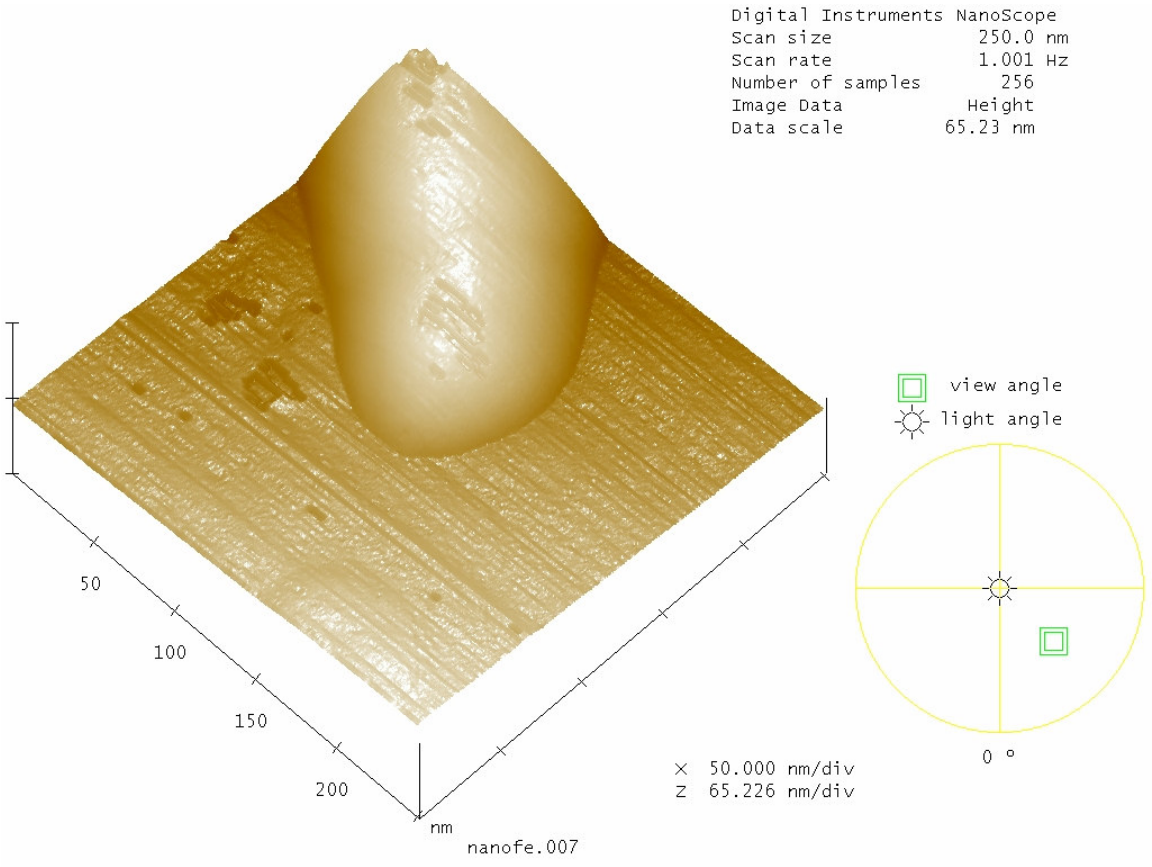

Figure 6.5.2 AFM image of a nanotube end

Figure 6.6 shows the μ-Raman spectra of the CNT deposit grown on the substrate surface. It shows the D and G peaks at ~1350 and 1580 cm^{-1}, which are characteristic of a multi-walled nanotube. The sample was grown for 30 min with flow rates of 20, 40, and 40 sccm for CH_4, H_2, and N_2, respectively. The catalyst was coated for 30 sec.

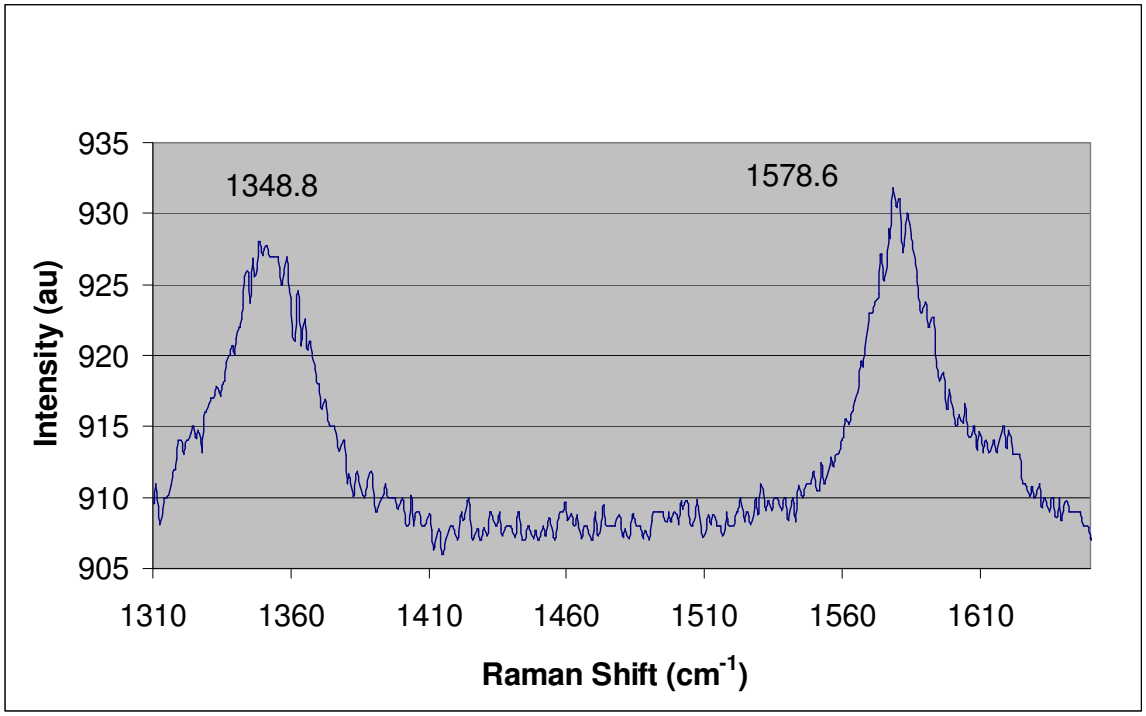

Figure 6.6 μ-Raman spectra showing D and G peaks characteristic of multi-walled carbon nanotubes

CHAPTER 7

DISCUSSION

7.1 Effect of pretreatment time

From Figures 6.2.1 to 6.2.10 in chapter 6, it can be noted that vertically aligned nanotubes are obtained in all cases. With increase in pretreatment time from 3 to 10 min the inner grey deposit increases in size and completely encompasses the catalyst coated region. The tubes are bundled along the scratch boundary in the outer dark region compared to the inner grey deposit. This can be explained by the fact that catalyst coating after PLD is not uniform and varies in thickness as one moves from the center of the catalyst coating to the edge. The catalyst is thick at the center and its thickness reduces as we move outwards. When the catalyst pretreatment time is gradually increased, the catalyst film at the center has more time to break into nanosized particles. This facilitates in forming nanosized catalyst particles which are conducive to growth of nanotubes. The size of the inner grey region increases with increase in pretreatment time as more and more larger islands of the catalyst are broken down into smaller nanoparticles for nanotube growth. The outer periphery of the catalyst film is very thin and forms nanoparticles of the right size for nanotube growth even when the pretreatment time is short. This helps in increasing the nucleation density compared to the central region and so dense growth of the nanotubes is seen. The nanotubes are closely packed, well aligned and are bundled along the scratch in the outer dark region. The difference in the nucleation density explains the difference in color of the two regions.

7.2 Effect of methane

The alignment improved with increase in flow rate of methane significantly. First, at methane flow rate of 10 sccm nanotubes are not formed. From Fig 6.1.1 it can be seen that at 15 sccm of methane, growth is seen and there are numerous terminating clusters on top. Straight and long nanotubes can be observed (Fig 6.1.2) but they are hardly aligned. With 20 sccm, the alignment improves to a considerable extent as seen from Figs. 6.1.3. At 30 sccm, we see well aligned CNTs grown perpendicular to the surface of the substrate. The nanotube film breaks into pieces and the tube density also increases. The nanotubes are more closely packed for methane flow rate of 30 sccm (Fig 6.1.4) than for 15 sccm (Figs. 6.1.4 and 6.1.5).

In the first case of 10 sccm of methane, the flow rate for 10 minutes appears to be too low for the initiation of nanotube growth. With a progressive increase in the flow rate to 15 sccm, nanotubes begin to form and at 20 sccm are well defined and well aligned. The sample is entirely covered with CNT deposit after CVD and hardly clusters are formed. The flow rate appears to be just adequate. With further increase, only the outer periphery (where the catalyst film is less thick than the center) forms well defined nanotubes, whereas the inner grey region shows a considerable number of terminating clusters. The central portion has amorphous carbon deposition which indicates that passivation of catalyst nanoparticles is taking place and the optimum flow rate might be between 20 and 30 sccm.

7.3 Effect of Growth time

The growth time was varied for three different flow rates and the results are summarized in Table 7.1. All samples are subjected to 30 sec PLD, while the last two for 45 sec.

Table 7.1 Summary of the effect of growth time

Sample name	Methane flow rate, sccm	Growth time, min	Observations
Fe-8-2	10	15	Long straight tubes (10 µm). Bushy growth. Lots of amorphous carbon on top.
Fe-8-3	10	10	No growth.
Fe-8-4	20	10	Aligned nanotubes (20 µm). Bundling of tubes along scratch mark
Fe-A-2	20	5	Alignment improved greatly. Minimal cluster formation on top. Nanotubes (6µm) are densely packed.
Fe-8-7	15	10	Grey region has lot of amorphous carbon and very short tubes. Dark region is made up of long ropes of nanotubes (15 µm). No significant alignment is seen. Terminating clusters on top for dark region.
Fe-T-1	15	10	Able to achieve growth on patterned blocks. Randomly aligned and coiled.
Fe-9-1	15	5	Aligned tubes (10-12 µm) in the piled material. Uniform in diameter.
Fe-T-4	15	5	Vertically aligned tubes in patterned blocks. (12 µm)
Fe-T-7	15	3	Vertically aligned tubes (10 µm). Lots of clusters when compared with 5 min.

For 10 and 20 sccm of methane:

At 10 sccm of methane and 15 min of growth time, nanotubes are observed but contained numerous amorphous carbon particles as shown in Fig 6.3.2. The tubes are ~10 µm long. However no particular orientation was observed. This can be considered as a

growth of a bush where the individual branches are not entangled and do not show any sort of alignment. When this is ploughed all the nanotubes attempt to align in that direction as seen in Fig 6.3.3. With a reduction in growth time, no growth was observed with 10 sccm of methane. So, the flow rate was increased to 20 sccm and the growth time of 10 min was retained.

As shown in Fig 6.3.6 aligned nanotubes 20 μm long were observed. The nanotubes are bundled along the scratch boundary (Fig 6.3.5). Terminating clusters were observed on top of CNTs. When the growth time is reduced to 5 min, a remarkable improvement in the alignment is observed. The nanotubes are vertically aligned to the substrate surface which is shown in Fig 6.3.8. The tubes are closely packed. The number of clusters on top also decreased. The nanotubes are ~6 μm long. This large difference in length can be attributed to the growth time.

For 15 sccm of methane:

Experiments were conducted at methane flow rate of 15 sccm and the growth time was varied. When grown for 10 min, the sample shows two regions of different colors. The outer region was dark black and the inner region grey. Considerable amount of amorphous carbon is observed in the grey region (Fig 6.3.10) while long nanotubes (15 μm) with terminating clusters are found in the outer region (Fig 6.3.11). A template is used to pattern the samples to grow tubes at selective areas and check the alignment without scratching the deposit. It can be seen from Fig 6.3.13 and 6.3.14 the nanotubes are grown in selective spots but there is no alignment.

At 5 min of growth time and 15 sccm of flow rate, aligned nanotubes are observed as shown by Fig 6.3.15. The nanotubes are vertically aligned and are ~10-12 μm in

length. So, with decrease in growth time from 10 to 5 min there is significant improvement in alignment while the length decreased marginally. So, 5 min of growth time at 15 sccm appears to be the optimum combination.

As aligned nanotubes are observed for the above stated optimum combination, the sample is patterned using a template. The catalyst deposition time has been increased to 45 sec. It can be seen from Fig 6.3.16, vertically aligned nanotubes with deposition in patterned blocks are obtained. The tubes are ~12 μm long. Very few terminating clusters are seen on top of the nanotubes. It can also be seen from Figure 6.3.16 nanotubes are grown where there is catalyst deposition. This is significant as it enables to grow aligned nanotubes selectively at the desired locations.

The growth time is further reduced to 3 min and still aligned growth is seen (Fig 6.3.17). The tubes are ~10 μm long. So, there is not appreciable decrease in length. But there are many more terminating clusters compared to the 5 min sample.

From the above discussion it can be seen that the flow rate and growth time complement each other and the optimum growth time varies with variation in flow rate.

Finally, the pretreatment was increased to 10 min and the synthesis was carried out under the same conditions. Nanotube growth is only seen on the outer periphery and the inner region has large catalyst nanoparticles agglomerated (Fig 6.3.18). Near the periphery, where nanotube growth is not observed, the catalyst nanoparticles are very small and agglomeration is not observed (Fig 6.3.19).

CHAPTER 8

CONCLUSIONS AND FUTURE WORK

8.1 Conclusions

Based on the results of the present investigation the following specific conclusions may be reached:

1. Carbon nanotubes are synthesized on silicon wafers by MPECVD using iron as catalyst.
2. Orientation of the nanotubes is controlled by the growth process and vertically aligned nanotubes are synthesized.
3. Catalyst film is patterned using a template thereby allowing the growth of carbon nanotubes at the desired locations.
4. Concentration of methane effects the growth of carbon nanotubes. Improvement in alignment is observed with increase in methane flow rate.
5. Carbon nanotubes grow on catalyst deposited areas only. Without catalyst, no nanotube growth is observed.
6. Pretreatment of the catalyst film plays a crucial role in the growth of nanotubes. Pretreatment is required to break the thin film of catalyst into nanoparticles which are conducive to nanotube growth.

7. Growth time (or duration of deposition) determines the alignment and length of the nanotubes. The optimum growth time is dependent on the concentration of methane and the catalyst thickness.

8.2 Future work

Following are some suggestions for future work:

1. Multi-walled carbon nanotubes have been synthesized in the present investigation. Further work is needed to synthesize single-walled nanotubes using PECVD.
2. In the present investigation a single catalyst layer (iron) is used. Multi-layer films are reported to increase the number of reactive sites through the formation of surface clusters.
3. Synthesize nanotubes on different substrates such as glass, plastics etc.
4. The catalyst has been deposited at pressure of 10^{-2} torr. Lowering the pressure may help in obtaining film with uniform thickness and/or more pure CNTs.
5. Methods to integrate the nanotubes grown on patterned blocks into devices need to be explored. For example flat panel displays need bundles of aligned CNTs. Composites with nanotubes as the reinforcing material have them dispersed randomly. New type of composite materials can be developed if the bundles of aligned nanotubes are kept intact.

REFERENCES

1. Dresselhaus, M.S., Dresselhaus, G., and Ph. Avouris, "Carbon Nanotubes: Synthesis, Structure, Properties, and Applications," Topics in Applied physics 80 (2001) 2.
2. Dresselhaus, M.S., Dresselhaus, G., Eklund, P., and R. Saito, "Carbon nanotubes," Physics world January (1998) 33-45.
3. Dresselhaus, M.S., Dresselhaus, G., and R. Saito, "Physics of carbon nanotubes," Carbon 33 (1995) 883-891.
4. Graham, A.P., Duesberg, G.S., Hoenlein, W., Kreupl, F., Liebau, M., Martin, R., Rajasekharan, B., Palmer, W., Siedel, R., Steinhoegl, W., and E. Unger, "How do carbon nanotubes fit into the semiconductor roadmap?," Appl. Phys. A 80 (2005) 1141-1151.
5. Meyyappan, M., Delzeit, L., Cassell, A., and D. Hash, "Carbon nanotube growth by PECVD: a review," Plasma Sources Sci. Technol. 12 (2003) 205-216.
6. Iijima, S., "Helical microtubules of graphitic carbon," Nature 354 (1991) 56-58.
7. Gupta, S., Wang, Y.Y., and R.J. Nemanich, "Role of thin Fe catalyst in the synthesis of double- and single-wall carbon nanotubes via chemical vapor deposition," Appl. Phys. Lett. 85 (2004) 2601-2603.
8. Bower, C., Zhu, W., Jin, S., and O. Zhu, "Plasma-induced alignment of carbon nanotubes," Appl. Phys. Lett. 77 (2000) 830-832.

9. Ren, Z.F., Huang, Z.P., Xu, J.W., Wang, J.H., Bush, P., Siegal, M.P., and P.N. Provencio, "Synthesis of large arrays of well-aligned carbon nanotubes on glass," Science 282 (1998) 1105-1107.
10. Meyyappan, M., Delzeit, L., McAninch, I., Cruden, B.A., Hash, D., Chen, B., and J. Han, "Growth of multiwall carbon nanotubes in an inductively coupled plasma reactor," J. Appl. Phys. 91 (2002) 6027-6033.
11. Stoner, B.R., Zhou, O., and H. Cui, "Deposition of aligned bamboo-like carbon nanotubes via microwave plasma enhanced chemical vapor deposition," J. Appl. Phys. 88 (2000) 6072-6074.
12. Silva, S.R.P., Haq, S., Khan, R.U.A., Stolojan, V., and B.O. Boskovic, "Large-area synthesis of carbon nano fibres at room temperature," Nature Materials 1 (2002) 165-168.
13. Lin, J., Wang, Y.H., Huan, C.H.A., and G.S. Chen, "Synthesis of large area aligned carbon nanotube arrays from C_2H_2-H_2 mixture by rf plasma-enhanced chemical vapor deposition," Appl. Phys. Lett. 79 (2001) 680-682.
14. Kim, U., Pcionek, R., Aslam, D.M., and D. Tomanek, "Synthesis of High Density carbon nanotubes films by microwave plasma chemical vapor deposition," Diamond and Related Materials 10 (2001) 1947-1951.
15. Gao, J.S., Umeda, K., Uchino, K., Nakashima, H., and K. Muraoka, "Plasma breaking of thin films into nano-sized catalysts for carbon nanotube synthesis," Mat. Sci. & Eng., A 352 (2003) 308-313.
16. Kim, T.Y., Lee, K.R., Eun, K.Y., and K.H. Oh, "Carbon Nanotubes growth enhanced by nitrogen incorporation," Chem. Phys. Lett. 372 (2003) 603-607.

17. Lee, J.Y., and B.S. Lee "Nitrogen induced structure control of vertically aligned carbon nanotubes synthesized by microwave plasma enhanced chemical vapor deposition," Thin Solid Films 418 (2002) 85-88.
18. Chhowalla, M., Teo, K.B.K., Ducati, C., Rupesinghe, N.L., Amaratunga, G.A.J., Ferrari, A.C., Roy, D., Robertson, J., and W.I. Milne, "Growth process conditions of vertically aligned carbon nanotubes using plasma enhanced chemical vapor deposition," J. Appl. Phys. 90 (2001) 5308-5317.
19. Qin, L.C., Zhou, D., Krauss, A.R., and D.M. Gruen, "Growing carbon nanotubes by microwave plasma-enhanced chemical vapor deposition," Appl. Phys. Lett. 72 (1998) 3437-3439.
20. Lee, Y.H., Choi, Y.C., Shin, Y.M., Lim, S.C., Bae, D.J., and B.S. Lee, "Effect of surface morphology of Ni thin film on the growth of aligned carbon nanotubes by microwave plasma-enhanced chemical vapor deposition," J. Appl. Phys. 88 (2000) 4898-4903.
21. Merkulov, V.I., Melechko, A.V., Guillorn, M.A., Simpson, M.L., Lowndes, D.H., Whealton, J.H., and R.J. Raridon, "Controlled alignment of carbon nanofibers in a large-scale synthesis process," Appl. Phys. Lett. 80 (2002) 4816-4818.
22. Sato, H., Takegawa, H., and Y. Saito, "Vertically aligned carbon nanotubes grown by plasma enhanced chemical vapor deposition," J. Vac. Sci. Tech. B. 21 (2003) 2564-2568.
23. Meyyappan, M and D.B. Hash, "Model based comparison of thermal and plasma chemical vapor deposition of carbon nanotubes," J. Appl. Phys. 93 (2003) 750-752.

24. Kato, T., Jeong, G.H., Hirata, T., and R. Hatakeyama, "Structure control of carbon nanotubes using radio-frequency plasma enhanced chemical vapor deposition," Thin Solid Films 457 (2004) 2-6.

25. Merkulov, V.I., Guillorn, M.A., Lowndes, D.H., Voelkl, E., and M.L. Simpson, "Shaping carbon nanostructures by controlling the synthesis process," Appl. Phys. Lett. 79 (2001) 1178-1180.

26. Dai, H., Fan, S., Chapline, M.G., Franklin, N.R., Tombler, T.W., and A.M. Cassell, "Self-Oriented regular arrays of carbon nanotubes and their Field Emission properties," Science 283 (1998) 512-514.

27. Ren, Z.F., Huang, Z.P., Xu, J.W., Wang, J.H., Bush, P., Siegal, M.P., and P.N. Provencio, "Growth of highly oriented carbon nanotubes by plasma-enhanced hot filament chemical vapor deposition," Appl. Phys. Lett. 73 (1998) 3845-3847.

28. Lee, Y.H., Choi, Y.C., Bae, D.J., Lee, B.S., Han, I.T., Choi, W.B., Lee, N.S., and J.M. Kim, "Low temperature synthesis of carbon nanotubes by microwave plasma enhanced chemical vapor deposition," Synthetic Metals 108 (2000) 159-163.

29. Dai, H., Kong, J., and A.M. Cassell, "Chemical vapor deposition of methane for single-walled carbon nanotubes," Chem. Phys. Lett. 292 (1998) 567-574.

30. Li, W.Z., Xie, S.S., Qian, L.X., Chang, B.H., Zou, B.S., Zhou, W.Y., Zhao, R.A., and G. Wang, "Large-scale synthesis of aligned carbon nanotubes," Science 274 (1996) 1701-1703.

31. Kenny, J.M., Valentini, L., Lozzi, L., and S. Santucci, "Formation of carbon nanotubes by plasma enhanced chemical vapor deposition: Role of nitrogen and catalyst layer thickness," J. Appl. Phys. 92 (2002) 6188-6194.

32. Ducati, C., Alexandrou, I., Chhowalla, M., Amaratunga, G.A., and J. Robertson, "Temperature selective growth of carbon nanotubes by chemical vapor deposition," J. Appl. Phys. 92 (2002) 3299-3303.
33. Wang, S.G., Wang, J.H., Ma, Z.B., Wang, C.X., Man, W.D., and B.H. Zhang, "Vertically aligned carbon nanotubes grown on geometrically different types of surface," Diamond and Related Materials 12 (2003) 2175-2177.
34. Meyyappan, M., Teo, K.B.K., Hash, D.B., Larceda, R.G., Rupesinghe, N.L., Bell, M.S., Dalal, S.H., Bose, D., Govindan, T.R., Cruden, B.A., Chhowalla, M., Amaratunga, G.A.J., and W.I. Milne, "The significance of plasma heating in carbon nanotube and nanofiber growth," Nano Letters, 4 (2004) 921-926.
35. Meyyappan, M., Delzeit, L., Nguyen, C.V., Stevens, R.M., and J. Han, "Growth of carbon nanotubes by thermal and plasma chemical vapour deposition processes and applications in microscopy," Nanotechnology 13 (2002) 280-284.
36. Maruyama, S., Chiashi, S., Maurakami, Y., and Y. Miyauchi, "Direct synthesis of high-quality single-walled carbon nanotubes on silicon and quartz substrates," Chem. Phys. Lett. 377 (2003) 49-54.
37. Dai, H., Li, Y., Mann, D., Rolandi, M., Kim, W., Ural, A., Hung, S., Javey, A., Cao, J., Wang, D., Yenilmez, E., Wang, Q., Gibbons, J.F., and Y. Nishi., "Preferential growth of semiconducting single-walled carbon nanotubes by a plasma enhanced CVD method," Nano letters, 4 (2004) 317-321.
38. Yoo, J.B., Han, J.H., Yang, W.S., and C.Y. Park, "Growth and emission characteristics of vertically well-aligned carbon nanotubes on glass by hot

filament plasma-enhanced chemical vapor deposition," J. Appl. Phys. 88 (2000) 7363-7365.

39. Wong, W.K., Li, C.P., Au, F.C.K., Fung, M.K, Sun, X.H., Lee, C.S., Lee, S.T., and W. Zhu, "Fabrication and characterization of pure and well-aligned carbon nanotubes using methane/nitrogen-ammonia plasma," J. Phys. Chem. B. 107 (2003) 1514-1517.
40. Cassell, A.M., Ye, Q., Cruden, B.A., Li, J., Sarrazin, P.C., Ng, H.T., Han, J., and M. Meyyappan, "Combinatorial chips for optimizing the growth and integration of carbon nanofiber based devices," Nanotechnology 15 (2004) 9-15.
41. Terrones, M., Grobert, N., Olivares, J., Zhang, J.P., Terrones, H., Kordatos, K., Hsu, W.K., Hare, J.P., Townsend, P.D., Prassides, K., Cheetham, A.K., Kroto, H.W., and D.R.M. Walton, "Controlled production of aligned-nanotube bundles," Nature 388 (1997) 52-55.
42. Nyugen, C.V., Chao, K.J., Stevens, R.M.D., Delzeit, L., Cassell, A., Han, J., and M. Meyyappan, "Carbon nanotube tip probes; stability and lateral resolution in scanning probe microscopy and application to surface science in semiconductors," Nanotechnology 12 (2001) 363-367.
43. Ajayan, P.M., Koratkar, N., Modi, A., Lass, E., and B. Wei, "Miniaturized gas ionization sensors using carbon nanotubes," Nature 424 (2003) 171-174.
44. Lieber, C.M., Hafner, J.H., and C.L. Cheung, "Growth of nanotubes for probe microscopy tips," Nature 398 (1999) 761-762.

45. Lieber, C.M., Hafner, J.H., and C.L. Cheung, "Direct growth of single-walled carbon nanotube scanning probe microscopy tips," J. Am. Chem. Soc. 121 (1999) 9750-9751.

46. Ren, Z.F., Huang, Z.P., Wang, J.H., and D. Wang, "Free-standing and aligned carbon nanotubes and synthesis thereof," U.S. Patent No. 6,863,942, dated Mar. 8, 2005.

47. Komanduri, R., Choo, K.L., Ogawa, Y., Otra, V., Raff, L.M., and G. Kanbargi, "Micromachining of silicon by short-pulse laser ablation in air and under water," Mat. Sci. and Eng. A. 372 (2004) 145-162.

48. Ramakrishnan, M.P., "Experimental study on microwave assisted CVD growth of carbon nanotubes on silicon wafer using cobalt as a catalyst," M.S. Thesis, Oklahoma State University, May 2005.

49. Raghavan, D., "Synthesis of multi-walled carbon nanotubes by plasma enhanced microwave CVD using colloidal form of iron oxide as a catalyst," M.S. Thesis, Oklahoma State University, May 2005.

50. Hone, J., Whitney, M., and A. Zettl, "Thermal conductivity of single-walled carbon nanotubes," Synthetic Metals 103 (1999) 2498-2499.

VITA

Anandha G R Nidadavolu

Candidate for the Degree of

Master of Science

Thesis: SYNTHESIS OF CARBON NANOTUBES BY PLASMA ENHANCED CVD ON SILICON USING IRON CATALYST

Major Field: Mechanical Engineering

Biographical:

Education: Received Bachelor of Engineering degree in Mechanical Engineering from Jawaharlal Nehru Technological University, Hyderabad, India in July, 2001; completed requirements for the Master of Science degree at Oklahoma State University in May, 2005.

Experience: Graduate research assistant in the department of Mechanical and aerospace engineering at Oklahoma State University, Stillwater, Oklahoma; May 2002 – May 2005.